2017

Moisture Sensing in Baled Crops

John Just
Iowa State University

Follow this and additional works at: http://lib.dr.iastate.edu/etd

Part of the Agriculture Commons, Bioresource and Agricultural Engineering Commons, Electrical and Electronics Commons, and the Statistics and Probability Commons

Moisture sensing in baled crops

by

John Just

A dissertation submitted to the graduate faculty

in partial fulfillment of the requirements for the degree of

DOCTOR OF PHILOSOPHY

Major: Agricultural and Biosystems Engineering

Program of Study Committee:
Matt Darr, Major Professor
Lie Tang
Phillip Jones
Steven Hoff
Mehari Tekeste

The student author and the program of study committee are solely responsible for the

content of this dissertation. The Graduate College will ensure this dissertation is

globally accessible and will not permit alterations after a degree is conferred

Iowa State University

Ames, Iowa

2017

TABLE OF CONTENTS

GENERAL ABSTRACT

This dissertation is comprised of three papers. The first paper describes in detail a planar dielectric probe design using finite element analysis to determine sensing range and efficiency. The probe is subsequently connected to a Keysight impedance analyzer to measure dielectric properties of raw cotton at controlled levels of moisture content, compressed densities, and source frequency sweeps. Sensitivity to compositional differences such as turnout (lint vs seed) and variety is also explored. The response to the different factors is shown graphically and further quantified statistically in the form of a predictive model for the complex permittivity (dielectric constant and loss tangent).

The second paper extends the dielectric probe used in the first paper to real-time harvesting on a round-module cotton harvester by leveraging a packaged sensor with embedded impedance measurement circuit and probe all in one mobile unit. A moisture prediction model based on permittivity is developed from lab-measured data and adjusted based on field data collected during cotton harvesting in Fall of 2014 for pickers and Spring of 2015 for strippers. Verification of the prediction accuracy is performed on field data collected during cotton harvesting in 2016. Sources of variability and sensitivity to confounding factors are investigated and quantified. Finally, plots of diurnal trends of predicted and actual moisture content are overlaid for several days of harvesting.

The third paper draws on the first two in applying capacitive-based moisture sensing to large-square bales of alfalfa. A lab characterization is performed on alfalfa over a wide range of moisture contents and densities using both the Keysight impedance analyzer and packaged sensor to measure permittivity. Field data (on-machine permittivity measurements of bales and corresponding ground truth moisture content) is subsequently collected during baling in 2015 and 2016 for alfalfa hay (<30%) and silage (>30%) and used for training and validation of prediction models. In following with the other two papers, sources of variability are discussed and sensitivity to factors quantified. Limitations in sensing range of the packaged sensor lead to multiple prediction models: a simple but limited model restricted to hay and another using modern fitting techniques (feature engineering and artificial neural network) for both hay and silage. Real-time filtering of the prediction signal is investigated using the simple model in light of what seems like mechanically induced oscillations, using a Kalman filter to isolate and remove them while minimizing delay. The real-time prediction signal is finally overlaid with actual moisture content found from core samples of the same bales.

Note: Text, figures, and tables are redacted where the sponsor deemed that information that is proprietary or otherwise of sensitive nature and not to be released to the public.

CHAPTER 1:   GENERAL INTRODUCTION

Moisture sensing is a classic subject in the electronic sensing industry, having been studied in grains since early in the 20th century when a correlation was found between moisture and electrical resistance in wheat [1]. Not long thereafter research transitioned to examining dielectric properties via capacitive-based measurements at radio frequencies, eventually leading to permittivity-based moisture predictions in mid-20th century. Research on the dielectric properties of grain and other seeds has been adopted as a standard reference by ASABE since 1965 and revised as late as 2012 [2]. The permittivity is modeled in terms of the specific material properties (density, moisture content, temperature) as well as the frequency of the applied voltage source. Compared to grain and seed, relatively little work has been published on the dielectric properties of baled crops such as hay or cotton, although some published research exists [3] [4] [5]. From the context of moisture sensing, baled crops such as hay and cotton are challenging due to low bulk modulus, which can lead to increased probability of confounding effects from density changes. Additionally, cotton and hay do not flow easily and thus can be more difficult to position a dielectric probe consistently when measuring permittivity. These challenges are exacerbated when attempting to measure dielectric properties with a probe mounted on a machine during harvesting, where the probe must function within the existing operation of the machine (i.e., the machine is not modified in any way to encourage consistent contact of the probe with material).

This dissertation is focused on rapid determination of moisture content (MC, or MC%) in raw cotton and alfalfa hay using a capacitive sensing probe operating in the radio frequency range. The primary objective aimed to extend the innovation to real-time on harvesting equipment. In order to do so, the first paper sets out to characterize the influence that factors such as moisture content, density, frequency, and constituents have on the dielectric properties of raw cotton. Since the probe design that enables moisture sensing in baled crops is a critical link, this initial work also takes time to carefully explore the region of influence around the probe which can have an effect on dielectric measurements. This is accomplished by modeling the electrostatic field and surface charge simultaneously via Finite Element Analysis (FEA). Following the typical path of similar research, the probe is subsequently connected to a commercial impedance analyzer and tests conducted to measure the permittivity of raw cotton in a lab setting that controls factors such as density, MC, frequency, and temperature. The conditional means of the dielectric constant and loss tangent are modeled with respect to the MC, density, and frequency as explanatory variables. Cotton variety is also included as a fixed effect. This work is the most thorough to date in characterizing the dielectric properties of cotton, introduces probe design considerations leveraging FEA, and also served as

a gateway to extend the probe design to MC sensing on mobile harvesting equipment.

The full intention of the innovation is realized in the second paper, aimed at real-time on-machine prediction of MC during cotton harvesting. Unlike most other work where the research ended after the ideal lab characterization [4] or off-the-shelf sensors were simply evaluated for performance on a machine [3], this research extends the novel probe design and lab characterization of the first paper to harvesters. The probe is packaged with an impedance measurement circuit to facilitate permittivity measurements in the module chamber of the machine. Over 550 modules from various locations and both stripper and picker machines were sampled and used for development and validation, with the on-machine performance approaching that found in gins under more controlled conditions (material composition, moisture range, temperature). Resulting diurnal trends in the filtered predicted MC match actual MC closely and clearly indicate the value in decision making during typical harvesting operations. This innovation is unique since no other in-chamber moisture sensor exists for round-module cotton harvesters, and offers an effective low-cost solution for moisture sensing on round-module cotton harvesters.

The third paper is a natural extension of the work in cotton to alfalfa hay and silage. A nominal lab characterization is performed in a similar fashion as first paper (with commercial impedance analyzer and planar probe) to determine the influence of density and MC. An important result shows the sensitivity to density changes is relatively small compared to moisture for typical ranges in alfalfa, and thus use of dielectric measurements for moisture prediction in alfalfa is justified. For this study over 1000 bales of alfalfa are weighed and sampled during 2015 and 2016 harvesting to obtain ground truth MC and density. Sources of variation are discussed and a moisture prediction model is trained and tested using multivariate regression on a random bifurcation of from field data for alfalfa hay ($< 30\%MC$); a range where the packaged sensor showed less issues with saturation. Some additional filtering and constraints are also discussed and applied to the dataset prior to evaluation. The accuracy is compared to a commercial microwave sensor and showed similar performance for hay under filtered conditions. While this alone stands as a useful invention since the cost of the capacitive-based sensor is much lower than competing microwave-based sensors, further value was found in the ability of the sensor to predict MC in silage alfalfa ($>30\%$ MC), which stands as the physical limit for the microwave technology tested. To and overcome the nonlinearity associated with saturation and gain additional accuracy with the packaged sensor above $30\%MC$, machine learning techniques were employed that included feature engineering and use of an Artificial Neural Network (ANN) to predict beyond the range for which the sensor response behaves nicely, which was up to $50\%MC$ in this work. Thus the sensor is very competitive by approaching the accuracy of more expensive technology while having a larger range.

1.1   REFERENCES

[1]   S. O. Nelson and S. Trabelsi, "A Century of Grain and Seed Moisture Sensing through Electrical Properties," in *ASABE*, Louisville, Kentucky, 2011.

[2]   *Dielectric Properties of Grain and Seed,* St. Joseph, Mich.: ASABE, 2012.

[3]   C. B. Behringer, "Performance Comparison of Moisture Sensor Technologies for Forage Crops," Madison, Wi, 2004.

[4]   W. Guo, J. Yang, X. Zhu, S. Wang and K. Guo, "Frequency, Moisture, Temperature, and Density-Dependent Dielectric Properties of Wheat Straw," *Transactions of the ASABE,* vol. 56(3), pp. 1069-1075, 2013.

[5]   C. E. Kirkwood, N. S. Kendrick and H. M. Brown, "Measurement of dielectric constant and dissipation factor of raw cottons," *Textile Research Journal,* p. 24:841, 1954.

[6]   A. Kraszewski and S. O. Nelson, "Composite Model of the Complex Permittivity of Cerial Grains," *J. agric. Engng. Res,* pp. 43,211-219, 1989.

[7]   D. K. Cheng, Field and Wave Electromagnetics, Pearson Education, 1989.

[8]   "Impedance Measurement Handbook, 4th Edition," Keysight Technologies, 2014.

[9]   "Basics of Measuring the Dielectric Properties of Materials," Keysight Technologies, 2015.

[10]   "E4990A Impedance Analyzer: Data Sheet," Keysight Technologies.

[11]   S. O. Nelson, "Dielectric properties of grain and seed in the 1 to 50-mc range," *Transactions of the ASAE,* pp. vol. 8, no.1, pp. 38-48, 1965.

[12]   D. Funk and Z. Gillay, "Unified Grain Moisture Algorithm," USDA, 2012.

[13]   D. B. Funk, "New Official Moisture Technology Implementation Briefing," in *NAEGA-GIPSA Regional Meeting*, Destrehan, LA, 2012.

[14]   "GAC 2500-UGMA Grain Analysis Computer," 2 2016. [Online]. Available: http://www.dickey-john.com/product/gac2500/.

[15]   S. O. Nelson, "Dielectric Property Measurements and Techniques," in *AIChE*, Austin, TX, 2004.

[16]   S. O. Nelson, Dielectric Properties of Agricultural Materials and Their Applications, elsevier, 2015.

[17]   W. L. Balls, "Dielectric properties of raw cotton," *Nature,* p. 158: 9–11., 1946.

[18]   L. Han Ming, L. Ma, C. Q. Ma and J. F. Hong , "Estimation of the moisture regain of cotton fiber using the dielectric spectrum," *Textile Research Journal,* p. Vol. 84(19) 2056–2064, 2014.

[19]   C. E. &. D. Team, "Turnout Percentages -- Factors Involved," CSD Extension, 2010.

[20]   B. Goodman and C. D. Monds, "A Farm Demonstrations Method for Estimating Cotton Yield in the Field for Use by Extension Agents and Specialists," *Journal of Extension,* vol. 41, no. 6, 2003.

[21]   S. C. P. Ltd., "Moisture Management a Must," Southern Cotton Pty Ltd., Whitton, NSW, 2013.

[22]   J. Quinn, R. Eveleigh, B. Ford, J. Millyard, A. North and J. Marshall, "Cotton Picking Moisture," Cotton Seed Distributors, Wee Waa, NSW, 2014.

[23]   "Cotton Pcker Management and Harvesting Efficiency," Clemson University Extension, 1996.

[24]   R. Fiore, "Circuit Designers' Notebook, Document #001-927, Rev. E," American Technical Ceramics, 2005.

[25]   "Tests for thermoplastic materials used in the electrical and electronic industries," DuPont.

[26]   "Moisture Restoration of Cotton," USDA-ARS, 2004.

[27]   R. K. Byler, M. G. Pelletier, K. D. Baker, S. E. Hughs, M. D. Buser, G. A. Holt and J. A. Carroll, "Cotton Bale Moisture Meter Comparison at Different Locations," *Applied Engineering in Agriculture,* vol. 25, no. 3, pp. 315-320, 2009.

[28]   M. H. Willcutt, E. M. Barnes, M. J. Buschermohle, J. D. Wanjura, G. W. Huitink and S. W. Searcy, "The Spindle-Type Cotton Harvester," Texas A&M Agrilife Research and Extension Center, Lubbuck, TX, 2010.

[29]   "Cotton Picker Management and Harvesting Efficiency," Clemson University Extension, 1996.

[30]   J. P. Just and M. J. Darr, "COMPOSITE MODEL OF THE COMPLEX PERMITTIVITY OF RAW COTTON," *ASABE,* 2016.

[31]   *Standard Test Method for Moisture in Cotton by Oven-Drying,* West Conshohocken, PA: ASTM International, 2012.

[32]   J. G. Montalvo Jr. and T. M. Hoven, "Review of Standard Test Methods for Moisture in Lint Cotton.," *The Journal of Cotton Science,* pp. 12:33-47, 2008.

[33]   R. K. Byler, "Comparison of Selected Bale Moisture Measurements in a Commercial Gin," in *2012 Beltwide Cotton Conferences*, Orlando, Florida, 2012.

[34]   R. K. Byler, "The Accuracy of Cotton Bale Moisture Sensors Used in a South Texas Commercial Gin with Lint Moisture Restoration," in *2014 Beltwide Cotton Conferences*, New Orleans, LA, 2014.

[35]   D. Cash and H. F. Bowman, "Alfalfa Hay Quality Testing," Montana State University Extension, Bozeman, MT, 1993.

[36]   W. K. Coblentz, "Spontaneous Heating," in *Idaho Alfalfa and Forage Conference Proceedings*, Burley, Idaho, 2013.

[37]   W. Coblentz and M. Bertram, "Effectiveness of Buffered Propionic-Acid Preservatives for Large Hay Packages," Midwestforage.org, 2011.

[38]   K. E. Webster, M. J. Darr, J. C. Askey and A. D. Sprangers, "Production Scale Signle-pass Corn Stover Large Square Baling Systems," in *2013 ASABE Annual International Meeting*, Kansas City, MO, 2013.

[39]   J. P. Just and M. J. Darr, "COMPOSITE MODEL OF THE COMPLEX PERMITTIVITY OF RAW COTTON," *ASABE,* 2017.

[40]   J. Just and M. Darr, "Real-Time Moisture Prediction on Round-Bale Cotton Harvesters," *ASABE,* 2017.

[41]   D. Funk, "Engineering Considerations for Dielectric On-Line Grain Moisture Measurement," in *ASABE*, Kansas City, MO, 2013.

[42]   J. O. Rawlings, S. G. Pantula and D. A. Dickey, Applied Regression Analysis: A Research Tool, Second Edition, Springer, 1998.

[43]   "Impedance Measurement Handbook, 5th Edition," Keysight Technologies, 2015.

[44]   G. E. Shewmaker and R. Thaemert, "Measuring Moisture In Hay," in *Proceedings, National Alfalfa Symposium*, San Diego, CA, 2004.

[45]   M. Rankin, "Understanding Corn Test Weight," UW Extension Team Grains, 2009.

[46]   J. T. Documentation, "Standard Least Squares Report and Options -- Row Diagnostics," JMP From SAS, [Online]. Available: http://www.jmp.com/support/help/Row_Diagnostics.shtml#184200. [Accessed 17 Jan 2017].

[47]   S. O. Nelson and S. Trabelsi, "Use of Grain and Seed Dielectric Properties for Moisture Measurement," in *Southeastcon. 2011 Proceedings of IEEE*, Nashville, TN, 2011.

[48]   D. M. Mitchell, J. Johnson and C. Wilde, "IMPACTS OF DECREASING COTTONSEED TO LINT RATIO ON COTTONSEED MARKETS," in *Beltwide Cotton Conference*, New Orleans, 2007.

[49]   D. Blackham, F. David and D. Engelder, "Dielectric Materials Measurements," in *RF & Microwave Measurements Symposium and Exhibition*, 1990.

[50]   D. Funk, B. Gillay, S. Burton and Z. Gillay, "Engineering Considerations for Dielectric Online Grain Moisture Measurement," in *2013 ASABE International Meeting*, 2013.

[51]   R. K. Byler, "Resistivity of Cotton Lint for Moisture Sensing," *Transactions of the ASABE,* vol. 41, no. 3, pp. 877-882, 1998.

[52]   M. Digman and K. Shinners, "Technology Background and Best Practices: Yield Mapping in Hay and Forage," in *Proceedings, Idaho Hay and Forage Conference*, Burley, ID, 2013.

[53]   R. Benning, S. Birrell and D. Geiger, "Development of a Multi-Frequency Dielectric Sensing System for Real-TIme Forage Moisture Measurement," in *2004 ASAE/CSAE Annual International Meeting*, Ottawa, Ontario, Canada, 2004.

[54]   J. Banta, "Bale Weight: How Important Is It?," AgriLife Communications.

CHAPTER 2:   COMPOSITE MODEL OF THE COMPLEX PERMITTIVITY OF RAW COTTON

John Just, Matt Darr

ABSTRACT

A novel planar capacitive-type dielectric probe is described and modeled using electrostatic finite element analysis, with intuition about the range and sensitivity obtained. A measurement setup is then described which uses a Keysight E4990A impedance analyzer along with the dielectric probe. Parasitic impedances of the measurement setup are investigated and the accuracy of the setup quantified. A statistical model was developed for predicting the real part of the permittivity (dielectric constant) and the loss tangent (dissipation factor) of raw cotton. The three primary factors included in the model are frequency (100kHz to 30MHz), moisture content (4% - 15% wet-basis), and density (160 kg/m³ to 288 kg/m³). Cotton turnout and variety are also investigated for significance. Data is divided into training and (performance) verification data sets. The model for the dielectric constant explained 91% of variation about the mean (i.e., R^2=91%) in the training data set. The fit increased to 94% when the slope and bias from the original model was adjusted for each crop variety. The loss tangent model explained 85% of variation about the mean. The loss tangent model R^2 increased to 89% with inclusion of variety. The findings showed cotton turnout was not an influential factor on the dielectric properties of raw cotton, while significant differences were found between varieties. When the model was tested on the verification data set, crop variety again played a large role, with significant reduction in residuals for both the dielectric constant and loss tangent after adjusting for variety.

2.1   INTRODUCTION

While much has been published in the agricultural scientific community regarding the dielectric properties of grains, very little has been published regarding the same for raw cotton. Grain crops are a very homogenous kernel-air mixture, but cotton fiber tends to be a much more challenging material to characterize in general due to the highly non-homogenous nature of the material. Raw cotton contains a diversity of components including lint fiber, seeds, air, pods, dirt, and other foreign material. Additionally, local clumping and dispersion of these materials is prevalent within any given sample and cotton has a very small bulk modulus compared to grain.

Pod   Leaf Pieces   Twig   Boll (lint covering a seed)

Figure 2.1: Typical sample of cotton from a round bale cotton stripper harvester with diverse mixture of constituents. The relative composition of samples used in this work was seen to change across machine types (picker/stripper), crop varieties, and geographic regions. The clumpy texture of the materials is due to the nature of how the bolls form with lint surrounding the seed.

Therefore, simplified assumptions used in grain crops such as a two-phase [binary] mixture of air and kernels [6] and the Landau & Lifshitz, Looyenga mixture equation cannot be extended to cotton. Development of a predictive model for dielectric properties in raw cotton is therefore presented as mostly a heuristic process in this work, using empirical data to guide the construction of an adequate analytical expression as opposed to the more desirable theoretical approach.

While it is understood that the non-homogeneous nature of raw cotton will result in a less precise relationship between the dielectric properties of raw cotton and the absolute moisture content of the sample there is still value in a predictive model of reasonable accuracy. For instance, such an expression can aid in quickly determining a rough moisture content in raw cotton, which in turn has many uses in industry.

2.2   LITERATURE REVIEW & BACKGROUND PHYSICS

Use of dielectric measurement devices to estimate other correlated physical properties or qualities of materials has been widely demonstrated in scientific literature [2] [4]. The dielectric properties are represented by the complex permittivity of the material, which is a steady-state quantity describing the way in which electric fields interact with the material. It

consists of an energy storage (or lossless) component typically referred to as the dielectric constant ϵ', and a dissipative (or lossy) component referred to as the loss factor ϵ''. The dielectric constant of a material is a function of several different polarization mechanisms of charges in the Material/Device Under Test (MUT/DUT) that neutralize charges at the source, thus facilitating larger charge storage than otherwise possible in air. The measured loss is more generally an [unknown] combination of dielectric loss (primarily via dielectric relaxation, which is analogous to magnetic hysteresis) and charge conductivity [7].

For a capacitive-type sensor, the dielectric probe is the point at which the electrical current/voltage transitions to an electric field that extends into the material. It provides the crucial function of interfacing directly with the MUT and allows the MUT to change the impedance characteristics of the circuit, thus offering a means by which the dielectric properties of the material can be measured. The geometry of an ideal dielectric probe is generally designed to maximize capacitance (more charge per volt applied leads to relatively higher signal-to-noise ratio) and consists of simple symmetry in the geometry such as a parallel plate electrode configuration. From basic physics the equation of the E-field for the theoretical case of a parallel plate capacitor is well known (Equation 2.1) and it is seen that this configuration is optimal due to the uniformity of the E-field inside the volume of such a cell (all E-field directed perpendicular to plates and no dependence on spatial coordinates).

Equation 2.1: Theoretical equation of E-field for a parallel plate capacitor.

$$E = \frac{\sigma}{\epsilon}, where\ \sigma = surface\ charge\ density, \epsilon = permittivity$$

Therefore, all parts of the MUT will have equal weighting in the measurement. Additionally, in practice, with the exception of relatively small amounts of fringing effects around the edges, virtually all charge on the plates is due to E-field passing through the MUT, and thus a very high measurement "efficiency" is achieved with this design. In the case of flowing materials such as grain that can easily conform to a container shape, there is considerable latitude in developing a near-ideal probe that still has a functional design (usable for many applications). A material like cotton has much more restrictions, and thus a compromise is sought that balances functional design with ideal geometry to maximize measurement reliability. The work presented in this paper is focused on a frequency range of 100 kHz – 30 MHz, which is classified as Low-Frequency (LF) through High-Frequency (HF) range per the International Telecommunication Union (ITU) designation. For this range, the standard model of a parallel RC circuit for measuring permittivity is typically used, and has been thoroughly documented in tech bulletins and various other research [8] [9]. The primary advantage of this model is in the simple conversion from impedance to permittivity. In particular, a simple derivation shows the ratio of admittance of the

MUT over the empty cell condition produces the complex permittivity shown in Equation 2.2. This model assumes that the open or empty cell condition is simply an air capacitor with no dissipative element. The terminology, simplified model, and related mathematics as found in the Keysight reference documentation [8] [10] can be assumed to be followed for results reported in this paper if not stated otherwise.

Equation 2.2: Complex permittivity derived from impedance of a capacitive cell. The following equation uses standard electrical symbol designations, with G = conductance, C = capacitance, Y = admittance, ϵ' = dielectric constant, ϵ'' = dielectric loss factor, "ω" = frequency, and j = imaginary number.

$$\frac{Y_{MUT}}{Y_{open}} = \frac{G_{MUT} + j\omega C_{MUT}\epsilon'}{j\omega C_{open}} = \frac{G_{MUT}}{j\omega C_{open}} + \epsilon' = \epsilon' - j\epsilon'', where\ \epsilon'' = \frac{G_{MUT}}{\omega C_{open}}$$

Relating dielectric properties to physical properties such as MC and bulk density, as well as source frequency, has been ongoing for over 50 years in the grain and seed industry [11] with much success. A subset of the research of Dr. Stuart Nelson on grain and seed has been adopted into ASAE standard D293.4 [2], which contains equations and graphs of the relationship between the dielectric properties and major factors such as moisture, density, and temperature. Dr. David Funk, while at USDA-GIPSA, developed the UGMA that is certified for official trade in determination of moisture content [12] [13]. This has in turn been commercialized by companies such as Dickey-John in the form of the GAC 2500 [14]. The UGMA has foundations in much of the work of Dr. Nelson and also leans strongly on the work of physicists Landau, Lifshitz, and Looyenga relating permittivity and bulk density [15]. The same or very similar methods used to measure dielectric properties in grain and seed have been extended to a wide variety of other applications and agricultural materials (e.g., wheat straw, soils, and meats) [4] [16].

There is a dearth of current information regarding applying these same methods to cotton, and especially raw cotton. A few published works exist on dielectric properties of cotton dated from the mid-19th century [5] [17]. However, these works have very limited scope, in one case focusing on anisotropy of the dielectric constant based on strand orientation [17] and in another case investigating dielectric constant and dissipation factor at one frequency. Both works are greatly in need of updating given advancements in technology, methods, and knowledge. Some more recent research exists in the textile industry for cotton fiber that has similar scope as the much earlier work [18], but the resulting dielectric measurements are specific only to cotton fiber and does not extend to raw cotton, which as mentioned is a highly non-homogenous and disoriented mixture. In ASAE standard D293.4 there is limited dielectric information available for acid-delinted cotton seeds, but it is unclear what research the information was drawn from since it could not be located in published literature and there are several references to unpublished work.

2.2.1 OBJECTIVES

The primary objective of the research described in this paper is to develop a statistical model relating the dielectric properties of raw cotton to various factors with known or suspected influence, such as moisture content, source electric field frequency, density, and cotton turnout to fill the gap of knowledge/information in this area. Specifically, the dielectric constant and loss tangent are intended to be predicted over a frequency range of 100kHz to 30MHz, moisture contents of 4% - 15% w.b., and a density range of 160 kg/m^3 [10 lbs/cu-ft] to 288 kg/m^3 [18 lbs-cu-ft]. Cotton turnout is also examined for significance with respect to influence on the permittivity. A custom test and measurement stand built to support the primary objective is also thoroughly detailed herein. The most defining part of any dielectric measurement setup is the material probe, and therefore a unique planar-electrode dielectric probe designed specifically for measuring permittivity in baled crops is modeled and tested for accuracy using standard industrial materials with known dielectric properties prior to use with cotton.

2.3 MATERIALS AND METHODS
2.3.1 IMPEDANCE ANALYZER

A Keysight E4990A Impedance Analyzer [10] was selected to measure the raw cotton impedance and thus the permittivity. This instrument was determined to be the best available for the projected impedance and frequency range under consideration, with some key specifications shown in the Table 2.1.

Table 2.1: Summary of Key Specifications for E4990A taken from [10]

Function/Feature	Values/Range
Operating Frequency	20Hz – 120 MHz
Impedance Measurement Parameters	|Z|, |Y|, θ, R, X, G, B, L, C, D
Basic Impedance Accuracy	$\pm$ 0.08% ($\pm$0.045 typical)
Sweep Type (Frequency)	Linear or Log
Sweep resolution	2 to 1601 measurement points
Measurement Type	4-terminal pair with cable compensation
Voltage/Current Level	5mV_{rms} to 1 V_{rms} /200 uA_{rms} to 20 mA_{rms}, 1mV/20uA resolution
Data Analysis	Equivalent Circuits Available

2.3.2 FIXTURE/PROBE AND MEASUREMENT CIRCUIT

2.3.2.1 Planar Probe

Since cotton is a baled crop, a probe design that can be easily used to obtain a measurement a bale is desirable. In the hay and forage industry there are many products available with pronged-leads that are inserted into bales, but these are tiresome to use by hand if done repeatedly and could not be extended to online use on a harvester. Instead the design should facilitate the ability to drag the electrodes along the surface of the bale to obtain a measurement, since this would be easy to use by hand and could also be mounted in a bale-chamber of a cotton harvester to interface with a bale and obtain online

measurements. The particular design which this research utilizes is detailed below, including figures detailing both the mechanical design and electrical operation.

The planar design is advantageous in that it has no moving parts (such as a sampler) and simply needs to be in contact with the material. In most baling applications from cotton to hay and forage crops this could be mounted flush in a bale chamber and presumably work just fine with no other maintenance. In terms of electrical operation, the center plate acts as a source of E-field and the two surrounding/outer plates as return paths. The enclosure is a direct return back to the source and bypasses the measurement circuit. Since the case extends up between the electrode plates to the measurement plane (minimizing/shielding any interaction between the source and sink electrodes up to the measurement plane) almost all charge present on the outer plates is related to the portion of the electric field (E-field) that has passed through the MUT/DUT. A virtual ground created by an operational amplifier acts as the key element to facilitate measurement with minimal interference.
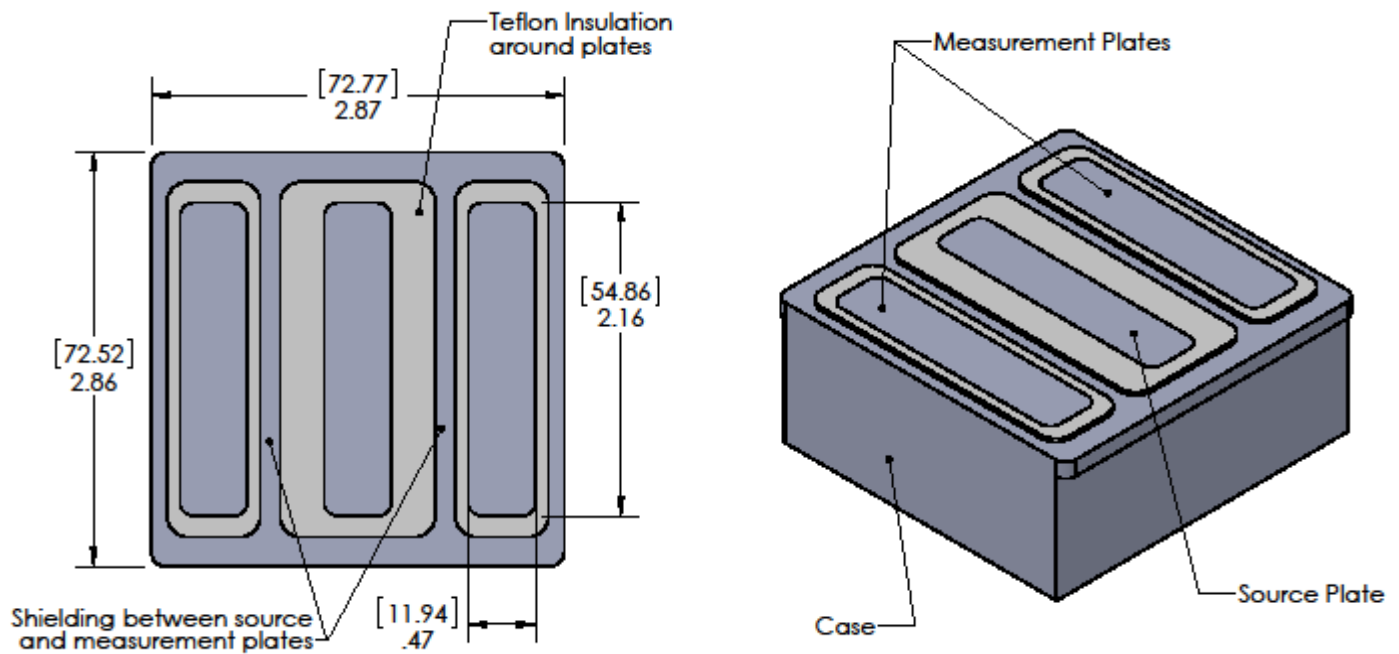
Figure 2.2: Dielectric Probe with dimensions in inches [mm]. A planar design is used due to practicality of interface with the material. This design lends itself to convenient measurements of a cotton bale (round or square) as well. Note that the case is direct return to voltage source that bypasses the measurement circuit. Thus any flux linkage between plates and case is not measured. Shielding extends between plates up to measurement plane to limit any interaction between plates that is not projected through MUT
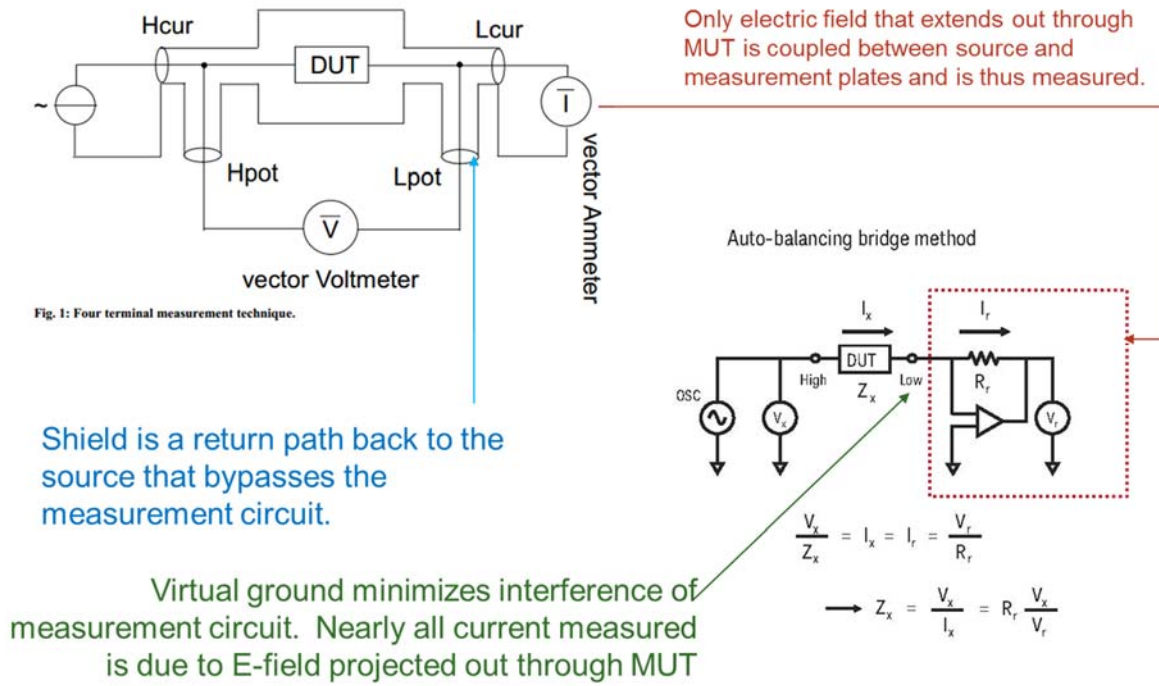
Figure 2.3: Basic diagram of the impedance analyzer and probe measurement circuit. Diagrams referenced from Keysight literature [8]. Hcur and Hpot are the voltage source and high-side potential measurement terminals, respectively. Lcur and Lpot are the current measurement and low-side potential measurement terminals, respectively. DUT is the same as MUT.

2.3.3   TEST STAND APARATUS

In order to measure cotton dielectric properties in a consistent manner at different densities, a test stand was built that

supported manipulating the material to desired bulk densities without interfering with the measurements of the material.

The main components that comprised the stand consisted of the probe bolted to a larger steel mount that also supported a

large, open-ended cylinder. The cylinder could be filled with cotton and then subsequently the cotton compressed to various

densities by a pneumatically powered piston attached to a wooden plunger. The cables from the E4990A connected to the

fixture underneath the mount. The setup was positioned on a table such that the impedance analyzer was within reach of

1m long cables, which is one of the two lengths that the E4990A had built in compensation functions to accommodate. One

meter is also the longest cables that were tested and found to have consistent and reliable impedance readings over the

desired frequency range prior to beginning this work.

By electrostatic FEA it was found that approximately 2.5 cm perpendicular to the sensor face was the maximum distance

for which any material can exert influence on the permittivity measurements. This was also confirmed by holding several

different materials above the sensor and bringing them closer until the permittivity values began to change. Additionally,

some influence was encountered around the edges of the sensor when testing, but this influence dropped off very quickly as

distance from the electrodes along the plane of the sensor face increased. Since the sensor face is approximately 7.5cm^2, it was decided that packing a cylinder of 19cm in diameter with cotton would mitigate any material besides the MUT in the cylinder from having influence on the permittivity measurements around the edge. Functionally, it was determined that a conservative approach would be to compress the cotton to no closer than 8 cm above the sensor face.
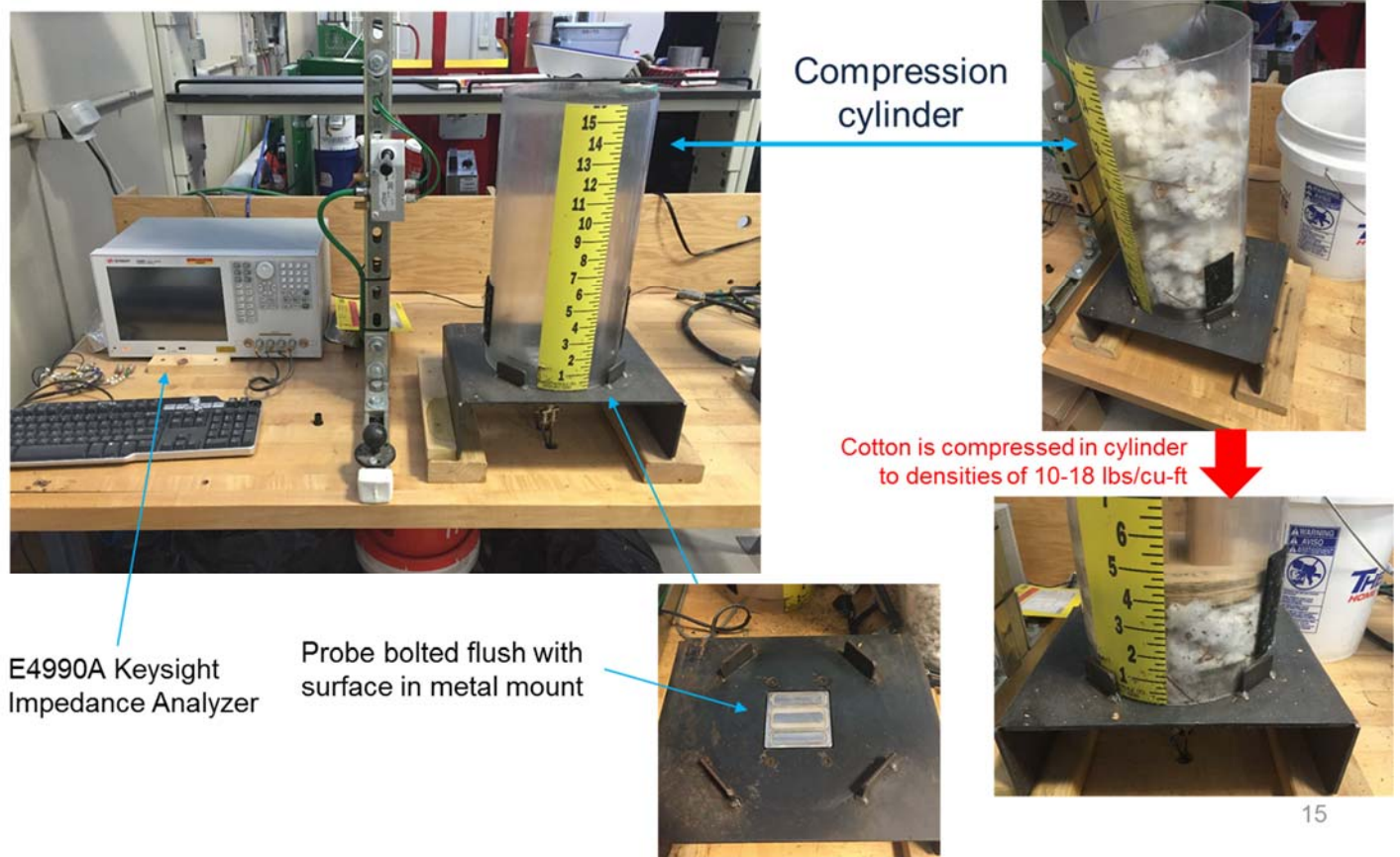

Figure 2.4: Test stand used to take dielectric measurements of cotton. Adhesive measurement tape was used to measure compression height and achieve target densities based on the wet weight of the sample being measured. The amount of cotton used was enough that the wooden compression cylinder is kept from entering the region of influence that the MUT has on the impedance of the circuit.

2.3.4 DESCRIPTION OF COTTON SAMPLE PROPERTIES USED IN DIELECTRIC MEASUREMENTS

Cotton samples evaluated during the completion of this work were collected from a broad range of field conditions in order to capture the diversity of raw cotton (Table 2.2). The variety of cotton, when known, was provided by the grower. Both picker and stripper cotton were included in the study to capture differences in cleaning and foreign matter ratios in the raw cotton. All samples were collected from the United States and included cotton from four regions (CA, TX, AK, GA). Note that the "unknown" variety from GA in Table 2.2 (not Dublin, GA) consists of 29 unique samples that amounted to about 1/3 of the measurements in the dataset, and are samples taken from bales during a couple weeks of harvesting. These were reserved as a test set of data to gauge the performance of the predictive model.

Table 2.2: Cotton Samples Included in Study. Note that turnout was reported as an average for the field from which the sample was taken. **29 individual samples from field measured "as is" (without rehydrating)

Crop Variety	Region	Machine Type	Avg Field Turnout
Unknown	Dublin, GA	Picker	
Stoneville 4946	Lake City, AR	Picker	39.6%
Stoneville 0912	Senath, MO	Picker	39.3%
Phytogen 499	Blythe, CA	Picker	39.5%
DP 1359	Blythe, CA	Picker	37.7%
DP 0949	Blythe, CA	Picker	37.4%
*Unknown**	GA	Picker	
DP 1133	Ennis, TX	Stripper	31.4%
Fibermax 2484	Floydada, TX	Stripper	33.5%
Phytogen 811 (Pima)	Uvalde, TX	Picker	32.9%
Phytogen 499	Newellton, LA	Picker	39%

2.3.4.1 Cotton Turnout

Cotton turnout was obtained for a subset of the data to analyze the effect on dielectric properties (total of 50 samples). This was found by separating each sample with a custom mini-gin after permittivity measurements were complete, and then dividing the weight of lint by the total sample weight. The two primary constituents of seed and lint post-ginning are shown below. Trash such as pods, sticks, leaves, and dirt also comes out during ginning, but the quantity is small (generally found to be <10% of raw sample weight in this work and other sources investigated [19]) in comparison to seed and lint. The weight is taken with the samples at ambient conditions and equilibrium moisture (generally 7-8% MC).

Figure 2.5: 287g of seed (left) and 241g of lint (right) after ginning a sample. The large disparity in bulk density between these two constituents makes cotton turnout a variable of great interest when examining and quantifying the dielectric properties of raw cotton.

The distribution of turnouts found in the samples tested is shown below. Note that while the turnout as found using the mini-gin has nearly the same range as obtained by the mills for average field turnout, it is shifted about 10% higher. Other literature discussing turnout noted values more similar to what was measured from the samples in this research (also noting roughly 10% trash content by weight) [20] [19].
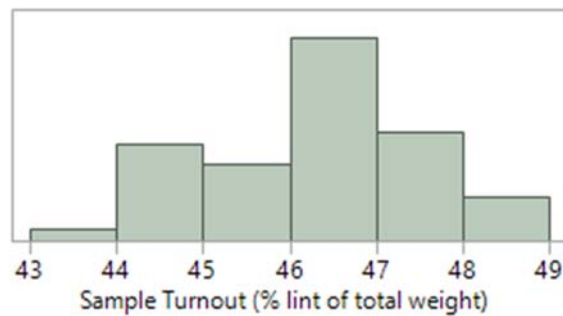
Figure 2.6: Distribution of [relative] cotton turnout from the sample dataset described in Table 2.2

2.3.4.2   Moisture Content

The varieties of cotton listed above were included over target ranges of moisture content that spanned 4% to 15% wet-basis (w.b.). This was determined to represent the typical range of cotton moisture found in raw cotton bales during industrial harvesting of cotton [21]. Beyond 15% moisture cotton is difficult to harvest and risks quality deterioration even if ginned immediately after picking [22]. In the field, the moisture in cotton naturally follows a cyclic process each day from dew coming on in the evenings and drying off in the mornings/early afternoon [23]. Even though dew will form as droplets, by the time it has passed through a harvester and rolled into a bale the dew has been absorbed into the fibers and seed. In order

to prep cotton samples to the desired moisture content, a procedure was developed with intentions to closely emulate the process by which harvested cotton in bale form takes on moisture. Upon receipt of a large raw cotton sample the initial baseline moisture content of the sample was determined using gravimetric methods following ASTM D2495-07, which requires drying of a cotton samples at 105C for 24 hours in a forced-air oven. After determining the baseline moisture content, the larger samples were subdivided into smaller samples and rehydrated to specific moisture levels. The rehydration method involved misting water on the raw cotton samples in accordance with the quantity of water that was calculated to increase the MC% by a target amount. The samples were then left in closed 5-gallon buckets for 24 hours, flipping the buckets several times to ensure no settling of water and good mixing. These samples had a mean sample size of $\mathbb{N}(\mu = 635, \sigma = 91)$ grams w.b., since this quantity of material was found to adequately fill the region around the probe that has influence on circuit impedance measurements. The rehydrated samples were then run across the test stand to obtain dielectric measurements, and subsequently oven-dried per aforementioned protocol to obtain ground truth MC%. It was determined by experimentation that drying the samples longer than 24hrs did not produce any additional mass loss.

2.3.4.3   Density

Density refers to the physical wet density of the raw cotton. The bulk modulus of raw cotton is very small compared to grain, and can change dramatically with very little force. Therefore, the density of cotton is not considered as an analog to the more static property of test weight in grain. The mean targeted density range for this testing was that found in round cotton modules made by machines such as the John Deere Cotton Harvester Model 7760. For a round module 2.3 m [7.5 ft] in diameter, 2.4 m [8 ft] wide and weighing 2268 kg [5000 lbs], this amounts to a density of approximately 224 kg/m3 [14 lbs/cu-ft] at harvest. The density in this work was controlled to be in the range of 160 kg/m3 – 288 kg/m3 [10 – 18 lbs/cu-ft].

2.3.4.4   Temperature

Temperature is classically included in dielectric property models, but it is especially difficult to simulate and measure in a disperse fibrous material like cotton, which is also an insulator and does not transfer heat very well. A method used in research on the dielectric properties of wheat straw was considered, which measured samples with the test stand apparatus and sample in a constant temperature oven to achieve target temperatures [4]. In practice the temperature variable is difficult to control while also limiting moisture loss that occurs with increasing temperature, and additionally makes it difficult to achieve various densities and positions using the same sample without affecting temperature and moisture content. Including temperature would also greatly reduce the coverage of moisture content and density for the same effort. Consequently, all measurements were performed with the samples at room temperature of approximately 25℃.

2.3.4.5   Frequency

The effect of frequency on permittivity measurements is well-documented as a nonlinear phenomenon [9]. In addition to the theoretical effects, the hardware, cables, and measurement device impose natural limitations on the frequency range and accuracy. A frequency range of 100 kHz to 30 MHz was determined to be within the capabilities of the impedance analyzer, cables, and probe combination used for this research and still attain an accuracy of the impedance measurements within 1%. Over this range 111 discrete samples were taken on a logarithmic sampling interval.

2.3.5   RAW COTTON DIELECTRIC MEASUREMENT PROCEDURE

The process of evaluating samples on the test stand involved several steps to ensure quality and accuracy of results. Prior to measurement, the samples were rehydrated per described in section 2.3.4.2. The wet weight of any sample was taken before and after permittivity measurements to ensure no substantial moisture loss occurred during permittivity measurements that could affect results. The scale was accurate to smaller than 1g, and on 600g this resulted in negligible measurement error. This weight was also used to determine the compression heights needed to reach target densities. For each sample, four densities were targeted, and at each density the sample was flipped twice, divided, and flipped twice more to thoroughly measure each part of the sample. This provides a hedge against the event where the added moisture was not uniformly distributed throughout the sample.
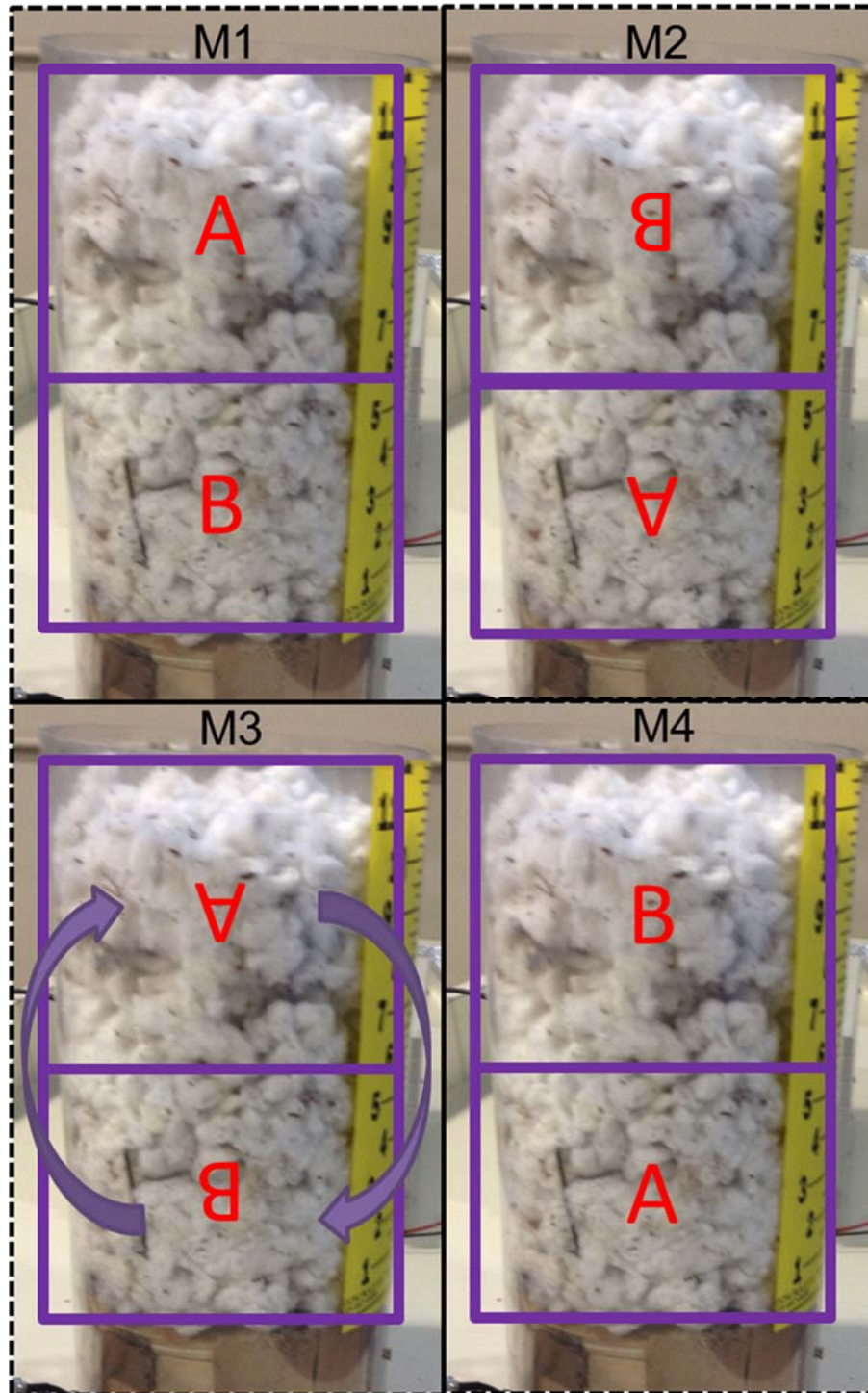
Figure 2.7: Images depicting dividing and flipping the sample. The top half and bottom half positions are swapped. In the case of a flip, the entire sample is simply rotated such that the top becomes the bottom, but not divided apart.

2.3.6   SUMMARY OF EXPERIMENTAL DESIGN FOR TRAINING DATA

The target factors and levels are shown in Table 2.3.

Table 2.3: Note, 5%MC was taken when available naturally (i.e., without inducing by oven-drying).

Factor	*Levels/Quantity*
Bulk Sample	10
Variety	8
Target Density	4 densities per sample: 256 [16], 240 [14.9], 223 [13.9], 197 [12.3] kg/m^3 [lbs/cu-ft]
Positions	4 per density
Moisture Content	5,7,9,11,12,13,14,16
Frequency	111 measurements per sample, 100kHz – 30MHz range sweep at uniform intervals on a log10 scale.

A total of (10 samples) * (7 MC levels) * (4 densities) * (4 positions) results in 1120 unique measurements to train a model.

2.3.6.1   Predictive Model Verification Data Set

A total of (29 module samples) * (4 positions) * (4 densities) = 464 unique measurements, or slightly less than a third of

total are reserved as a test set for the predictive model. These were taken as smaller individual samples from 29 round

modules. The exact crop variety was unknown for the verification samples.

2.4   RESULTS
2.4.1   GENERAL ELECTRICAL CHARACTERISTICS OF FIXTURE

The $\frac{Measured\ Charge}{Supplied\ Charge}$ is herein referred to as the efficiency of a probe design, and is one simple metric to judge the efficacy

of the design in measuring dielectric properties of materials. A high efficiency in this case is desirable primarily to maximize

the signal to noise ratio, and bears some relation to how well the E-field can be made to penetrate the MUT. Solidworks

was used to model the probe design and subsequently imported into Ansys Maxwell to perform electrostatic FEA and obtain

the charge density on the plates in open air. A source voltage of 1V DC was applied in the simulation to match the maximum

output used and tested with the E4990A Impedance analyzer. A total charge of 1.71 pC is obtained on the center (source)

electrode, and correspondingly -0.17 pC total on the outer electrodes. The findings show that the charge distributed between

the two outer plates is smaller by an order of magnitude than supplied by the source and present on the center electrode. By

far the majority of the supplied charge bypasses the measurement circuit, and thus one of the drawbacks of a more

"convenient" (for application) probe design required for real-time measurement of a fibrous crop.
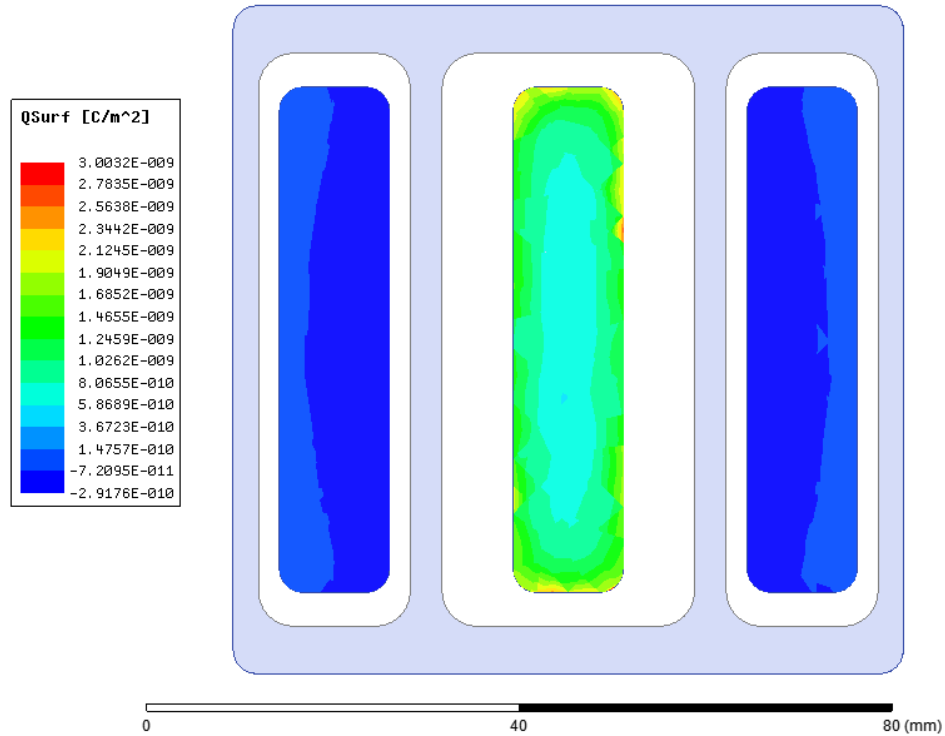
Figure 2.8: The surface charge density is obtained from electrostatic FEA and shaded contours shown overlaid on the probe electrodes.

Using the same FEA model to find capacitance of the probe obtained a value of 0.085pF between each outer electrode and the center electrode, for a total of 0.17pF. This value was compared to a 20 Hz measurement obtained from the E4990A (lowest frequency available) using the probe in open air and found to be exactly the same, thus providing validity of the FEA results. The open-air measurement of capacitance using the E4990a connected to the probe, and sweeping over a frequency range of 1kHz to 30MHz is included below.
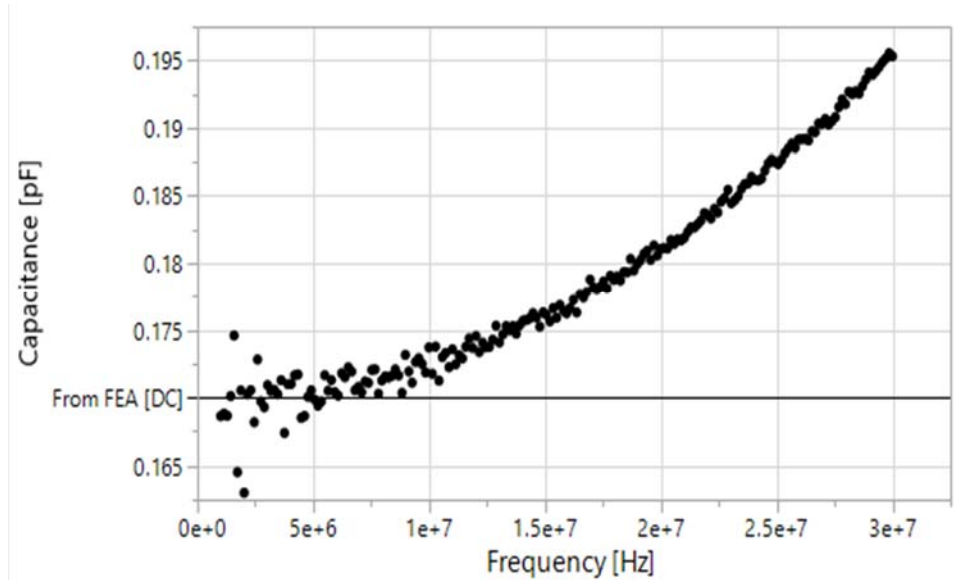
Figure 2.9: Open air capacitance measured by E4990a over a frequency range of 1kHz to 30MHz, with the range divided into 201 points at equal log-based frequency intervals. A reference line is included for the DC open-cell capacitance calculated by FEA.

Note in Figure 2.9, the measured capacitance can be seen to increase beyond nominal in open-air as frequency increases, while from an ideal stance capacitance should not be affected by frequency. Though it might be tempting to blame parasitic capacitance, an open-circuit test confirmed that the impedance is too high to accurately measure by the E4990A when no flux is linked from the center plate to the outer plates, and therefore provides evidence to reject this hypothesis. A better explanation attributes this to a parasitic series inductance [24], as described by the equation

$C_E = \frac{C_0}{[1-\omega^2 \, L_S C_0]}$ where

C_E = Effective/Measured Capacitance (F)

C_0 = Nominal Capacitance (0.17 pF for this probe)

ω = Source Frequency (Hz)

L_S = Parasitic inductance (H)

When this equation is used to solve for the parasitic inductance using the nominal and the measured capacitances and subsequently plotted against frequency, a line of fit drawn through the median (quantile regression) finds that the value is essentially constant and converges to 23uH.an inductance, as expected by the proposed phenomenon (left plot of Figure 2.10). Finally, this parasitic inductance value is in turn used in the formulation to predict effective capacitance and overlaid on the measured values in the right plot of Figure 2.10. The prediction explains 98% of the variation (R^2 = 98%), thus strongly supporting that the proposed phenomenon is the cause.
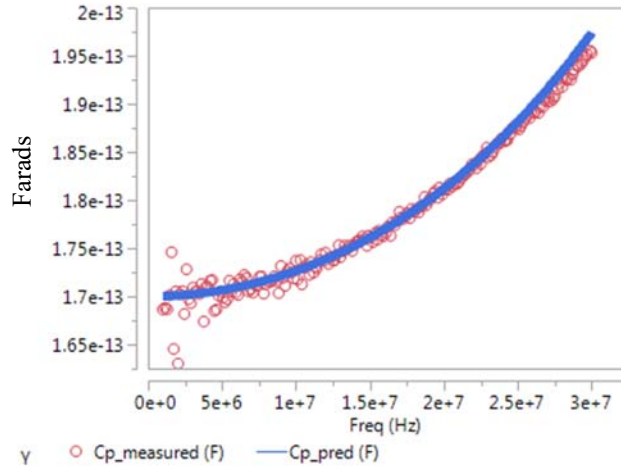
Figure 2.10: Using a value of 23uH for parasitic series inductance Ls in the formulation for effective capacitance, the prediction overlaid on measured values over the measurement frequency range very closely matches ($R^2 = 98\%$).

When the same investigation was done on a 12.7"D x 15.2"L cylindrical Teflon block, an inductance of less than half that of open air (~10uH) was found. Teflon was recommended as a test material by Keysight engineers due to known stable dielectric properties. Ultimately this parasitic inductance is typical of capacitors [24] and in this application is absorbed in the MUT impedance, which as mentioned earlier is assumed as the ubiquitous parallel RC circuit model to directly calculate complex permittivity. It was not possible to identify the parasitic series inductance for the materials tested other than pure plastics and air, and consequently it is an example of choosing convenience over fidelity of the circuit model.

2.4.2   DIELECTRIC PROBE REGION OF INFLUENCE

Since the geometry of the planar-type probe is complex and will not have the optimal uniform E-field throughout the measurement space that a parallel plate capacitor has, some intuition of how the MUT will be volumetrically weighted is desirable. As part of the electrostatic FEA modeling, the spatial E-field found and plotted in Figure 2.11. The spatial vector field plot of the E-field provides a visual of the influence throughout the measurement space. When a single line perpendicular to the electrode plane and located at the geometric center of the fixture is considered, a plot of the E-field magnitude against distance is obtained. In both cases the results indicate an exponential decrease in E-field (and consequently a corresponding decrease in influence on dielectric measurements) with distance. It is important to reiterate though that only a fraction of this E-field actually couples with the measurement circuit and therefore "counts" (as was also noted with the order of magnitude difference between charge on the center plate compared to outer plates).
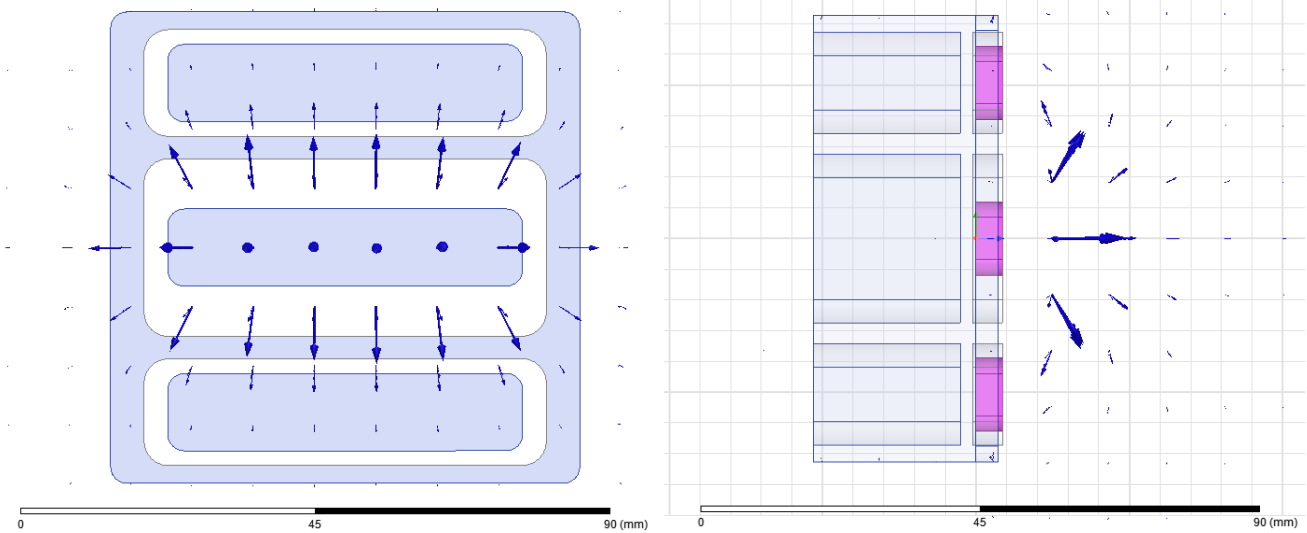
Figure 2.11: The E-Field can be seen to decrease rapidly when moving away from the probe in a direction perpendicular to the plates, such that at only a couple cm from the plates the MUT will have negligible effect on the measurement.
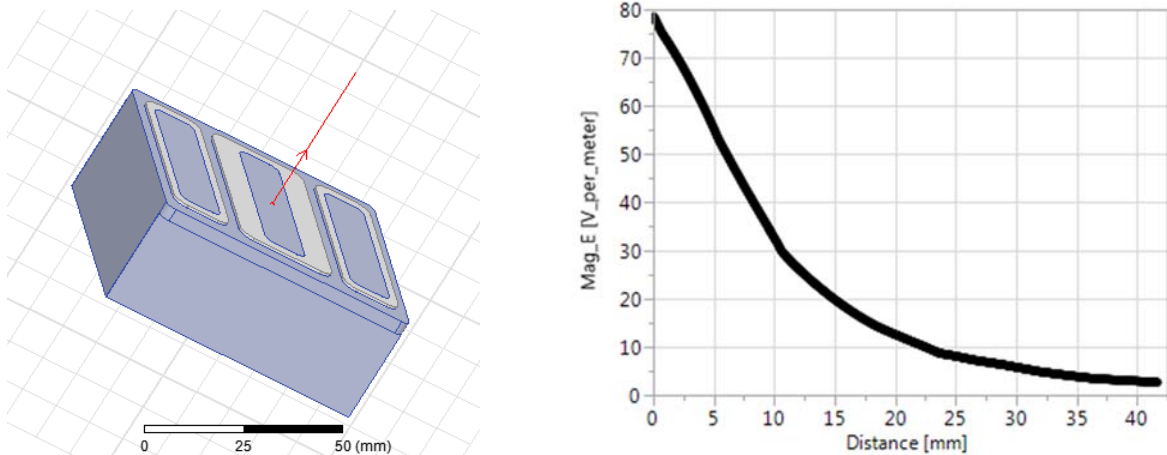
Figure 2.12: The E-field along an axis perpendicular and center to the measurement plane (shown left) is plotted against distance (right). The nonlinear decay quantifies how quickly the E-field (and likewise general influence of material) reduces with increasing distance. Only a fraction of this E-field actually couples with the measurement circuit.

FEA using Ansys Maxwell also enabled the total range of the probe and magnitude of influence on capacitive measurements at increasing distances to be quantified. In order to do so, 2.54mm [0.1 inch] layers of PTFE were successively stacked on the sensor plane per the configuration shown in Figure 2.13, and the capacitance then solved for. PTFE was used since it has a published permittivity value of 2.1, which closely matches the mid-range of raw cotton. The same simulations were also run when excluding the first layer and compared to gain insight into the effect a small gap can have on the measured values. A plot showing capacitance [pF] for each case (gap & no gap) are shown in Figure 2.14. In the case of a small gap the final capacitance value is 18% less than the case with no gap $\left(\text{i.e. } C_{gap} = 0.82 * C_{no\_gap}\right)$. This shows that even a small gap can cause a dramatic decrease in capacitance due to the nonlinear decrease in E-field

with perpendicular distance from the center. In terms of the individual influence of each layer though, the effect that adding another layer of PTFE at any point has on calculated capacitance (as a ratio of the total capacitance of all layers) indicates the total capacitance is a superposition of the capacitance of each individual layer. Thus the relative influence that any particular layer has on the total measurement appears unaffected by the presence (or lack) of other layers. Note that with this geometry, 90% of the capacitance is determined by material within 12.7mm [0.5 inch] of the face of the sensor, and the other 10% within the next 12.7mm [0.5 inches]. Thus the probe has a sensing range of less than 25.4 mm (1 inches).
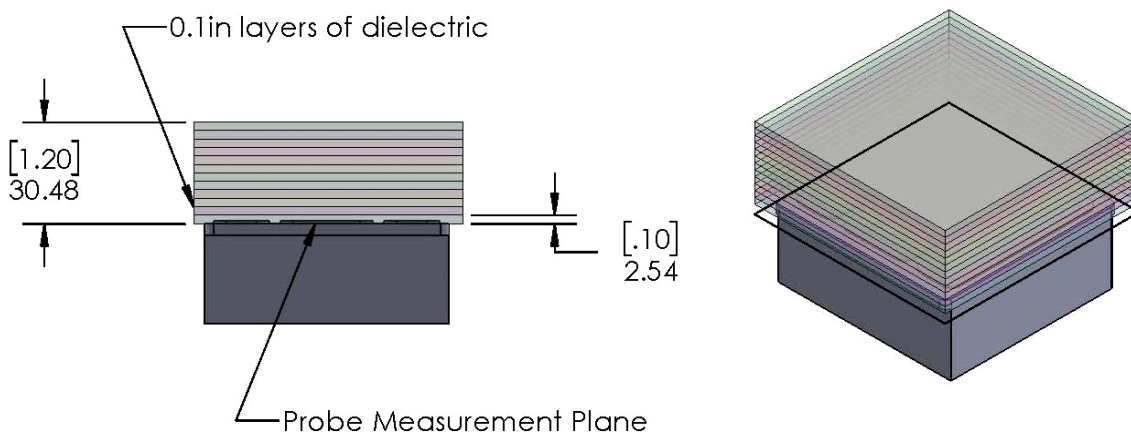
Figure 2.13: 2.54mm [0.1 inch] layers of PTFE are stacked on the probe measurement plane and simulations run successively to examine the range of influence (i.e. the volume around probe which has non-negligible effect on capacitance). The simulation is subsequently repeated while omitting the 2.54mm [0.1 inch] layer of PTFE closest to the sensor (i.e., with a 2.54mm [0.1 inch] air gap between sensor face and PTFE).
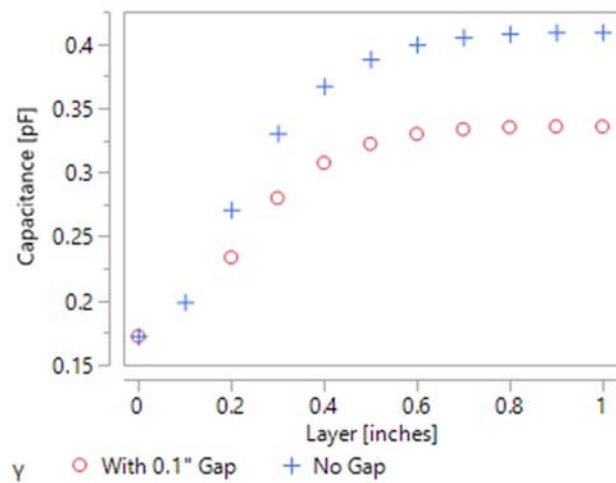
Figure 2.14: Capacitance found from FEA as a function of the thickness of PTFE layer being measured. Both with and without a 2.54mm [0.1 inch] gap are overlaid. A gap results in an 18% reduction in the measured capacitance for the same layer thickness. The range of the sensor was unchanged whether an air-gap exists or not.

2.4.3   FIXTURE PARASITIC IMPEDANCE

As noted in the Keysight literature [9] [8], the calculation of permittivity is based on impedance measurements of the MUT, and any impedances between the point of measurement and the MUT (such as the fixture itself) could potentially confound the material measurement by introducing what is termed as parasitic impedances. While the impedance and phase shift of the one-meter cables connecting the fixture to the impedance analyzer were compensated for using the E4990A built-in compensation functions, the impedance of the fixture itself was simply evaluated to determine if a corrective action was necessary to mitigate fixture parasitics. In order to assess the parasitic impedance of the fixture, open and short circuit tests were performed in accordance with the standard practices as described in Keysight literature. If the source plate is electromagnetically shielded from the ground electrodes, any remaining impedance can be attributed to coupling or other circuit paths not associated with the MUT. Physically shorting the plates using a conductor exposes series impedance that otherwise artificially inflates the apparent impedance of the MUT. The open/short impedances are then compared to the approximate impedance range for raw cotton. Measured impedances from the open/short circuit test are plotted in Figure 2.15, and the mean of the upper and lower 2.5% quantile values for cotton are shown in Figure 2.16.
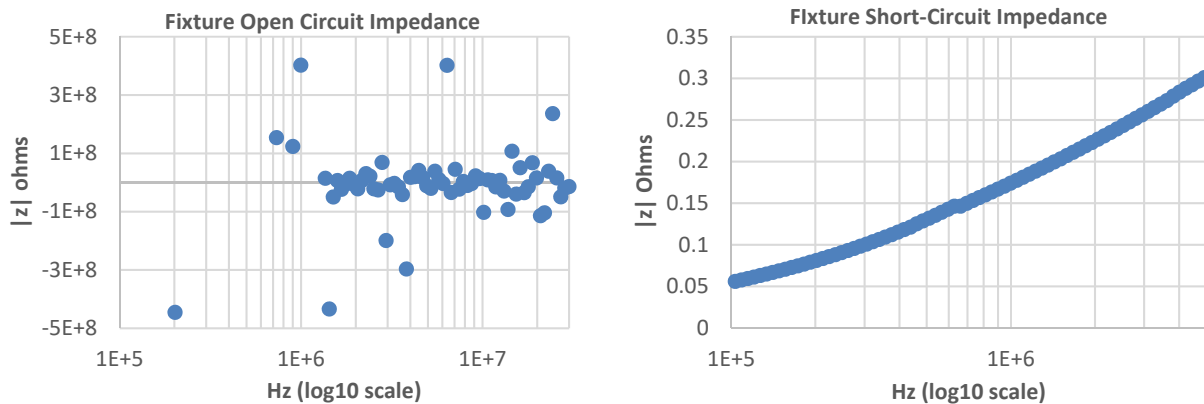
Figure 2.15: Open and short circuit tests on the fixture reveal the fixture parasitic impedances. (Left) Shorting the electric field from the source plate to ground is the open-circuit test, which effectively isolates the measurement plates on the probe unless any leakage occurs. In this case there is virtually none as can be seen by extremely high impedances. (Right) Shorting the source and measurement plates using an aluminum bar accomplishes the short circuit test and determines if any series impedance is on the order of the MUT.
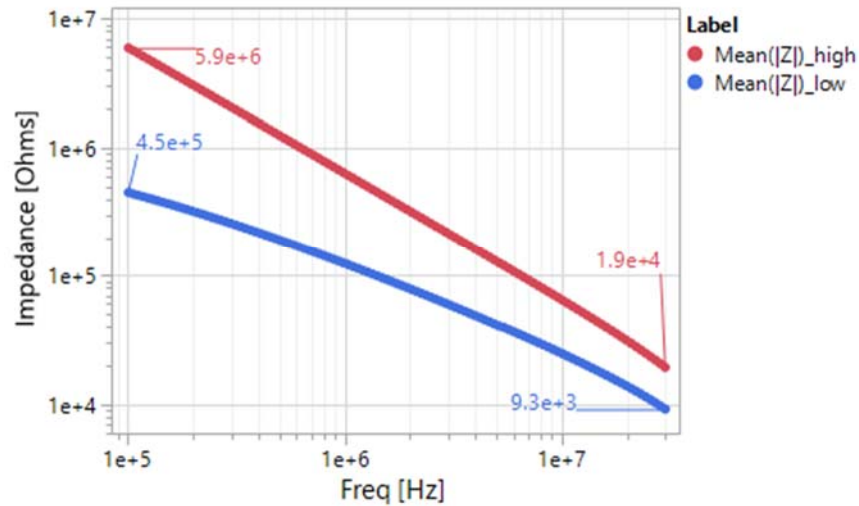
Figure 2.16: Impedance (in Ohms) VS frequency is plotted for the mean of the highest and lowest 2.5% samples measured. This is compared to open and short circuit impedance, and also used to determine E4990A measurement accuracy.

The open-circuit impedance values are beyond the range of the sensor at all frequencies, which is why the left plot in Figure 2.15 shows extremely large variations (including negative impedance) throughout the frequency range displayed. Note that the open-circuit measurements at frequencies below 1-Mhz produced much higher magnitude impedances, and so only the smaller range of impedances is shown for clarity. As a conservative approach the open circuit impedance is taken to be the upper limit of impedance range specification of the E4990a. The upper 2.5% quantile value of cotton is well within the E4990A specified measurement capabilities, and if the conservative estimate of the open-circuit value is used then the impedance of cotton is still well over an order of magnitude smaller than any parallel parasitic impedance. Therefore, there is no concern of any parasitic impedance in parallel with the MUT. Likewise, the lower 2.5% quantile recorded at any frequency for cotton was greater than 9.3 kOhms, which is well over four orders of magnitude larger than the series impedance found from the fixture short-circuit data. Thus the series impedance is far too small to have any appreciable effect on the impedance measurements of the MUT.

The data shown in Figure 2.16 was also overlaid on the accuracy spec of the E4990A below to the impedance of raw cotton would fall within the 1% or less error range. In Figure 2.17 the cotton from this work had impedances anywhere vertically between the red dotted lines, and is generally well within 1% for the majority of the material as shown in Figure 2.16.
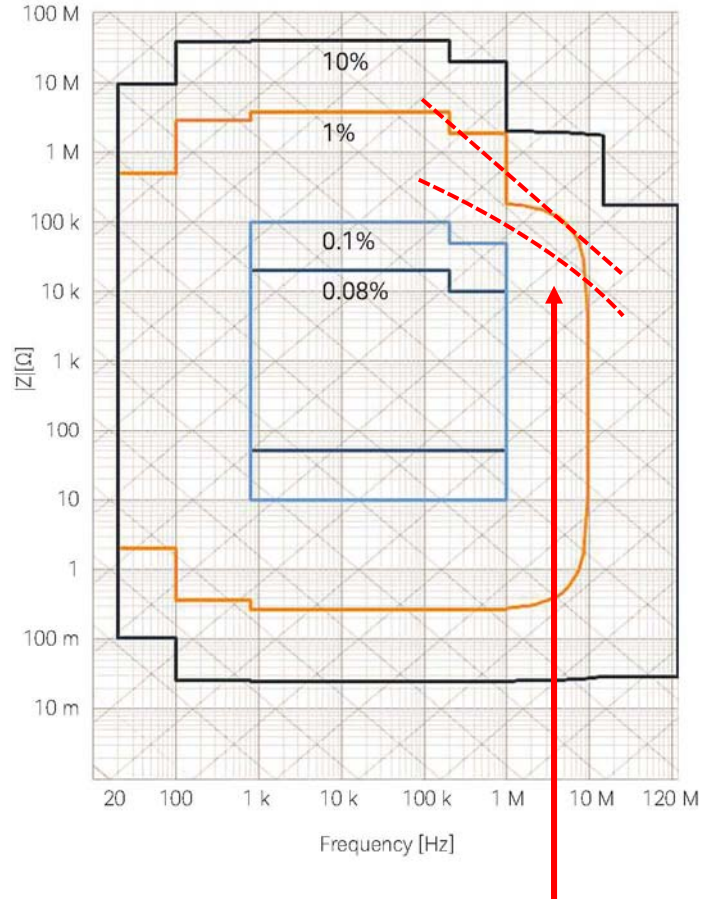
Figure 2.17: More than 95% of the cotton measurements for the range of variables tested falls vertically between the bands overlaid on the E4990A accuracy spec from Keysight. Therefore, in the range of impedances seen for cotton, the impedance values reported by the analyzer have <1% error.

2.4.4   STANDARD MATERIAL TESTS USING MEASUREMENT FIXTURE

The measurement setup (Impedance analyzer, one-meter cables, and test fixture) accuracy was tested with Acetal and

PTFE, materials with known and stable dielectric properties. The results shown in Figure 2.18 and Figure 2.19 for the

dissipation factor $\left(\text{a. k. a. the loss tangent}, \tan\_d = \frac{\epsilon''}{\epsilon'}\right)$ and the real component of the relative permittivity (dielectric

constant) were compared to published values in DuPont literature and documentation from various other plastics

manufacturers [25]. Generally, values at 1-MHz are most widely available. At this frequency values of the dielectric

constant between 3.3 - 3.9 were found in literature for Acetal, and 2.05 – 2.1 for PTFE. Therefore, with measured values of

3.78 for Acetal and 2.12 for PTFE at 1-MHz, the setup used for this research was deemed to be accurate and acceptable for

this research.
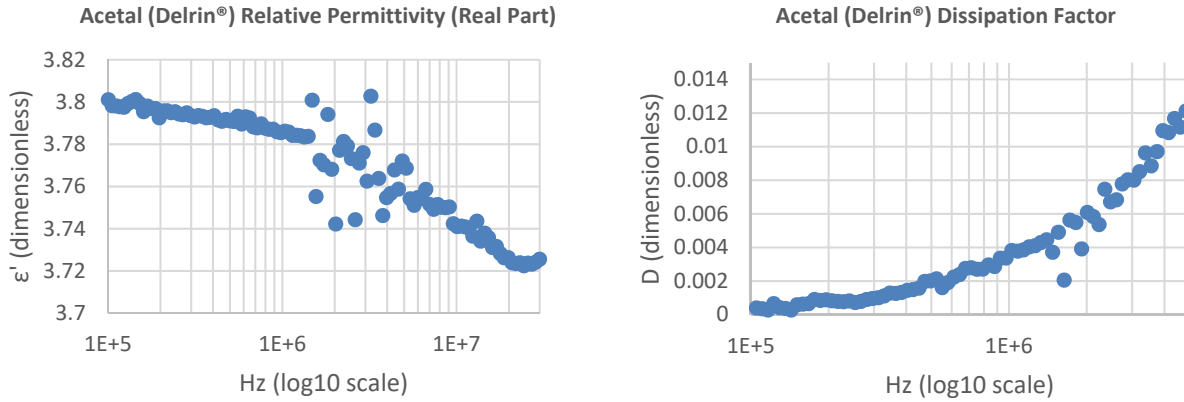
Figure 2.18: Dielectric Measurements of Delrin using measurement setup (fixture, cables, & E4990A). A value between 3.7-3.8 at 1-MHz is in the mid-range of values published by DuPont for the dielectric constant. Similarly, a value of 0.004 is very close to DuPont's published values of the dissipation factor.
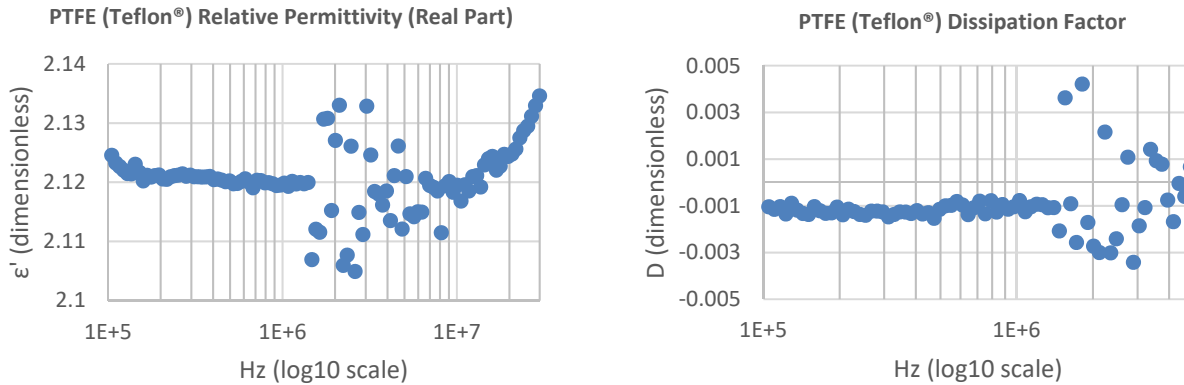
Figure 2.19: Dielectric Measurements of Teflon using measurement setup (fixture, cables, & E4990A). Teflon has a permittivity in the mid-range of raw cotton tested, so it is especially important to have accurate results in measuring the permittivity of it. DuPont published values are 2.05 for dielectric constant and nearly zero for dissipation factor. Most other sources note 2.1 for the dielectric constant and zero for the dissipation factor (e.g., this is the default value in Ansys Maxwell). In any case, the measurements found using the prescribed setup are nearly identical to these values.

At first glance the negative values for the disspation factor of PTFE appear problematic, but like the large variation seen in the open circuit impedance measurements, this is due to the assumed simplified model of the MUT and the magnitude of parallel resistance exceeding the measurable range of the impedance analyzer. Published values of the dissipation factor (loss tangent) for PTFE are exceedingly small (as expected from these results).

2.4.4.1.1   *Seed VS Lint Permittivity*

Since changes in cotton turnout was postulated as a factor of influence on dielectric measurements, as part of the investigation of this factor several kg of raw cotton was ginned to obtain the separated lint and seed and subsequently used to compare the dielectric response at extreme and typical mixtures of lint and seed. All material was equalized to room

conditions to have the same moisture content and temperature during testing. Tests were conducted the same as with raw cotton using the setup described in Figure 2.4. The resulting dielectric constant and loss tangent at 1-MHz through a range of densities are shown in Figure 2.20. Since the densities of lint and seed are very disparate, fitted lines using least-squares regression are extrapolated to compare the dielectric response by adjusting for density. The intercepts are expected to be similar since at zero density the values would theoretically be the same as open air, and with exception of the intercept for the dissipation factor of seed, the intercepts were found not to be statistically different than open air values when using a 95% confidence interval. By examination of the fitted lines in the plots it is easy to see visually that the seed and lint do not have similar responses. Unsurprisingly, a t-test for the dielectric constants shows the mean slopes are not the same with significant p-value < 0.0001. The dissipation factor is visually different enough no statistical test is necessary, and furthermore lint required a square root transformation for fitting, while the seed could be fit best with a linear function, which confirms a difference without any further statistical testing. The results indicate that the composition of the lint causes a stronger response than seed for both permittivity and dissipation factor for the same density and MC.
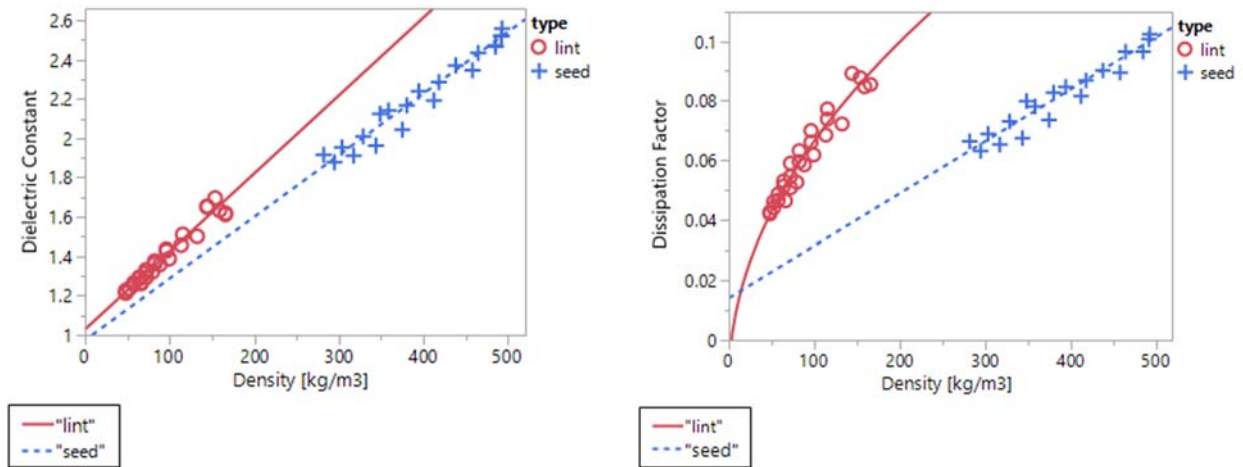
Figure 2.20: Dielectric properties of pure lint and seed compared at equilibrium room moisture as material is compressed (bulk density is increased)

Although there will be some local clumping, the lint clumps around the seed to form the cotton bolls and thus both the lint and seed are relatively evenly distributed throughout the volume of material. Therefore, since cotton lint showed a stronger dielectric response than seed (all else the same), it is projected the dielectric properties will be positively correlated with turnout. Generally the turnout of cotton falls somewhere between 35%-45% [19], and at a nominal 10% trash that means seed will comprise approximately the same or slightly more of the composition by weight as lint. If there is an impact, it would seem the dissipation factor is much more sensitive than the dielectric constant to changes in turnout.

2.4.5   GENERAL RESPONSE OF PERMITTIVITY AND LOSS TANGENT

Since density and moisture content are well known from other literature as the factors of highest influence, the response of permittivity and loss tangent using the setup described in Figure 2.4 and tests described in Table 2.3 was investigated prior to developing a statistical model. To create these plots, the data was grouped into 2% bins of MC, 20 kg/m3 bins of density, and by source frequency. Then for each set of plots, one of these variables was held constant at a given level and the data averaged at unique combinations of the other two variables. The plots in Figure 2.21 and Figure 2.22 with frequency on the x-axis have responses very similar to those found for grain and seed [2]. If there were no interaction between the grouping variable and the variable plotted on the x-axis, the lines would all have the same slope (at a given frequency) but different offsets. However, it is clear there is an interaction between both MC and density with frequency since the slope of the plots in each case changes for different levels of MC (when density is held constant) or density (when MC is held constant). The plots in Figure 2.23 the effect on dielectric measurements when changing density may increase with increasing MC (again suggesting a possible interaction), although not as clearly as between frequency and these variables. The results of this visual exploration are subsequently used to drive the predictive model development, with emphasis on the apparent nonlinear interaction between frequency and other variables. Note that these plots are very similar to plots of the dielectric constant and loss factor available for various grains and seed [2].
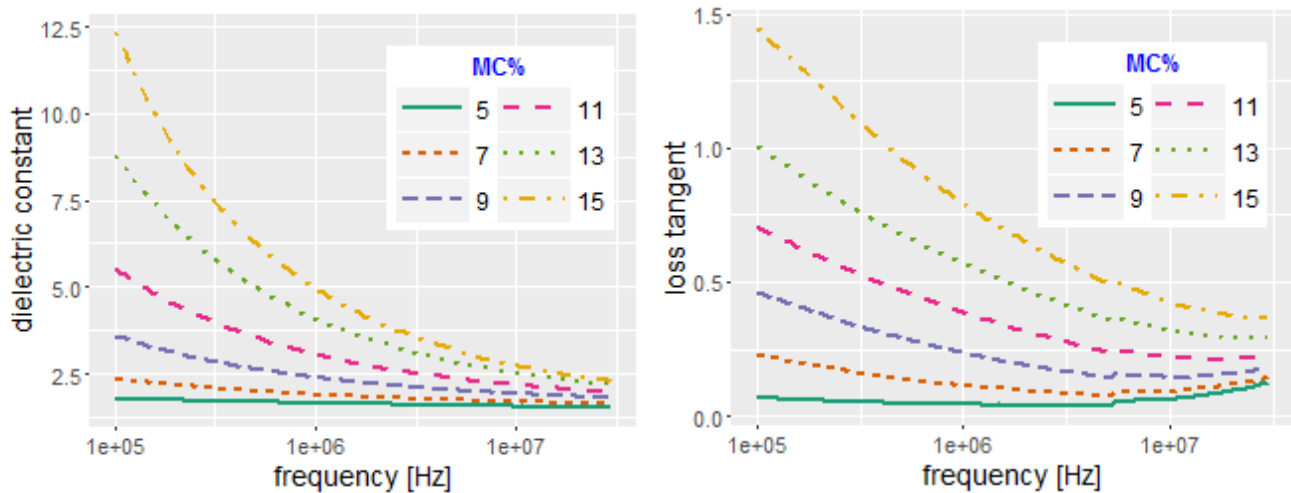
Figure 2.21: Effect of moisture content and frequency on the dielectric constant (left) and loss tangent (right) of raw cotton at a density of 230 kg/m3. The plots were obtained by binning the measured density into 20 kg/m3 bins and MC% into 2% bins and subsequently calculating the mean values of permittivity and loss tangent by MC% and frequency at a binned density of 230 kg/m3.
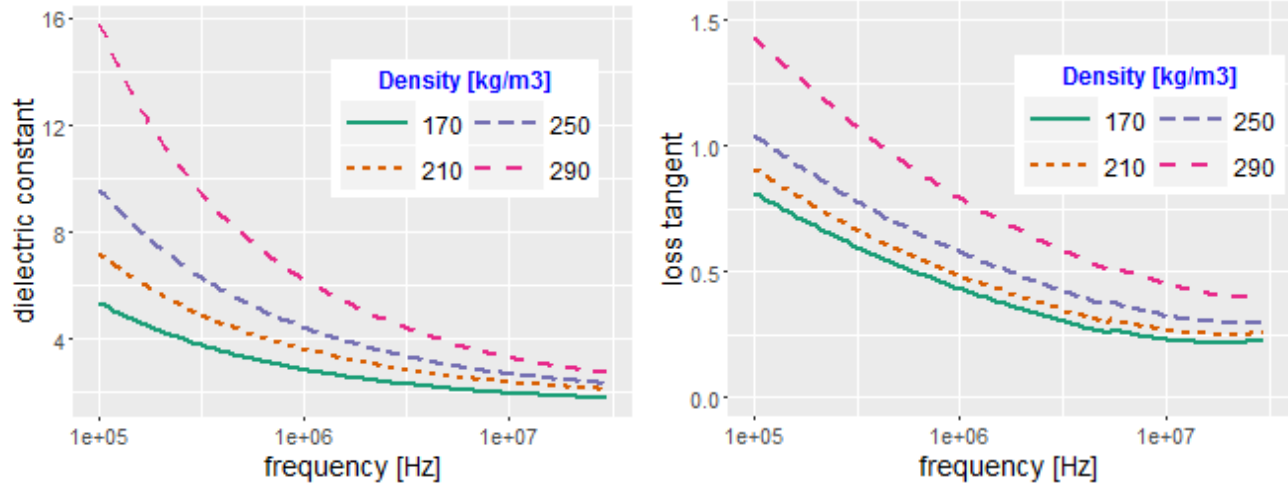
Figure 2.22: Using a similar binning method as described in the previous figure, here the measured dielectric constant and loss tangent are plotted for several densities against frequency at 13%MC.
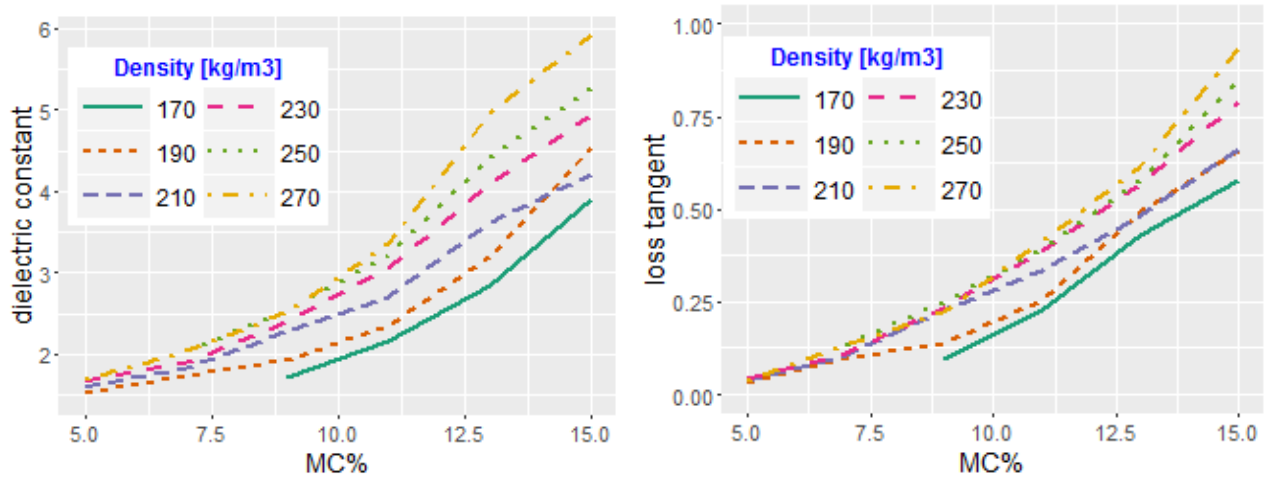
Figure 2.23: Using the same binning strategy as the previous two figures, the effects of density and MC on the dielectric properties at 1-MHz are plotted.

2.4.6   MODEL DEVELOPMENT

The major factors under consideration in the development of a statistical model for the dielectric constant and dissipation factor of raw cotton are MC, density, frequency, turnout, and crop variety. Crop variety however is not desirable as part of the model since it does not directly refer to a physical measurable quality (and not easily decoupled from the region where the cotton is harvested). Nonetheless it is investigated as a random effect.

Utilizing the intuition gained from the visual exploration presented earlier, it was determined that isolating the frequency component when fitting coefficients for the other terms was a good approach. This method is more targeted than simply including interaction with frequency for each term because it facilitates highly nonlinear relationships with frequency that were found to exist. Models were fit at nine discrete frequency levels evenly spaced over the frequency range under

consideration (Figure 2.24), and subsequently leverage plots and p-values (less than 0.05) were used to determine parameter significance (sans frequency). Then at each frequency, the coefficients for each term included in the model were recorded, and finally the coefficients mapped as continuous polynomial functions of $\log_{10}(frequency)$ as in Table 2.4, Table 2.5.

Both the dielectric constant and loss tangent of raw cotton displayed nonlinearity even after isolating frequency, and therefore the response had to be either fitted in a generalized linear model (GLM) with a nonlinear link function or simply transformed by a nonlinear function and modeled in the transformed space. In most use cases the dielectric properties are the quantity of measurement used to predict another unknown physical property such as moisture content, and applying transformation of the permittivity to linearize the nonlinear relationships is typical. Therefore transformation of the dielectric values by a nonlinear function prior to modeling was used here as well.

2.4.6.1   *Dielectric Constant Composite Model for Frequency between 100 kHz and 30 MHz*

A reciprocal transformation on the dielectric constant attained the best performance of all functions tested when using R^2 as the primary means to judge models. At each discrete frequency, MC, MC^2, density, and $[density]^2$ were fit and found to be significant (with P-values < 0.0001 in most cases). Conversely, an interaction between MC and density was not found to be significant, with P-value > 0.05 and/or no trend in leverage plots when fit at the nine discrete frequencies. Additionally, the same crop varieties from different regions were observed to be more similar in response (slopes and biases) than different varieties when examining predicted VS actual plots (Figure 2.25). Phytogen499 was represented from two regions with six months between collecting each bulk sample, but is still more similar in response than Phytogen811 Pima variety. To test for the effect of variety, a base model was fit as described earlier and the output subsequently stacked in another linear model with crop variety. The stacked model consisted of the base model prediction output, with crop variety and an interaction term between base model output and crop variety as random effects. This strategy used much less degrees of freedom than including crop variety in the original model since the interactions between the nine varieties and four predictors would have four times the number of parameters. The stacked model enhancement to the base prediction model is significantly easier to interpret as well. Both crop variety and the interaction of crop variety with the base prediction model output were significant as random effects (Wald p-values < 0.05).

Cotton turnout was not found to be a significant variable for either permittivity or loss tangent. It is hypothesized that the range of turnouts present in the dataset do not cause substantial changes in dielectric properties, and when investigating the effects, the variation due to other factors such as crop variety mask any effect that may be present. Given the significant effect of crop variety, it would likely take a much more extensive dataset that has a sizable range of turnout within each

variety to contain the power to discern if there is an effect from turnout.

As noted previously, the coefficients for each term included were fit at nine frequencies evenly distributed over the $\log_{10}(freq)$ range of 100kHz to 30MHz. Figure 2.24 shows the interpolated curve over frequency for the nine fitted coefficients for density and moisture, and Table 2.4 contains the equations of the mappings for each coefficient from frequency. Similar curves were fit for quadratic terms of each. Note the highly nonlinear relationship and thus why this method is used. At any individual frequency, it was observed that the intercept for MC and density terms was not statistically different than 1.0 (the relative permittivity of air), which lends credibility to the model and measurements. For the training data, the model achieved a coefficient of determination (R^2) of 91% and RMSE of 0.049 in transformed (reciprocal) dielectric constant units. Including crop variety (stacked model) results in an R^2 of 94% and RMSE of 0.039.
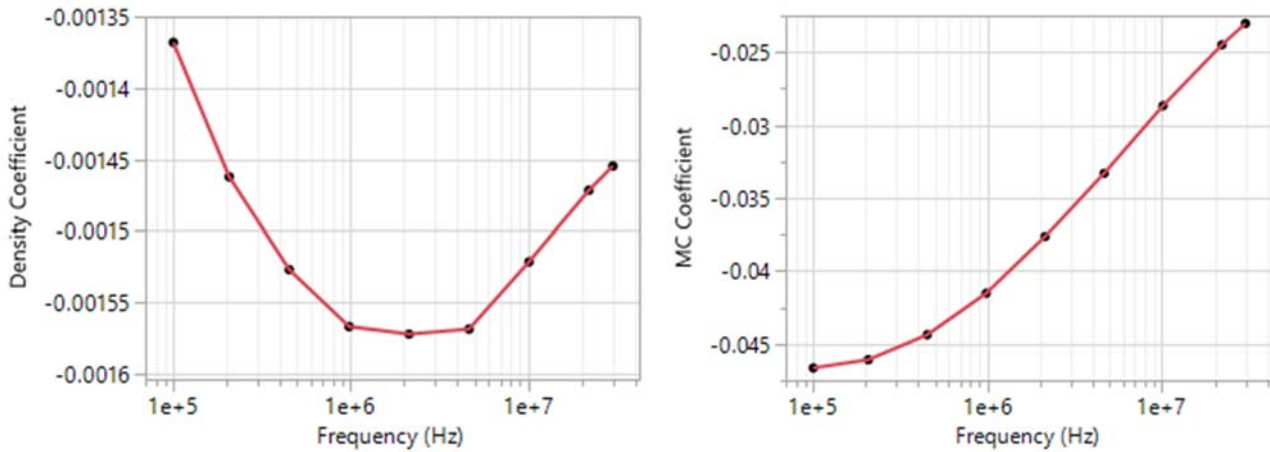
Figure 2.24: Mapping curve for the coefficients for density and moisture content by frequency in the dielectric constant formulation. Black data points represent discrete frequencies where the coefficients were fit, and then polynomial functions used to interpolate as a continuous function over the whole frequency range.

Table 2.4: Coefficients for the dielectric constant model are mapped as functions of the base 10 log frequency for each term from 100kHz to 30MHz. This mapping is interpolation for each of the model coefficients fit at the nine frequencies as shown in Figure 2.24.

General Formulation →		$[dielectric\ constnat]^{-1}= A(f) +\ B(f) * [density] + C(f) * [density]^2 +$ $D(f) * [MC] + G(f) * [MC]^2$
Factor	*Coefficient Designation*	*Coefficient Mappings (as a Function of Frequency)*
Intercept	**A(f)**	$1.2 - 0.009f - 0.072(f-6.3)^2 + 0.017(f-6.3)^3 +\ 0.006(f-6.3)^4$
Density	**B(f)**	$-0.0015 - 5.2E^{-6}f + 1.2E^{-4}(f-6.3)^2 + 1.4E^{-5}(f-6.3)^3 - 1.2E^{-5}(f-6.3)^4 - 1.7E^{-5}(f-6.3)^5$
[Density]²	**C(f)**	$4.8E^{-5} - 6.1E^{-6}f + 2.3E^{-7}(f-6.3)^2 + 8.3E^{-7}(f-6.3)^3$
MC%	**D(f)**	$-0.12 + 0.012f + 0.0028(f-6.3)^2 - 0.0016(f-6.3)^3 - 3.8E^{-4}(f-6.3)^4$
[MC%]²	**G(f)**	$4.6E^{-3} - 7.5E^{-4}f + 1.1E^{-3}(f-6.3)^2 - 1.1E^{-4}(f-6.3)^3 - 1.7E^{-4}(f-6.3)^4$

Note: $f=\log_{10}(freq)$

The predicted VS actual (measured) dielectric constant plot is shown for the training data in Figure 2.25. Crop variety is colored to contrast the difference between varieties, with two specific varieties (Phytogen499, Phytogen811 Pima)

highlighted as examples. A latent variable such as seed oil content differences or other constituent variations is hypothesized to be the underlying cause for response difference between crop varieties.
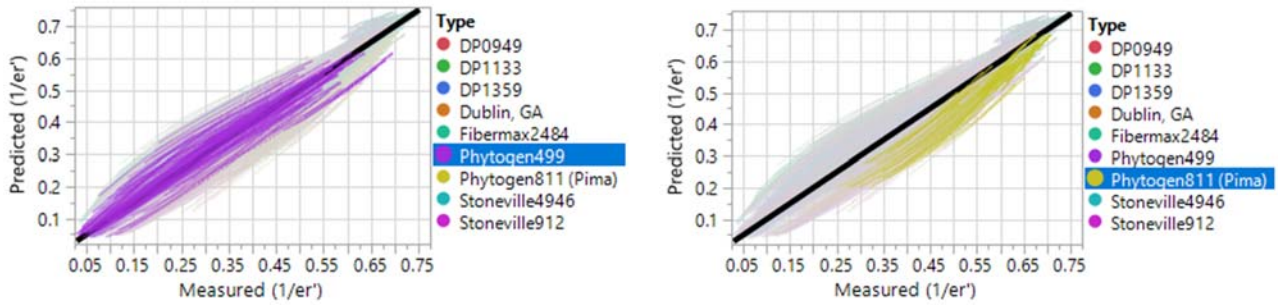
Figure 2.25: Predicted VS actual transformed dielectric constant values with Phytogen499 from two regions (left) and Phytogen811 Pima (right) highlighted. A black line overlaid is a one-to-one prediction line.

2.4.6.2 Dielectric Constant Prediction Performance Tested on Verification Data

Data consisting of 29 individual samples taken directly from bales shortly after being formed and dropped by harvesters were used to validate the prediction model. These samples were stored in sealed plastic bags to maintain moisture contents as experienced in the field until the time they were measured in the lab. Large residual error resulted due to slope and bias differences from base model. However when the verification data was overlaid with the rest of the data (Figure 2.26), it was seen to be very similar to the other bulk sample from GA that was rehydrated to controlled MC levels. The variety was not known for these individual samples, but it is presumed to have come from the same variety as the bulk sample since they were taken from the same area during the same timeframe (Dublin, GA). The prediction of this data using the base model has a 0.069 RMSE, but an RMSE of 0.042 is achieved when using the stacked model (corrected for variety and considering the verification data of the same variety as the bulk sample from Dublin, GA). The residuals before and after fitting with variety can be seen in Figure 2.28. This continued to support the hypothesis of dielectric property differences between varieties, given other significant influencing factors such as density and MC are the same.
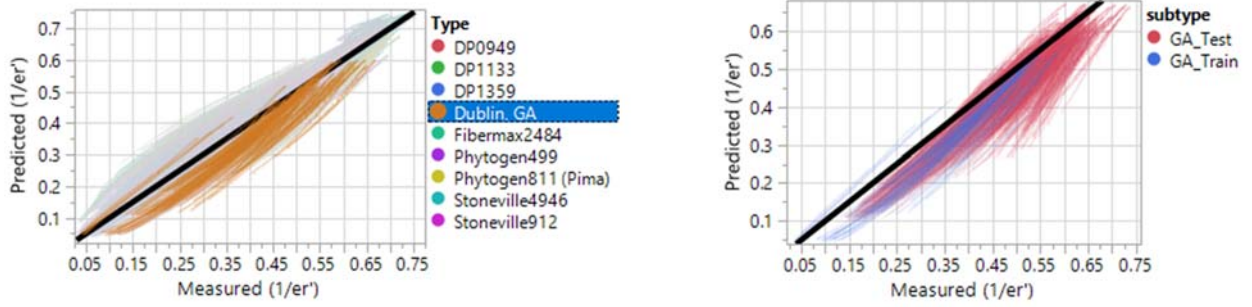
Figure 2.26: Samples from Dublin, GA are highlighted among rest of training data (left) and train VS test data compared separately for samples from GA (right). Thick black line overlaid is one-to-one prediction line.
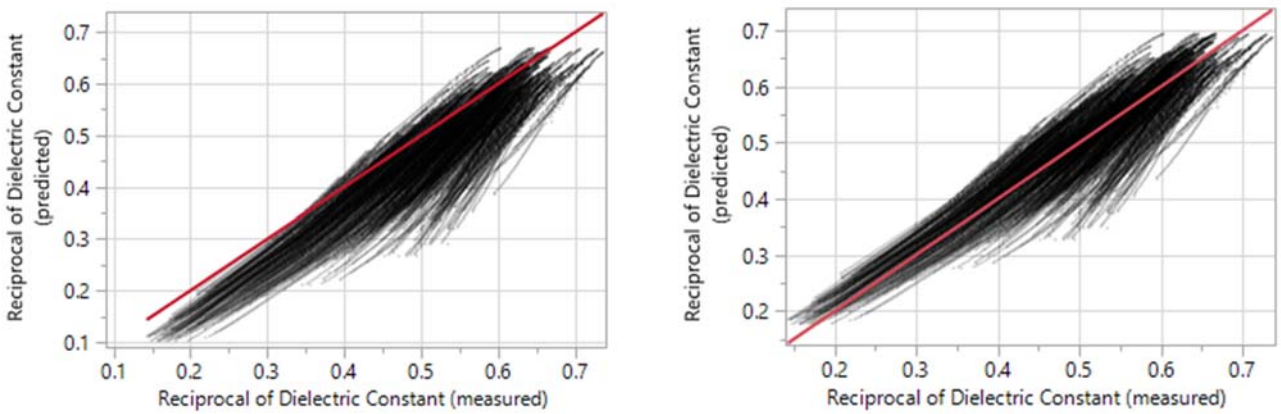
Figure 2.27: (left) Using the model from Table 2.4 to predict er' for the GA modules, a slope difference is observed by the one-to-one (45-deg) line that is draw with the data. (Right) Prediction outputs from model in Table 2.4 are slope and bias adjusted assuming crop variety is the same as the bulk sample from Dublin, GA.
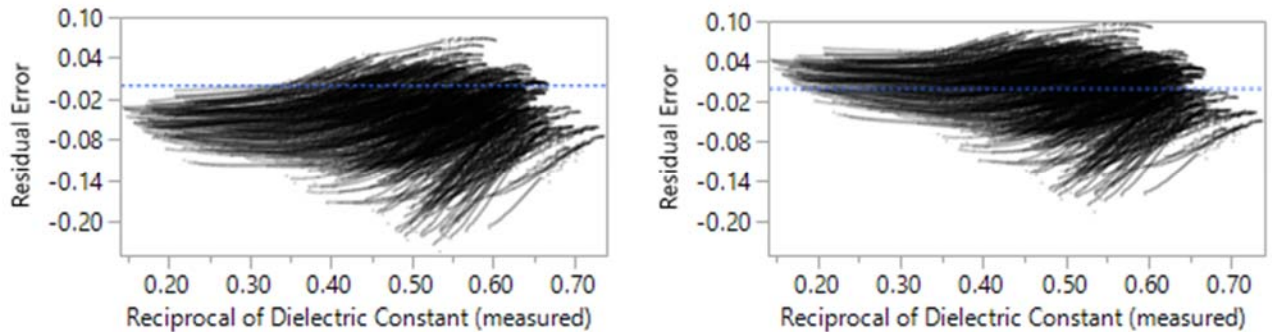
Figure 2.28: (Left) large bias in residuals of verification data when using base model without accounting for variety. (Right) stacking the base prediction model with factors to correct slope and bias by variety shows dramatic reduction in magnitude of residuals.

2.4.6.3   Loss Tangent Composite Model for Frequency between 100 kHz and 30MHz

Building predictive models for the loss tangent followed the same methodology as the dielectric constant, with the

primary differences being that a square root transform of the loss tangent was found to be optimal, and the quadratic density

term was not found to be significant (P-value > 0.05). All terms shown in Table 2.5 were significant (P-value < 0.0001).

An R^2 value of 84% and RMSE of 0.1 was obtained in fitting the base model. When variety is accounted for as with the dielectric constant, the R^2 increases to 89% with RMSE of 0.082, and a Wald p-value of <0.05 confirms statistical significance of variety as a random effect.

Table 2.5: Loss tangent coefficients mapped by frequency as was done with the dielectric constant in Table 2.4.   Unlike the dielectric constant model, inclusion of a squared-density term provided no additional benefit in the loss tangent model. The optimal transformation for loss tangent was found to be a square root function.

General Formulation →	$\sqrt{\textbf{loss tangent}} = \textbf{A(f)} + \textbf{B(f)} * [\textbf{density}] + \textbf{C(f)} * [\textbf{MC}] + \textbf{D(f)} * [\textbf{MC}]^2$	
Factor	*Coefficient Designation*	*Coefficient Mappings (as a Function of Frequency)*
Intercept	A(f)	$-1.9 + 0.22f + 0.10(f-6.3)^2 + 0.061(f-6.3)^3$
Density	B(f)	$0.0050 - 5.6E^{-4}f$
MC%	C(f)	$0.23 - 0.027f - 0.0031(f-6.3)^2$
[MC%]²	D(f)	$-0.0025 + 7E^{-4}f + 5.1E^{-4}(f-6.3)^2 - 4.4E^{-4}(f-6.3)^3 - 3.6E^{-4}(f-6.3)^4$

Note: "f" = $\log_{10}(frequency)$ and is in Hz.

2.4.6.4   *Loss Tangent Prediction Performance Tested on Verification Data*

As with the dielectric constant, the 29 samples taken from bales during harvesting in Georgia were used to assess performance. With the base model an RMSE of 0.13 is obtained, which is reduced to 0.05 after accounting for crop variety in a stacked model. Figure 2.29 shows the predicted VS actual along with a one-to-one prediction line before and after correcting for crop variety.
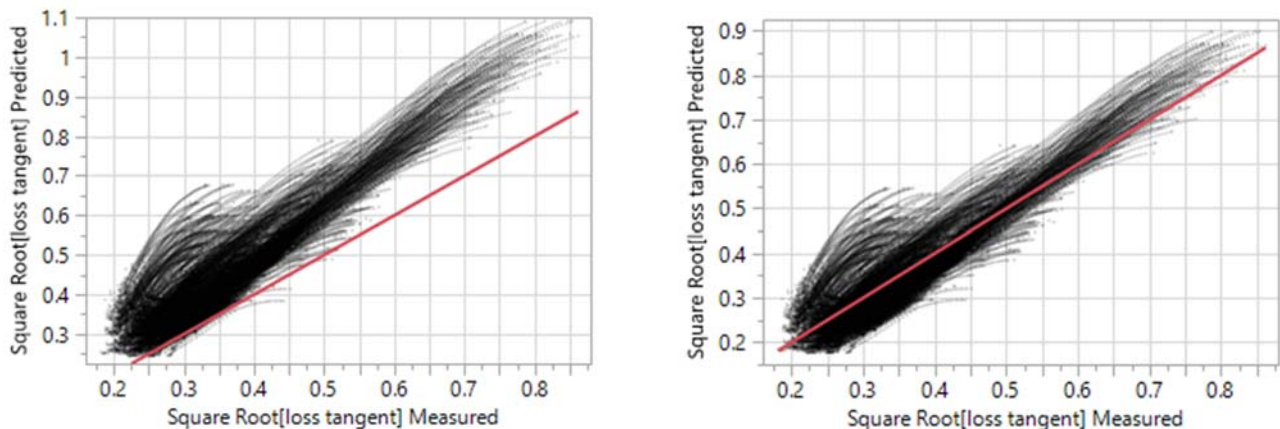
Figure 2.29: (Right) Base prediction model performance with one-to-one line overlaid. (Right) Base model adjusted (slope and bias) for crop variety with one-to-one line overlaid.
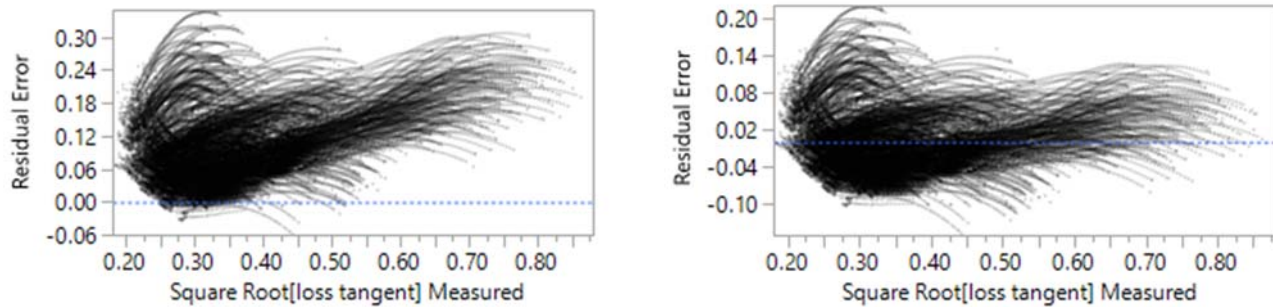
Figure 2.30: Before (left) and after (right) adjusting slope and bias (via stacked model) for crop variety.

2.5   CONCLUSIONS

Using an inexpensive capacitive-based sensing method, the authors have developed a reasonably accurate predictive model for raw cotton that achieves a coefficient of variation of 90% for the reciprocal of the dielectric constant and 85% for the square root of the loss tangent (dissipation factor). When conditioned on variety the prediction is improved with R^2 increased to 90% and 89% for the dielectric constant and loss tangent, respectively. The predictors used in the expression are moisture content over a range of 4% to 15%, frequency over a range of 100kHz to 30MHz, and density over a range of 160 kg/m^3 to 288 kg/m^3 [10 lbs/cu-ft to 18 lbs/cu-ft]. By fitting the coefficients for MC and density at several discrete frequencies and mapping the coefficients as functions of base 10 log frequency, the highly nonlinear nature of both variables with frequency could be accurately accounted for. Given the small bulk modulus of cotton, the inclusion of density, as expected, resulted in a noticeable improvement in fit and is therefore a significant factor on dielectric properties in raw cotton. The cotton turnout showed no impact, which seems likely due to the generally small difference in permittivity of lint and seed, the relatively larger volume of lint compared to seed, and the small range of ratios found in raw cotton. Since temperature was not included as a variable (but controlled to remain relatively constant), future efforts to construct a more extensive model could explore the effects of temperature. By showing a suitable predictive model is achievable in raw cotton, it is our hope that this research helps to stimulate further development of methods and equipment for measuring dielectric properties in biological materials with challenging physical characteristics and/or highly non-uniform mixtures.

On a final note, it is understood that dielectric values are rarely of interest themselves but are useful due to the ability to acquire rapid measurements using electronics and then plug into a prediction model that maps the values to physical quantities of interest, such as MC. The challenge is that any factors other than the one of interest that can change the measured quantity (permittivity in this case) will ultimately be a source of variability. If a sensor design similar to the one

presented herein is used, such applications will need to take into consideration several key points from this work, which includes the importance of presenting material consistently to the sensor face (avoiding small gaps which can have significant impact), and the effect that localized changes in density could have on the measurements.

2.6   REFERENCES

[1]   S. O. Nelson and S. Trabelsi, "A Century of Grain and Seed Moisture Sensing through Electrical Properties," in *ASABE*, Louisville, Kentucky, 2011.

[2]   *Dielectric Properties of Grain and Seed,* St. Joseph, Mich.: ASABE, 2012.

[3]   C. B. Behringer, "Performance Comparison of Moisture Sensor Technologies for Forage Crops," Madison, Wi, 2004.

[4]   W. Guo, J. Yang, X. Zhu, S. Wang and K. Guo, "Frequency, Moisture, Temperature, and Density-Dependent Dielectric Properties of Wheat Straw," *Transactions of the ASABE,* vol. 56(3), pp. 1069-1075, 2013.

[5]   C. E. Kirkwood, N. S. Kendrick and H. M. Brown, "Measurement of dielectric constant and dissipation factor of raw cottons," *Textile Research Journal,* p. 24:841, 1954.

[6]   A. Kraszewski and S. O. Nelson, "Composite Model of the Complex Permittivity of Cerial Grains," *J. agric. Engng. Res,* pp. 43,211-219, 1989.

[7]   D. K. Cheng, Field and Wave Electromagnetics, Pearson Education, 1989.

[8]   "Impedance Measurement Handbook, 4th Edition," Keysight Technologies, 2014.

[9]   "Basics of Measuring the Dielectric Properties of Materials," Keysight Technologies, 2015.

[10]   "E4990A Impedance Analyzer: Data Sheet," Keysight Technologies.

[11]   S. O. Nelson, "Dielectric properties of grain and seed in the 1 to 50-mc range," *Transactions of the ASAE,* pp. vol. 8, no.1, pp. 38-48, 1965.

[12]   D. Funk and Z. Gillay, "Unified Grain Moisture Algorithm," USDA, 2012.

[13]   D. B. Funk, "New Official Moisture Technology Implementation Briefing," in *NAEGA-GIPSA Regional Meeting*, Destrehan, LA, 2012.

[14]   "GAC 2500-UGMA Grain Analysis Computer," 2 2016. [Online]. Available: http://www.dickey-

john.com/product/gac2500/.

[15] S. O. Nelson, "Dielectric Property Measurements and Techniques," in *AIChE*, Austin, TX, 2004.

[16] S. O. Nelson, Dielectric Properties of Agricultural Materials and Their Applications, elsevier, 2015.

[17] W. L. Balls, "Dielectric properties of raw cotton," *Nature,* p. 158: 9–11., 1946.

[18] L. Han Ming, L. Ma, C. Q. Ma and J. F. Hong , "Estimation of the moisture regain of cotton fiber using the dielectric spectrum," *Textile Research Journal,* p. Vol. 84(19) 2056–2064, 2014.

[19] C. E. &. D. Team, "Turnout Percentages -- Factors Involved," CSD Extension, 2010.

[20] B. Goodman and C. D. Monds, "A Farm Demonstrations Method for Estimating Cotton Yield in the Field for Use by Extension Agents and Specialists," *Journal of Extension,* vol. 41, no. 6, 2003.

[21] S. C. P. Ltd., "Moisture Management a Must," Southern Cotton Pty Ltd., Whitton, NSW, 2013.

[22] J. Quinn, R. Eveleigh, B. Ford, J. Millyard, A. North and J. Marshall, "Cotton Picking Moisture," Cotton Seed Distributors, Wee Waa, NSW, 2014.

[23] "Cotton Pcker Management and Harvesting Efficiency," Clemson University Extension, 1996.

[24] R. Fiore, "Circuit Designers' Notebook, Document #001-927, Rev. E," American Technical Ceramics, 2005.

[25] "Tests for thermoplastic materials used in the electrical and electronic industries," DuPont.

[26] "Moisture Restoration of Cotton," USDA-ARS, 2004.

[27] R. K. Byler, M. G. Pelletier, K. D. Baker, S. E. Hughs, M. D. Buser, G. A. Holt and J. A. Carroll, "Cotton Bale Moisture Meter Comparison at Different Locations," *Applied Engineering in Agriculture,* vol. 25, no. 3, pp. 315-320, 2009.

[28] M. H. Willcutt, E. M. Barnes, M. J. Buschermohle, J. D. Wanjura, G. W. Huitink and S. W. Searcy, "The Spindle-Type Cotton Harvester," Texas A&M Agrilife Research and Extension Center, Lubbuck, TX, 2010.

[29] "Cotton Picker Management and Harvesting Efficiency," Clemson University Extension, 1996.

[30] J. P. Just and M. J. Darr, "COMPOSITE MODEL OF THE COMPLEX PERMITTIVITY OF RAW COTTON," *ASABE,* 2016.

[31] *Standard Test Method for Moisture in Cotton by Oven-Drying,* West Conshohocken, PA: ASTM International, 2012.

[32]   J. G. Montalvo Jr. and T. M. Hoven, "Review of Standard Test Methods for Moisture in Lint Cotton.," *The Journal of Cotton Science,* pp. 12:33-47, 2008.

[33]   R. K. Byler, "Comparison of Selected Bale Moisture Measurements in a Commercial Gin," in *2012 Beltwide Cotton Conferences*, Orlando, Florida, 2012.

[34]   R. K. Byler, "The Accuracy of Cotton Bale Moisture Sensors Used in a South Texas Commercial Gin with Lint Moisture Restoration," in *2014 Beltwide Cotton Conferences*, New Orleans, LA, 2014.

[35]   D. Cash and H. F. Bowman, "Alfalfa Hay Quality Testing," Montana State University Extension, Bozeman, MT, 1993.

[36]   W. K. Coblentz, "Spontaneous Heating," in *Idaho Alfalfa and Forage Conference Proceedings*, Burley, Idaho, 2013.

[37]   W. Coblentz and M. Bertram, "Effectiveness of Buffered Propionic-Acid Preservatives for Large Hay Packages," Midwestforage.org, 2011.

[38]   K. E. Webster, M. J. Darr, J. C. Askey and A. D. Sprangers, "Production Scale Signle-pass Corn Stover Large Square Baling Systems," in *2013 ASABE Annual International Meeting*, Kansas City, MO, 2013.

[39]   J. P. Just and M. J. Darr, "COMPOSITE MODEL OF THE COMPLEX PERMITTIVITY OF RAW COTTON," *ASABE,* 2017.

[40]   J. Just and M. Darr, "Real-Time Moisture Prediction on Round-Bale Cotton Harvesters," *ASABE,* 2017.

[41]   D. Funk, "Engineering Considerations for Dielectric On-Line Grain Moisture Measurement," in *ASABE*, Kansas City, MO, 2013.

[42]   J. O. Rawlings, S. G. Pantula and D. A. Dickey, Applied Regression Analysis: A Research Tool, Second Edition, Springer, 1998.

[43]   "Impedance Measurement Handbook, 5th Edition," Keysight Technologies, 2015.

[44]   G. E. Shewmaker and R. Thaemert, "Measuring Moisture In Hay," in *Proceedings, National Alfalfa Symposium*, San Diego, CA, 2004.

[45]   M. Rankin, "Understanding Corn Test Weight," UW Extension Team Grains, 2009.

[46]   J. T. Documentation, "Standard Least Squares Report and Options -- Row Diagnostics," JMP From SAS,

[Online]. Available: http://www.jmp.com/support/help/Row_Diagnostics.shtml#184200. [Accessed 17 Jan 2017].

[47]   S. O. Nelson and S. Trabelsi, "Use of Grain and Seed Dielectric Properties for Moisture Measurement," in *Southeastcon. 2011 Proceedings of IEEE*, Nashville, TN, 2011.

[48]   D. M. Mitchell, J. Johnson and C. Wilde, "IMPACTS OF DECREASING COTTONSEED TO LINT RATIO ON COTTONSEED MARKETS," in *Beltwide Cotton Conference*, New Orleans, 2007.

[49]   D. Blackham, F. David and D. Engelder, "Dielectric Materials Measurements," in *RF & Microwave Measurements Symposium and Exhibition*, 1990.

[50]   D. Funk, B. Gillay, S. Burton and Z. Gillay, "Engineering Considerations for Dielectric Online Grain Moisture Measurement," in *2013 ASABE International Meeting*, 2013.

[51]   R. K. Byler, "Resistivity of Cotton Lint for Moisture Sensing," *Transactions of the ASABE,* vol. 41, no. 3, pp. 877-882, 1998.

[52]   M. Digman and K. Shinners, "Technology Background and Best Practices: Yield Mapping in Hay and Forage," in *Proceedings, Idaho Hay and Forage Conference*, Burley, ID, 2013.

[53]   R. Benning, S. Birrell and D. Geiger, "Development of a Multi-Frequency Dielectric Sensing System for Real-TIme Forage Moisture Measurement," in *2004 ASAE/CSAE Annual International Meeting*, Ottawa, Ontario, Canada, 2004.

[54]   J. Banta, "Bale Weight: How Important Is It?," AgriLife Communications.

CHAPTER 3:   REAL-TIME PREDICTION OF MOISTURE CONTENT ON ROUND-MODULE COTTON HARVESTERS

John Just, Matt Darr

ABSTRACT

In this work, a sensor design and mounting location capable of obtaining a representative dielectric measurement for round cotton modules during harvesting is used, and a statistical model to predict MC is presented with consideration of influencing factors such as density. Hard performance goals for the system are specified on a per-module basis, with a target of no greater than 1%MC mean absolute error (MAE) over the range of 6-12%MC, and relaxing outside of those bounds. Also imposed is a goal that the module-to-module noise during operation be much less than the MAE of the aggregated data to provide reasonable tracking of changes in moisture throughout a single harvest day. A baseline prediction model was developed using dielectric properties of cotton as measured on a lab test stand. It was found that bulk density exerted strong influence on dielectric measurements during controlled lab testing and so an adjustable bias term that is based on density was included, preset at 208 kg/m³ [13 lbs/ft³]. Controlled machine testing revealed that variability of the predicted MC% increased with rotational speed but the mean prediction was unchanged. The sensor probe design was shown to be very sensitive to air gaps between the probe and material, but further testing which explored material force on the sensor plate area found evidence for consistent contact with the sensing area. A subsequent field experiment investigating the change in predicted moisture with changing average module density found sensitivity nearly twice that of the lab tests. A pre-validation (training) of the prediction formula, using a single prediction per module, found a bias of 0.74%MC for pickers and 2.55%MC for strippers. A bias was found between regions for pickers for machine-measured values in the training data. When samples from these regions were tested in the lab, it was concluded inherent material property differences was not the cause of the bias. More extensive field validation during 2016 continued to find similar bias for both pickers and strippers, and the sensitivity to density changes as they relate to machine-measured dielectric values was also firmly defined using average module densities in a multivariate regression, and was roughly 1.5 times the effect as measured in the lab. The cause of the bias between field and lab data was not conclusively established, but postulated due to lower density at the sensor interface on the machine than was found for the average of the entire module. Corrections for the bias by applying an offset for pickers and strippers separately was found to have the same performance as adjusting predictions for density, and in either case the performance goal of an MAE of less than 1%MC throughout the key range of 6-12%MC was achieved on a per-module basis. Finally, examining the output for several days of harvesting

on both pickers and strippers, the characteristic diurnal moisture cycle throughout the day was observed with the predictions closely following the actual trends in moisture, thus achieving the performance target.

3.1   INTRODUCTION

The moisture content (MC) of cotton has been noted to have a significant effect on lint quality throughout the entire process at cotton gins [26]. Wet cotton is generally defined to be anything greater than 7.5% wet basis [27]. A MC of 6%-7% is ideal, with higher or lower MC causing different problems. Problems with MC out of this range extend to harvesting equipment as well. Harvesting cotton too wet will reduce machine efficiency, risk clogging, and/or cause grade reduction during storage [28]. These risks increase sharply for MC greater than 12%-13% [22]. Growers may also be subjected to discount costs when selling high moisture cotton, and the increased drying required at the gin can cause fiber damage [21]. With the rapid adoption of round module cotton pickers and strippers, the risks associated with high moisture are increased since operators tend to run further into the evening [22] [21]. On the other hand, very dry cotton (4-6%) is more brittle and easily damaged when subjected to the mechanical harvesting actions. There is also the possibility of increased static electricity which could cause the fibers to stick to surfaces and choke the machine, or cause a fire [28].

The machine efficiency and fiber quality could benefit from a direct, real-time measurement of cotton moisture during harvesting. Moisture management starts with harvesting and the decisions heavily impact storage and processing. In addition to facilitating monitoring of the changes in moisture content throughout the day [28] [29] to mitigate aforementioned issues, a moisture sensor allows for flagging of very wet modules to be staged sooner in the ginning process. While some of the commercial moisture sensors used as part of the process control in gins have been extended to harvesting equipment, even the performance noted for these sensors in the very controlled environment of a gin for clean lint cotton leaves room for improvement [27]. The on-machine performance characteristics of gin moisture sensors is not published, but their application in the harsher environment of harvesting raw cotton with increased variability of the material composition makes achieving the same performance a much more difficult task. In addition, round modules are formed by rolling cotton onto the outer layer of the module, and can have varying densities and moisture contents throughout the layers. A typical process control meter can only measure a portion of a round module, which has the potential to be biased due to lack of representative measurements throughout the entire module. There is much room for improved options for measuring the moisture content of modules of round-module cotton in real-time. This work focuses on one such option using capacitance, and specifically discusses the details involved in building a predictive statistical model and follows with a performance evaluation in several geographic regions for both picker and stripper round-module harvesters.

3.1.1   PERFORMANCE CRITERIA

In terms of agricultural commodities, the typical cotton moisture range of 6 MC% (6-12 MC%) is fairly small and as such the performance criteria in terms of bias and standard deviation should reflect the limited operating range. Taking into consideration the typical range found in the field, and performance that was reported as acceptable for process control at gins with a more limited range, a criterion that targets a mean absolute error over various conditions should be no more than 1%MC over the typical operating range of 6-12 MC% on a per-module basis is deemed to be useful to operators for production decisions. Note that the MAE is similar to standard deviation in intent to measure dispersion, but always less than or equal to standard deviation (MAE = 0.8 * stdev for a Normal distribution), and more robust (less sensitive) to outliers. The MAE also facilitates an easier and more intuitive assessment of error over a range of moisture contents by implementing local smoothing and/or regression methods. In certain harvesting conditions it is plausible that there is a shift in response that may be appropriately defined as a bias due to factors that are not accounted for in the prediction model (such as density), and this can complicate the evaluation when error is quantified as MAE rather than bias. If these conditions are sampled unwittingly and/or go unidentified it could adversely influence the performance assessment. For simplicity biases are not considered part of the performance criteria in this work but bias is quantified in the performance assessment as applicable. Also note the additional simplistic assumption that all data points are treated as independent identically distributed (IID). Furthermore, a soft-target criterion considers how well the sensor tracks moisture changes through the day, since a sensor that operates with 1% MAE error module-to-module would be undesirable and make it difficult to track changes during key times in the day when the MC is rapidly decreasing/increasing. Reasonably smooth tracking from module-to-module throughout the day, and responsiveness to changes, should be expected for successful real-time implementation of cotton moisture measurement.

3.1.2   RESEARCH OBJECTIVES

With target performance in mind, the goal of this research was to develop and apply a capacitive-based dielectric sensor in the prediction of cotton module moisture. A base prediction model was initially developed using measurements of raw cotton obtained on a lab test stand data intended to emulate the machine-mounted scenario as closely as possible. Factors both known from previous work [30] and/or projected to have an influence on dielectric response were investigated for their effect while the sensor was mounted on the machine, and subsequently compared to the baseline prediction model. This includes density, interface pressure, and module dynamics. The field-collected machine data was divided into two phases: training and testing. The training data allows for tuning of the baseline prediction formula prior to validating. Finally, performance was assessed on field data obtained and further verification of the daily trends was observed in light of how the output of the sensor would typically be observed during real-time harvesting operations.

3.2   MATERIALS AND METHODS
3.2.1   DIELECTRIC PROPERTY SENSOR

A sensor was used which incorporates a measurement probe, driving voltage, analog-to-digital conversion of applied voltage and measured current signals, on-board processing of voltage & current into units of complex permittivity, and digital communication, to measure the real-time dielectric properties of cotton during harvesting. The sensor uses a planar probe design with approximate dimensions of 72 mm by 72 mm [7] ████████████████████████████. An open-air permittivity measurement was obtained when no material was in front of the sensor, and this was stored locally as a normalizing factor for the typical conversion equations from complex admittance to complex permittivity (both dielectric constant and loss factor). The sensor was programmed to obtain measurements at a rate of 1-Hz, ████████████████ ████████████████████████████████████. Permittivities were broadcast on the vehicle Controller Area Network (CAN Bus) at the same rate they were measured (1 Hz). The CAN bus output from the sensor was logged and included all other available real-time machine operating parameters associated with cotton module production (such as module diameter, weight, module serial number, etc).

Figure 3.1: Mobil sensor includes probe packaged with electronics and can be mounted on-machine.

3.2.2   MODULE FORMATION PROCESS

"Round" cotton modules are nominally 234 cm in diameter and 229 cm in width (Figure 1). The width of the round module is fixed based on the geometry of the cotton harvester but the diameter can be adjusted based on user settings. As cotton is harvested with either a stripper or picker, it is accumulated in an inner chamber to a certain level within the machine in loose form. When enough cotton is accumulated it is then ejected from the accumulation chamber and pressed onto the periphery of the cylindrical shaped module in the module chamber. The module is simultaneously spun with belts, effectively rolling and pressing the new cotton onto the outermost layer. This batched process continues until it reaches the preset module diameter. In a lab test observing the outer 30.5 cm [12 in] of the module radius, layers were found ranging from 0.64 to 3.8 cm [0.25 to 1.5 in] thick (Figure 3.3). Typical module weights differ based on the harvest machine configuration and are approximately 2041 kg [4500 lbs] for strippers and 2268 kg [5000 lbs] for pickers.
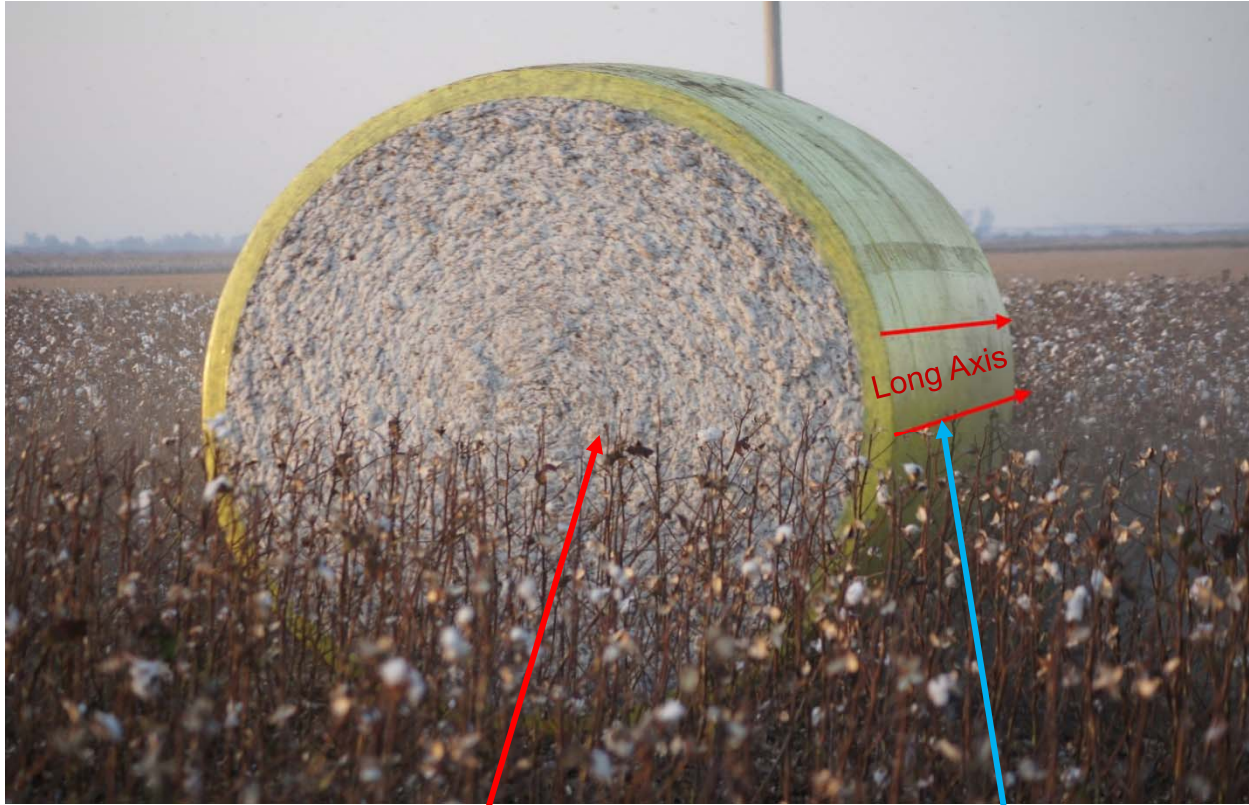
Figure 3.2: A typical round module, the moisture sensor is positioned to interface with material on the module face near the periphery such that measurements are taken of new material as it is spun into the module.

Figure 3.3: A lab test in which plastic wrap was rolled in with each layer of cotton into a module such that the layers could be visualized and unfolded. In the compressed state within the module the layers ranged from 0.64 to 3.8 cm [0.25 to 1.5 in] thick.

3.2.3   MOUNTING LOCATION

The sensor mounting position was such that measurements could be taken of new material as it is spun into the cotton

module, and therefore collect measurements of all layers in the module to ensure representative sampling throughout the

module (Figure 3.4). Due to mechanical operation and module chamber design there are limited mounting options for the sensor and a full location optimization was not feasible. The location of the sensor in the chamber was chosen as a balance between physical constraints and a desire for sensor interaction with nearly all layers in the module as new material is spun into the module. Note that in the chosen location, the sensor interfaces with the module face.

Long Module axis

This edge is the module chamber floor when door is closed. As new cotton is fed into the module, the module diameter grows and thus the sensor measures new material.

Sensor mounting location on side in module chamber.

Figure 3.4: Sensor mounting location within the module chamber. The flat end of the module presses against the sensor during formation. Dielectric measurements of the module are taken at 1Hz and converted to a predicted moisture.

3.2.4   SAMPLE COLLECTION AND DRYING METHOD

Validation of the performance was intended at a per-module level, and thus the sample collection method was designed to support the assessment of moisture prediction accuracy at that level. At least four sub-samples were collected from each module at different radii from center, which combined to form the sample that was used to determine moisture of the module. Multi-location sampling was important in order to account for the variation of moisture within a module and obtain an

estimate of the mean moisture of the module with manageably-sized samples (manageable in terms of handling, transporting, and lab analysis). Samples were taken from the open end of a wrapped module usually within 30 minutes after it was dropped by cutting away at the surface to expose layers deeper inside the module. By avoiding surface layers there is less risk of the moisture changing post-measurement due to interactions with the environment, which can occur quite fast [26] [22], prior to sample collection and placing in sealed bags. These samples were then stored in zip-top bags that were doubled to ensure no moisture loss until they were weighed and dried in forced-air ovens per ASTM D2495 [31] [32] to determine the MC%.

Figure 3.5: Example of sampling points from a round module per protocol. At least four different layers, corresponding to different radii, were sampled at quadrants around the module.

Since samples were transported to a lab for drying, which sometimes took up to a week before reaching the lab, a subset of the samples were tracked early on to determine if moisture loss was a concern. In 95% of the cases the difference between the wet weight of the sample as measured in the lab after a transport period and the field immediately after collection (lab weight – field weight) was less than 0.5%MC, which is considered acceptable. As expected the distribution is left-skewed due to moisture loss, but measurement error and very little moisture loss sometimes resulted in a small positive difference between the lab and field.

Quantiles		
100.0%	maximum	0.277%
99.5%		0.272%
97.5%		0.165%
90.0%		0.061%
75.0%	quartile	-0.038%
50.0%	median	-0.116%
25.0%	quartile	-0.205%
10.0%		-0.434%
2.5%		-0.607%
0.5%		-1.052%
0.0%	minimum	-1.106%
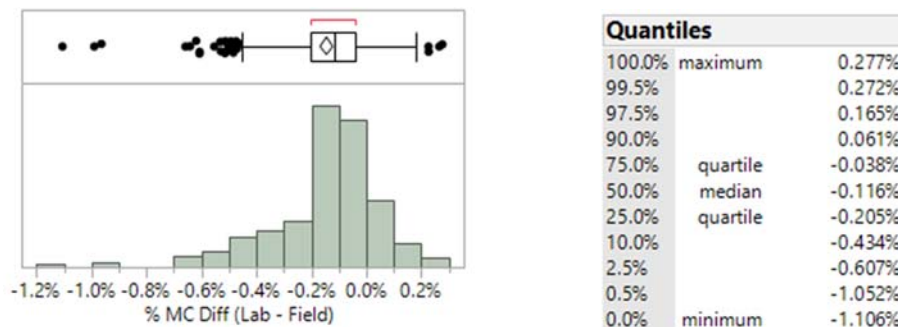
Figure 3.6: From 293 data points a distribution is shown of MC% difference between lab and field measured wet weights to investigate moisture lost in transit.

In order to gauge moisture variability within a module, an opportunity was taken to quantify it by collecting and drying (per protocol) a larger number of sub-samples from two individual modules. Twenty 30g samples from a relatively dry (mean of 8.4%MC) module and eight 100g samples from a relatively wet (mean of 12.3%MC) module were used to estimate the spread. While not exhaustive, it served to quantify variability and provide a baseline for comparison of the level of MC% variability that is present in modules of raw cotton soon after formation. A distribution of the MC% in each is shown in Figure 3.7. A range of ~2%MC was found in both modules, along with a standard deviation of 0.82%MC and 0.46%MC for the higher and lower MC modules respectively.
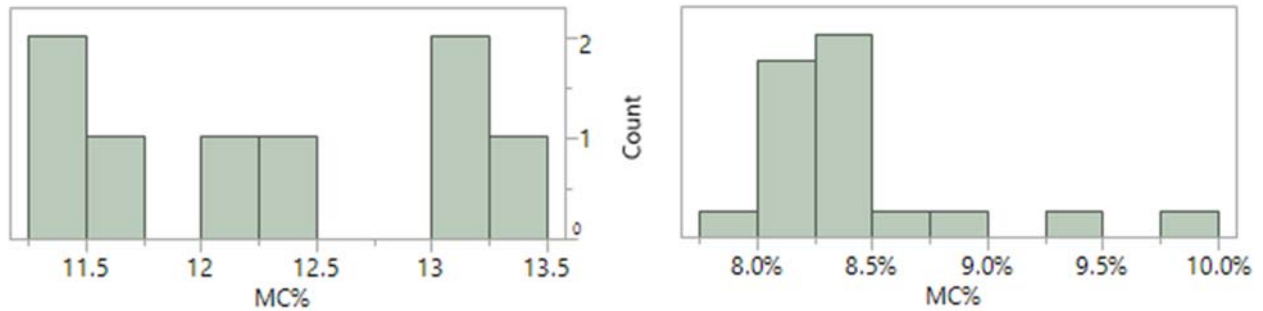
Figure 3.7: (Right) Distribution of MC% from eight 100g samples taken from a wetter bale. (left) Distribution of twenty 30g samples taken from a relatively dry mid-afternoon module.

ASTM D2495 is one of the most often cited voluntary standards in the USA for determination of cotton MC [32]. This method calls for sample sizes of 5-10g but also advises that a number of specimens should be taken such that the MC may be determined with an accuracy of ± 0.5 MC% at the 95% CI. Like this work, the primary sampling unit considered is a module. The ASTM states a known standard deviation of 0.378 as a basis, and thus 3 samples of 10g each will achieve the prescribed confidence. The evidence presented thus far suggests that level of variation may be approached by lower MC% modules, but evidence has also been presented that suggests the spread in MC% increases with mean MC%. Presuming MC% within a module is such that we are sampling from an approximately Normal distribution and that the 0.82%MC standard deviation is used to obtain more conservative inference, we can use a t-distribution to find the 95% CI of $\bar{X} - \mu$. When taking four-samples per module (which is the target number used in this work) and using a standard deviation of 0.82%MC this amounts to ± 0.8 MC% in 95% of the cases. It is notable that, by these numbers and using 100g samples, 10 samples of 100g each would be needed from each module to achieve the ASTM target of ± 0.5 MC% of the mean. Since the sample sizes taken in this work are 10x the ASTM target of 10g, and four of them are taken from each module, it was

decided that the sampling scheme was well beyond the ASTM standard and that the standard was relatively optimistic regarding variation, especially at high MC levels.

3.2.5   SUMMARY OF FIELD/MACHINE TESTS AND PERFORMANCE VALIDATION DATA (OUTLINE OF RESULTS)

3.2.5.1   Baseline Prediction Model Development

Previous work focusing on measurements of the dielectric properties of cotton under controlled lab conditions provides data that is used to develop a baseline predictive model for moisture. The characteristics of this data can be found summarized in other work [30] but is also repeated below as well. In this case the samples were artificially re-wetted to obtain a range of moisture contents for each.

Table 3.1: Characteristics and background of the raw cotton used to develop a baseline prediction model for MC%.

Variety	Region	Machine Type	Avg Field Turnout
*Unknown**	Dublin, GA	Picker	
Stoneville 4946	Lake City, AR	Picker	39.6%
Stoneville 0912	Senath, MO	Picker	39.3%
Phytogen 499	Blythe, CA	Picker	39.5%
DP 1359	Blythe, CA	Picker	37.7%
DP 0949	Blythe, CA	Picker	37.4%
*Unknown**	GA	Picker	
DP 1133	Ennis, TX	Stripper	31.4%
Fibermax 2484	Floydada, TX	Stripper	33.5%
Phytogen 811 (Pima)	Uvalde, TX	Picker	32.9%
Phytogen 499	Newellton, LA	Picker	39%

**GA samples came from the same general area and timeframe, but turnout information was unavailable.

3.2.5.2   Machine Response Testing

The response of a sensor in a laboratory is ideal since the density can be controlled and quantified, and the material is certain to maintain good contact with the sensor face due to the operation of the lab test stand. In light of the application of the sensor on a machine though, several factors were postulated to have confounding effects and needed to be investigated and quantified. Consistent contact with the sensor is a concern as previous work has theoretically shown a small gap can greatly reduce the magnitude of dielectric measurements [33], and there is no such guarantee of consistent contact on the machine. Density was likewise known to have a strong influence on dielectric measurements from previous work [30], but there was no guarantee the effect would be the same on the machine due to a different interface than the lab test stand, and thus is necessary to test further. Both these factors are quantified on the lab test stand as a baseline, also facilitating investigation of an interaction, and then further explored with testing on machines. Unique dielectric measurements of the cotton on the machine are considered only as new cotton is added onto the module, and thus most of the dielectric measurements occur during rotational movement that can be upwards of 120 rpm. In terms of linear speed this would appear to the sensor as 6.3 m/s at a radius of 0.5 m. Therefore, the effect of the dynamic interface between module and sensor on

the machine is unknown and to be quantified as well. Since it is desirable to quantify the MC% of a module by one value of central tendency, this is also investigated in terms of the best method to do so and for signs of any complicating factors.

3.2.5.3   Performance Validation

For validation the prediction model was evaluated on machine data collected during harvesting operations. There is an emphasis on obtaining data across different machines, field conditions, varieties, and regions in order to include a multitude of confounding factors in the data and bolster confidence in results. Prior to final validation, the lab-generated prediction model is tested on field data gathered in late 2014 and early 2015 to allow for adjustments to the prediction model due to unforeseen factors (and thus this is referred to as the training data). Performance is then assessed for the lab-generated MC% prediction model on the validation data, adjusted for findings during the training phase, and compared to the stated performance objectives. Note that module density information was not available during the early testing, but was available for the final validation data. It is accepted that adjustments made from training data may not be optimal without some knowledge of the population of module densities to ensure this factor has been properly accounted for. The result of this knowledge would indicate if centering the prediction model around one mid-point density across all conditions is a sufficient simplifying assumption, or if other factors which are easy to identify can be used as a proxy to density and facilitate adjustment of predictions in a reasonable manner. The presumption for performance assessment of this sensor is that module densities are not known such that they can be used to adjust predictions accordingly on a per-module basis, although the hypothetical scenario in which module densities are known is considered. Finally, using the validation data then the practicality of quantifying moisture on a per-module basis is revisited in terms of the real-time output to the operator as they would see it during operation.

Table 3.2: Summary of all field/machine data obtained for validation of the sensor MC prediction accuracy.

	Region	Time Frame	Number of Modules Sampled	Machine Type	Separate Days of Harvesting/Collection
TRAIN	Arkansas	Early Fall of 2014	25	Picker	4
	Southern California	Late Fall of 2014	14	Picker	3
	NSW, AU	Spring 2015	46	Stripper	4
VALIDATE	NSW, AU	Spring of 2016	53	Stripper	6
	NSW, AU	Spring of 2016	94	Picker	5
	South TX	Mid-Summer 2016	48	Stripper	4
	South, TX	Mid-Summer 2016	99	Picker	5
	North TX	Late Summer/Early Fall 2016	82	Stripper	4
	South TX	Late Summer/Early Fall 2016	98	Picker	4
	Georgia	Mid Fall 2016	5	Picker	1

3.2.5.4   Lab vs Field Response

As an additional initial check on the sensor response, the samples from modules collected in 2014 were also measured on the lab test stand the same way which was done to develop the baseline prediction model. This included repeated measurements of the samples in various orientations and over a 220 kg/m^3 density range. The only difference in this case was that MC% was not a controlled factor – it was measured on the test stand at the same MC% level as it was on the machine.

3.3   RESULTS
3.3.1   DEVELOPMENT OF BASELINE MC PREDICTION MODEL

3.3.1.1   Confounding Effects of Density and Material to Sensor Interface

The influence of density on raw cotton dielectric properties has been documented in other research by the authors [33]. That work targeted a range of densities between $160 - 250$ kg/m^3 (10-15 lbs/ft^3) to match typical densities found in harvesters that form round modules, since there has recently been widespread and rapid adoption of this style of harvesting equipment in industry [22]. Density can refer to the actual physical density as well as a dry density (after adjusting for MC). Physical density refers to total matter (in this case both dry material and water) in a given volume, while dry density refers to just the

dry matter independent of water. The applications that use moisture sensing are generally concerned with prediction of moisture content (MC), a quantity that is normalized to the mass of total material without regards to volume. On the other hand, the dielectric properties using typical electromagnetic sensing methods are highly dependent on the quantity of material packed into a given sensing volume, as well as the type of material. Thus both the effect of changing the mass in a given volume by compressing the material (all else constant) and the proportion of water to dry matter will be of significance and affect the dielectric measurements. Presentation, primarily as it relates to material interface with the sensor and including factors such as orientation or local clumping, is considered separate from density. The sensor design used for this work has been documented previously to be very sensitive to air gaps between the electrodes and material. Even a very small (0.254cm, or 0.1in) gap can have a large impact due to 90% of the final measurement influenced by material within the 1.27cm (0.5in) closest to the sensor, with the influence decreasing exponentially with distance perpendicular away from the sensor face. Since the location of the sensor is in the side of the machine and the belt tension on the cotton module is parallel to the sensor face plane (i.e., the cotton module is not being pressed directly against the sensor face), density and presentation may not be related. All else equal, it is conceivable that a higher density module could have poor contact and a lower density module have strong contact.

The effects of density and a small (0.24cm, or 3/32in) gap are shown in Figure 3.8 and include the results of testing four different samples: Two from pickers and two from strippers. These samples were all in equilibrium with typical room conditions of MC% and temperature prior to testing. Also, during testing they were kept in the same orientation before and after introducing a gap to control as many factors as possible. Visually it is easy to see a large discrepancy between gap and direct contact response for both the dielectric constant and loss tangent (the loss factors is not shown, but similar results were found as well).
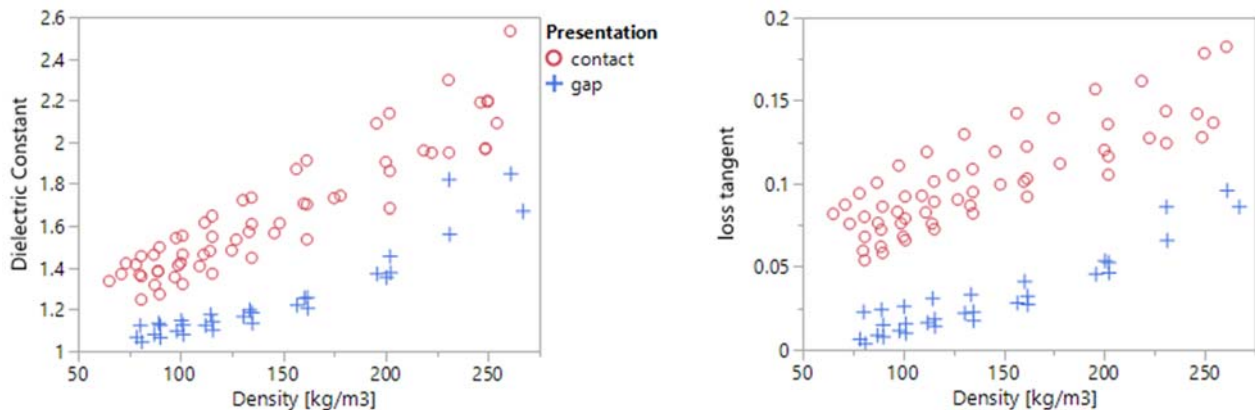
Figure 3.8: The effects of changes in density are shown for the dielectric constant and loss tangent using two samples of cotton harvested with pickers and two from strippers.

When the data is fitted while constraining the intercepts to theoretical values (Table 3.3) the difference can be quantified at any given density by taking the ratio of the mean dielectric value when a gap is present to the value when the same material is in direct contact with the sensor, as is plotted in Figure 3.9. Even with the same intercepts, since the slopes are very different the curves remain divergent over the typical density range. In the best case, when density is at the high end, the dielectric constant and loss tangent in the case of a gap will be 80% and 60% of their respective values sans gap.

Table 3.3: Fitted parameters of dielectric response to density from lab testing using cotton samples equalized to the same ambient temperature and MC conditions. With intercepts constrained to theoretical values, the response may be compared between presenting the same material with a 2.4mm [3/32in] gap VS direct contact as density changes.

Parameter = Fitted Slope + Intercept			
Parameter	Presentation	Fitted Slope	Intercept
Dielectric Constant	Gap	2.24E-5*Density	1
	No Gap	4.65E-3	1
Loss Tangent	Gap	2.69E-6*Density	0
	No Gap	$\dfrac{3.25E^{-3}}{Density^{0.4}}$	0
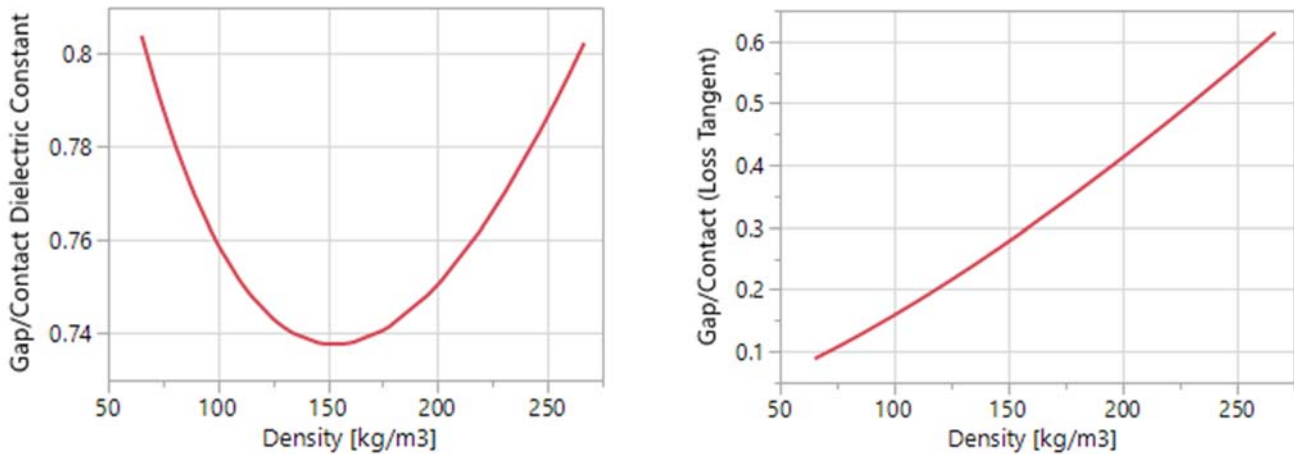
Figure 3.9: Comparative response of dielectric properties when gap is present to when there no gap. The y-axis is the ratio of the "Gap" to "No Gap" values (as calculated by the equations in Table 3.3) to indicate the level of difference at any given density.

In the case that the sensor maintains consistent contact with the material, density sensitivity is still a concern if the range of values in a given condition is large enough to induce substantial variability or local biasing in moisture predictions. In order to investigate the effects of density, first a prediction model must be fitted to examine the sensitivity in a way that relates to

57

biasing moisture predictions under controlled laboratory conditions. This is trivial to do using a multivariate regression, and in effect has already been done in previous work that includes a wide frequency range [30]. That same data is used here to build a predictions model ███████████████████████, and with focus on inverting the predictions such that dielectric properties are used to predict moisture. A dry density term is also included to quantify the confounding effect of density on moisture predictions. Further on, module densities are to be obtained during field testing and observed if any evidence of variation or biasing in predictions can be attributed to density under typical expected conditions for the sensor application.

3.3.1.2   Baseline MC Prediction Model from Lab Test Stand

Dielectric properties are not immune to density changes. Fitting the coefficients in the predictive model is done with consideration of known effects from previous research [30] and facilitates an adjustment to moisture predictions if any knowledge of density is available in a real-time application. Module densities and their associated effects are intended to be collected and quantified as part of the larger field testing and the performance assessment, but development from lab data serves as both a starting point and a basis for comparison. A prediction formulation for MC is developed that includes density as a covariate, and since the equation is a linear combination of the variables the density terms simply amounts to a bias applied that is relative to the effect of density. For a typical 2268kg [5000 lb] module of dimensions in Figure 3.2 at 8% MC, a mean dry density of 208 kg/m3 [13 lbs/ft3] was calculated for pickers and served as a baseline. The prediction model used for validation of the sensor was trained on lab measurements taken from a test stand designed with the intention to emulate module densities experienced on the machine. A more detailed description of the measurement process and the samples used to train the algorithm is available in previous work [30]. The relationships between dielectric values and MC% is known to be nonlinear from this previous research, and is shown for the lab-generated data in Figure 3.10. The loss tangent (dissipation factor) had a similar response and transformation as the loss factor and is thus not shown. As such, these transformations are the basis functions of the covariates used in the predictive model.
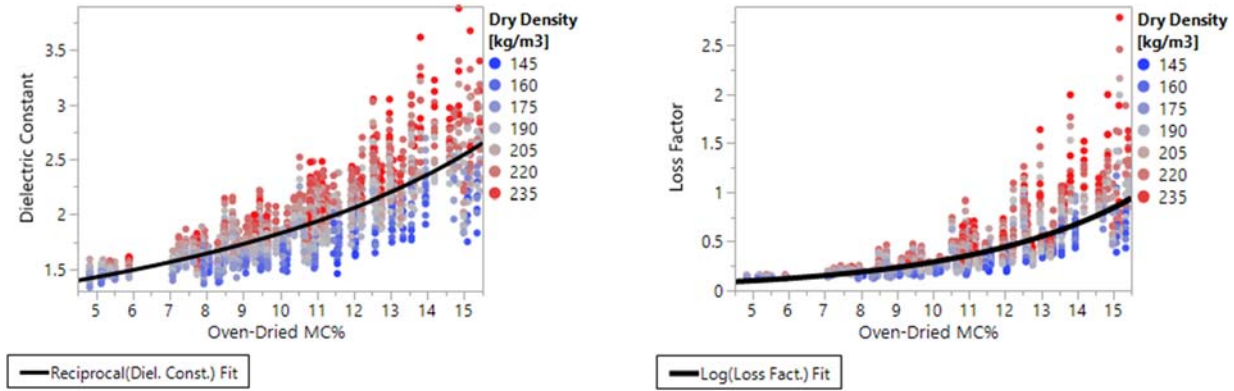
Figure 3.10: Raw dielectric response of sensor to moisture in cotton as found from lab testing. Points are colored by density; nonlinearity with MC and strong sensitivity to density as an orthogonal effect to MC is seen.

The fitted model is given in Table 3.4, and the sensitivity of MC% predictions (using dielectric properties) to changes in dry density of the material, all else constant, can be gleaned by the coefficient. Since increasing density has a positive correlation with the dielectric properties, the coefficient is negative to account for the effect when predicting MC.

Table 3.4: Fitted coefficients for moisture prediction statistical model.

FORMULATION	**Predicted MC%** $= \dfrac{1}{Dielectric\ Constant} * A + \text{LOG}_E(loss\ factor) * B + \text{LOG}_E(dissipation\ factor) * C + DRYDENSITY * D + E$				
LABEL	A	B	C	D	E
COEFFICIENT	-18.6	-1.66	2.64	-0.418 [1]	27.1

(1) Density is in lbs/ft^3. If density is in kg/m^3 then the coefficient is -.0261

Returning to the issue of density sensitivity, both the effect of increasing the concentration of material in a given area, as well as the effect of dry matter vs water are investigated using the above formulation. Since water in this case is constrained to be internal (or absorbed) into the material, changes in dry density result in changes of moisture within a given volume, while holding the moisture concentration constant in terms of percent by weight of material. Thus, for example, the effects of applying higher tension on the compressing belts in the module chamber can be observed. For the data generated in a lab environment, each change of 16 kg/m^3 (1 lb/ft^3) in dry density will induce changes in the dielectric properties that result in the equivalent change of 0.418 MC%, given all else remains constant. The true impact of density on performance of the sensor for moisture predictions is unknown though until the distribution of densities under typical operating conditions is known, and so field exposure while collecting module density information is imperative to understand the risk that changes in density pose to accurate predictions if they cannot be accounted for.

The main purpose of this work is moisture prediction, and so it is also desirable to understand the sensitivity to moisture compared to dry matter. An investigation was performed by a multivariate regression using MC% and physical (or "wet") density, such that holding the physical density constant it could be seen what replacing dry material with water would cause for a response in the predictions. The results indicate that replacing dry material with water induces 93% of the response as just increasing MC% but keeping dry density the same, and thus moisture has a significantly stronger effect than dry material.

3.3.2   CHARACTERIZATION OF GENERAL DIELECTRIC RESPONSE ON MACHINE AND RELATED CONFOUNDING EFFECTS

3.3.2.1   Rotational Dynamic Effects

In order to collect measurements from new material added as the round module is formed, unique dielectric measurements are obtained primarily while the module is spinning and module diameter is increasing. The operational states were logged from the machine communication bus. While variation from differences in moisture and constituents of cotton harvested is inevitable, the dynamics introduced at the module-to-sensor interface due to the rotational motion represents a potential additional source of error that had to be assessed. Results are presented in predicted MC using the formula in Table 3.4.

To begin investigation of discrete changes of measured dielectric values in the module, a module of approximately 1.75m diameter was rotated slightly in the module chamber and then stopped momentarily. This process was repeated many times during a single logging event to produce the figure below. Using the baseline MC prediction formula presented Table 3.3 this amounts to a mean of 8.3%MC with standard deviation of 0.3%, which serves as a baseline comparison to the measurements taken during subsequent dynamic tests on the same module. This variation is close to variation of actual MC found from sampling a dry module (Figure 3.7).

Discrete points can be seen as clumps of similar values close in time at which the module was static during dielectric measurement.
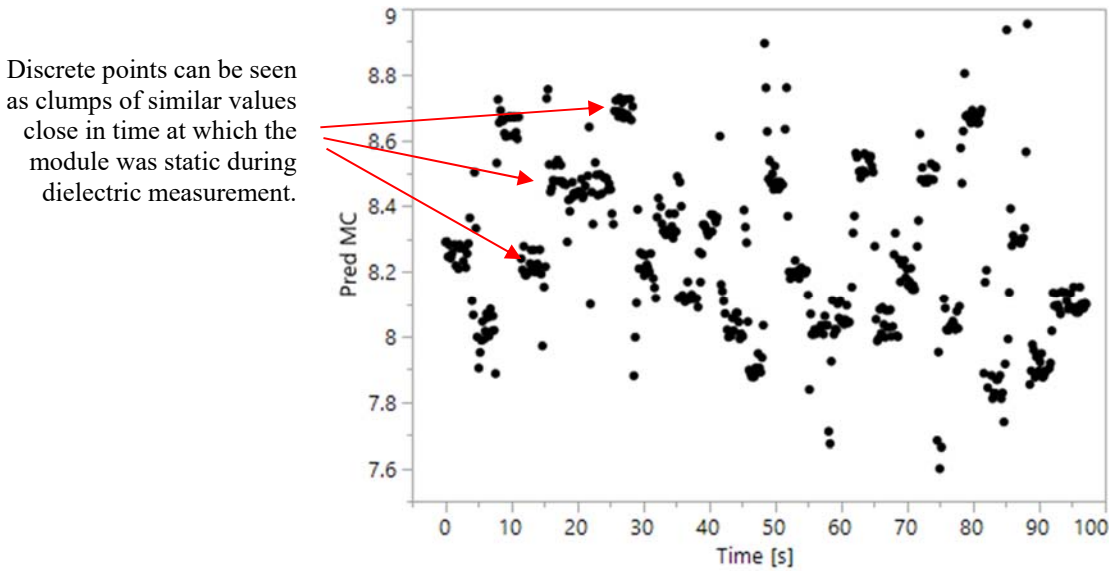
Figure 3.11: Discrete changes in the measured dissipation factor on a round module were seen by slightly turning a 1.75m module in the module chamber, stopping, and then repeating several times and recording the entire process.

Dynamic testing was then performed on the same module with the intent of observing any changes in the dielectric measurements induced by increasing rotational speeds. Testing was performed at seven different rotational speeds; from 0 to 120 RPM (in increments of 20 RPM). The results are shown in Figure 3.12 and Figure 3.13 for two quantities of specific interest; the mean and standard deviation of predicted MC. When compared using Tukey HSD and 95% CI, the mean for the module was found to be the same across all rotational speeds except at zero RPM. I.e., as long as the module is rotated to obtain a representative sampling around the module, the rotational speed does not influence the mean value. The standard deviation, on the other hand, does in fact change with rotational speed, following approximately a square root curve. The standard deviation of predicted MC for all rotational speeds except zero were larger than the standard deviation of static measurements taken around the module. The dynamics associated with increasing rotational speeds introduce variation in measurements above and beyond the actual variation in dielectric values in the module. It is presumed this is due to a combination of imperfection in the module face (e.g., variations in the density) and bouncing/jostling around of the module-to-sensor interface.

RPM	Group	Mean
100	A	8.3
80	A	8.3
20	A	8.3
40	A	8.2
60	A	8.2
120	A	8.2
0	B	7.6
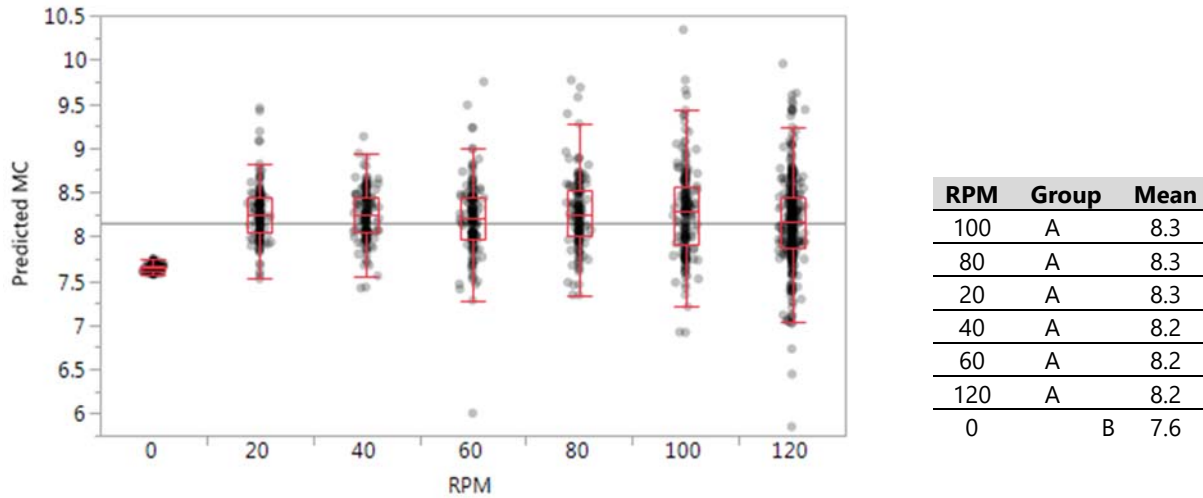
Figure 3.12: (Left) Box plots of predicted MC during each rotational speed test of the module on the machine. (Right) The mean predicted MC for each rotational speed was compared in the larger group using Tukey-Kramer HSD at 95% interval and a connecting letters report generated. The only mean that is significantly different than the others is the one with zero rotational speed (since it doesn't obtain a representative sampling of the entire module like the others).
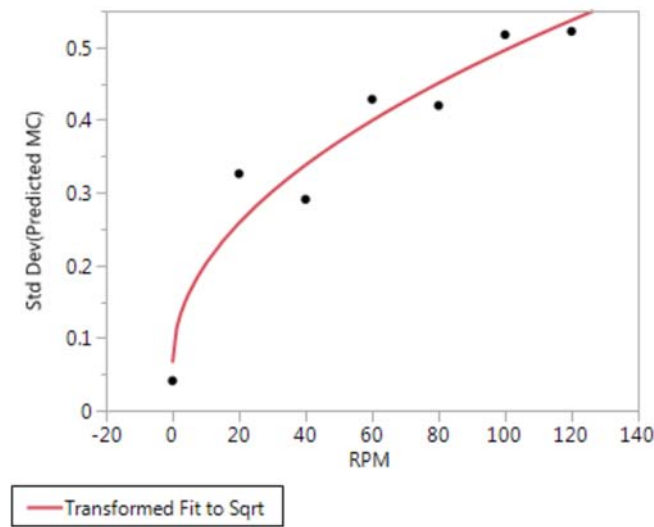
Figure 3.13: The standard deviation of predicted MC increased linearly with the sqrt of module RPM. For the same module, the stdev of predicted MC when static was 0.3%MC. The variation of measurements at typical operating speed of 120 RPM is therefore about twice the static case of Figure 3.11.

Earlier module variability testing showed consistency in the mean predicted module MC% (Figure 3.12) at all speeds, so long as the module was rotated at some speed above zero. This, however, does not preclude the possibility of a gap or similar situation, resulting in the material at the sensor interface to be otherwise less consistently in contact with the sensor such that a low bias is induced as was detailed in Figure 3.8.

3.3.2.2   Distribution of Measurements within a module

On average, individual modules were found to form somewhere between 10 and 11 minutes ███████, with only half that time or less devoted to rolling new material into the module. Two typical examples of the process taken arbitrarily from picker machine logs are shown in Figure 3.15, for which moisture predictions were made using the equation described in Table 3.3. Cotton is accumulated within the machine and rolled into the module in irregularly-spaced intervals, as can be seen by the times where the module diameter increases. The process variation indicates the need to filter the real-time output for the operator, as well as the need for some additional investigation into the most suitable method to summarize the moisture of the entire module, such as will be needed for performance evaluation. Measurements while the module is static and/or module diameter is not increasing indicates no new material is being fed into module, and thus a simple average or median of all measurements is not sufficient since it would weight long periods of inactivity very heavily. Additionally, when the module is static (as can be seen when the module diameter is not increasing), the measured values were found to sometime be far off the average value measured while the module is turning. It was not difficult to find such cases in the recorded data, and thus further investigation into whether the dynamics may induce a bias is needed. On the other hand, the mean predicted MC during each instance in which the module diameter was increasing (and thus rotating the module) tended to be much more consistent, as would be expected from the results in Figure 3.12.
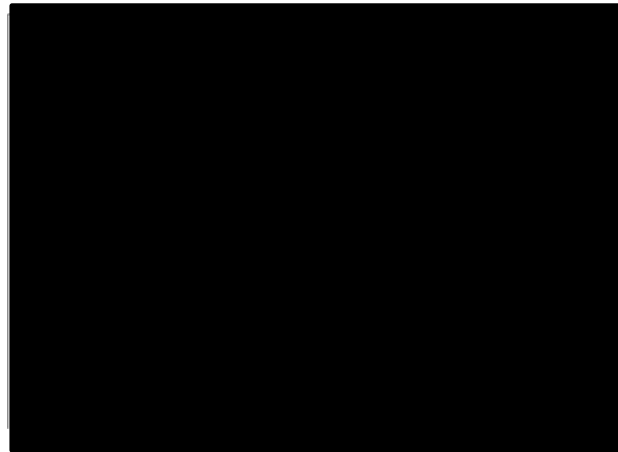
Figure 3.14: ███
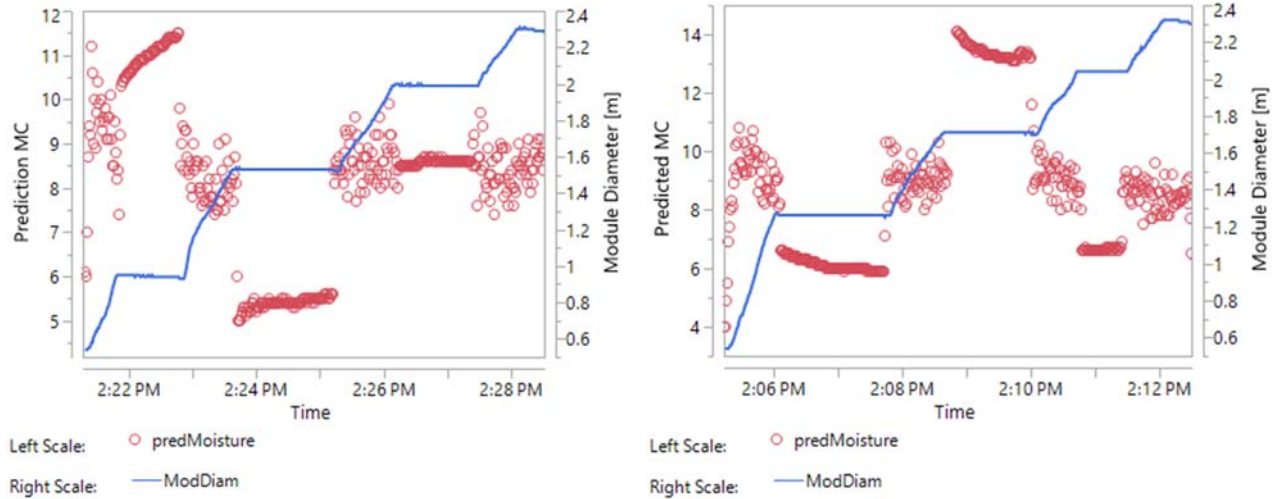
Figure 3.15: Predicted MC% values during a typical module formation process for a single module is shown in each plot.

A simple mean or median of all measurements is not satisfactory since it would weight non-rotational periods (in which the same material is measured for upwards of two minutes) very heavily. Since the module diameter signal is available on the machine communication bus and updated faster than 1 Hz, it can be used to limit predictions to specific states of machine functionality. This is step one of filtering. By taking the mean predicted MC at each unique module diameter value during the formation, the long periods of time where no new material is being added are not given undue weight in the determination of the module moisture from all the measurements of the module. An example of the resulting predicted MC during formation of a module after grouping and averaging predictions by module diameter to obtain one prediction for each unique module diameter can be seen in the left plot of Figure 3.16. This is step two of filtering. After doing so, the resulting number of measurement points per module is still large, with each data point representing unique material.
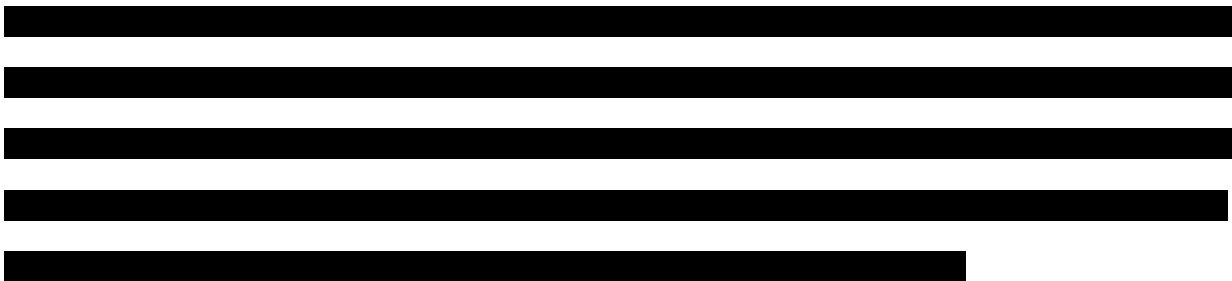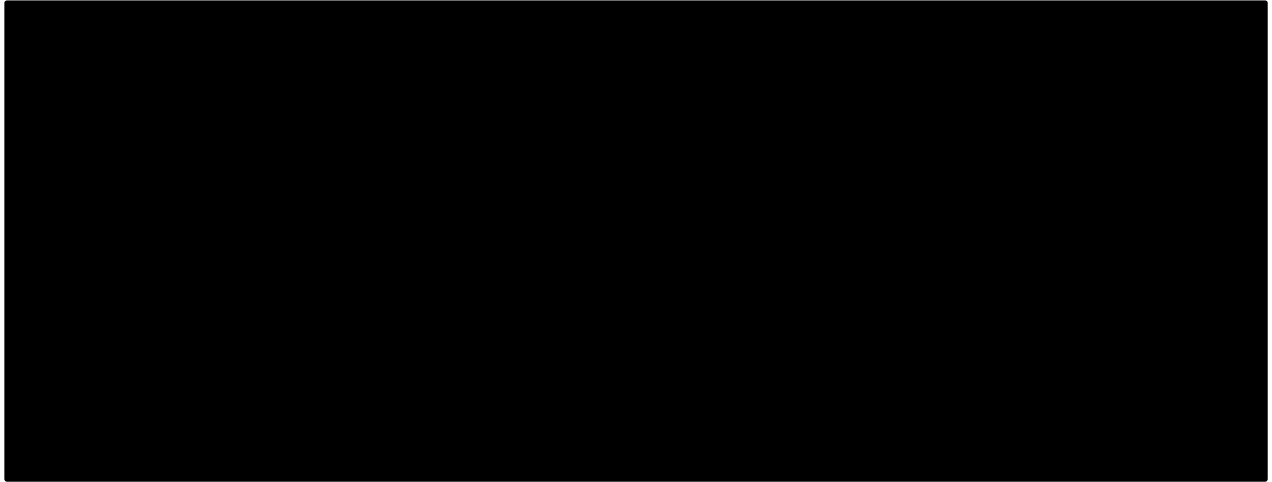
Figure 3.16:
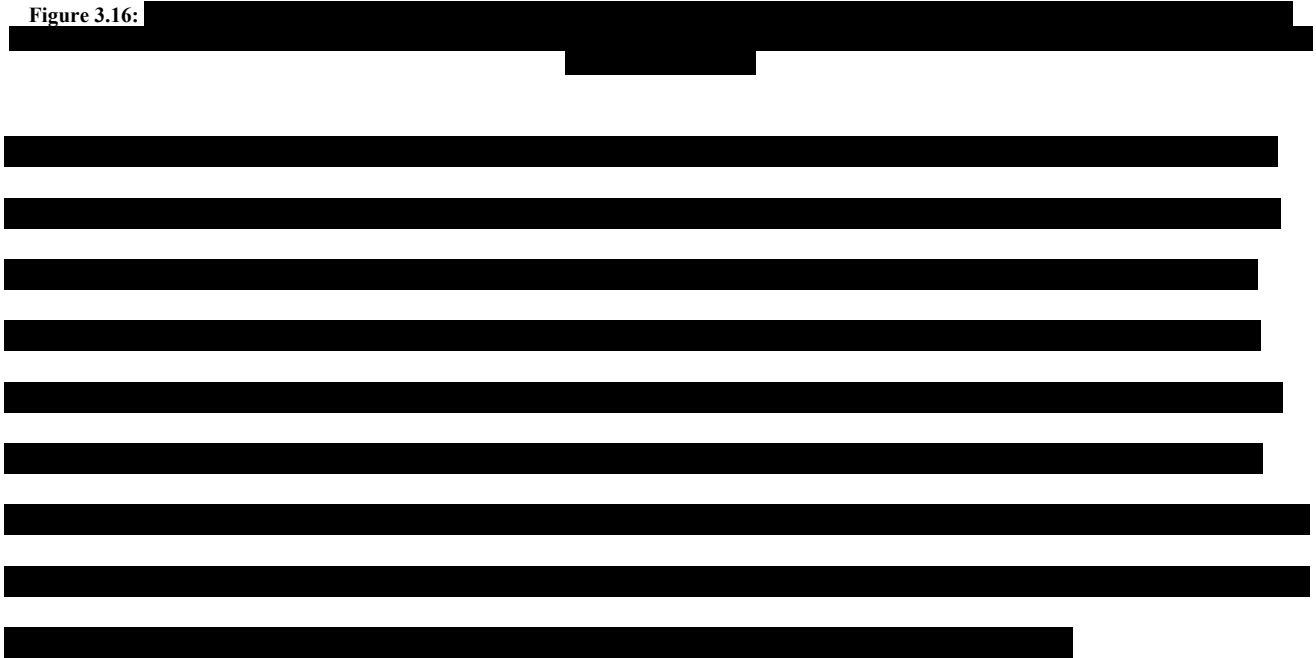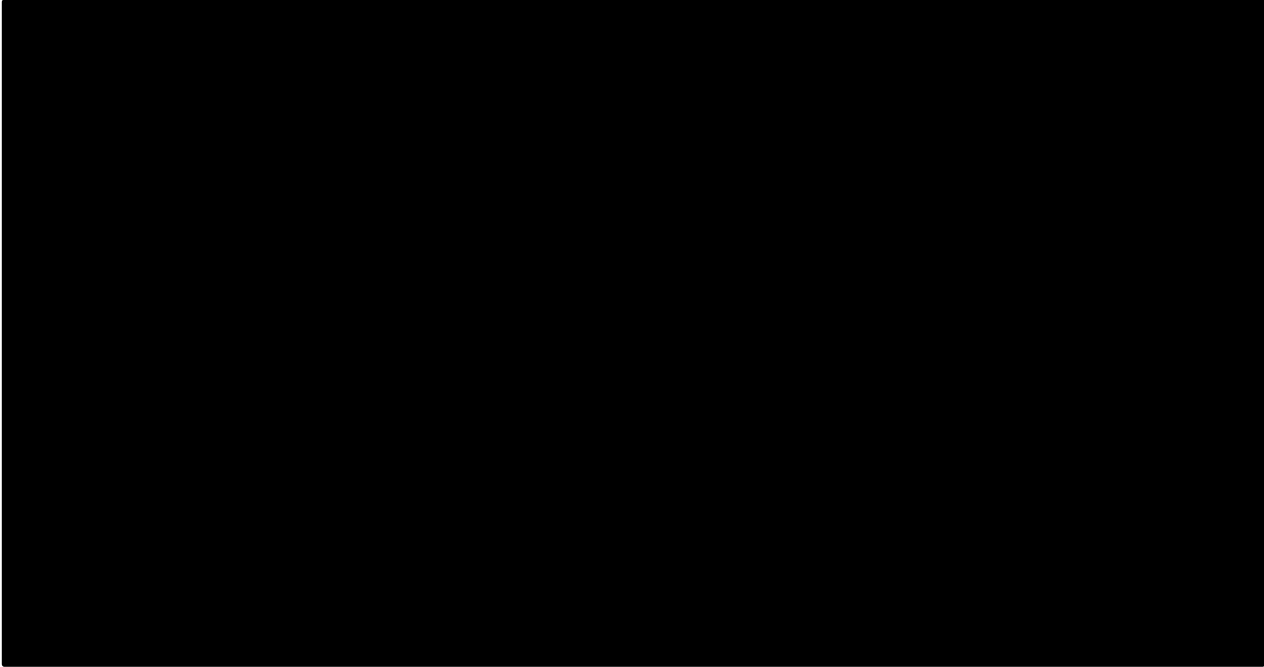
Figure 3.17: ██

3.3.2.3   Single Filtered Predicted MC per-Module

Once filtering and averaging by diameter has taken place to ensure all material is equally weighted, the module can be summarized by one predicted MC value. Since dew was found to be the primary cause of moisture changes in cotton, it was projected that the MC would not typically vary appreciably amongst the material in a round module (such as finding wet spots), and as such performance assessments on a per-module basis is appropriate. Other sources support this and indicate a diurnal (U-shaped) curve throughout the day that starts with high MC%, and as the dew dries off reaches a minimum in mid-afternoon, which subsequently increases again as the temperature drops towards and below the dew point ([28] [29]).   When distributions of the predicted MC of several hundred modules from both pickers and strippers are overlaid centered at zero as shown in Figure 3.18, attempting to fit a Normal distribution indicates the data is unlikely from a Normal distribution (p-value < 0.01). The corresponding Normal probability plot visually indicates skewness and an especially long tail on the high-side. Due to a strong deviation from normality, a median is used for single-module summaries since it is known to be a robust (especially to outliers) estimator of central tendency.
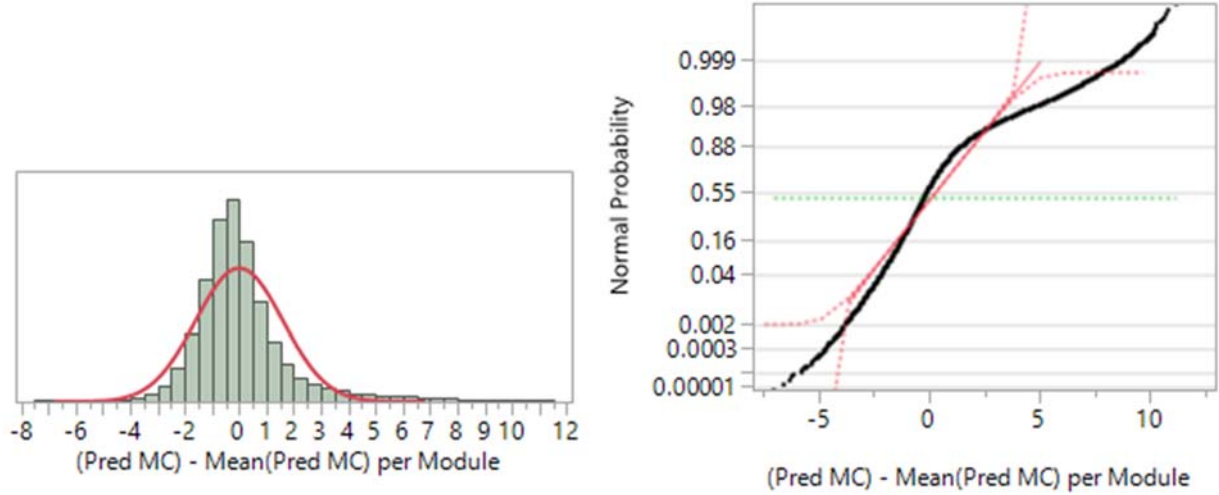
Figure 3.18: (left) Distributions of predicted MC for several hundred modules from pickers and strippers aggregated and centered at zero and overlaid with a [red] Normal distribution fit. A p-value < 0.01 suggests that the distribution is non-Normal. (right) A Normal probability plot of the same visually indicates the non-Normality.

The total filtering criteria to get to one prediction per module then is shown in Table 3.5. Using a median of the predicted MC per module then, diurnal trends of the predicted MC per-module appear (e.g. Figure 3.19) and demonstrate adequate resolution on a per-module basis to capture the larger daily trend. The smooth trend also shows promise that when filtering in this way the sensor can meet the criteria of smooth tracking, yet responsiveness to changes. Concurrent assessment of the trend of oven-dried samples is necessary to prove this though.

Table 3.5: Conditions for filtering predictions from sensor to obtain one value per module.

Step	Label	CONDITION
1	*FILTER_1*	Only consider measurements when module is rotating
2	*FILTER_2*	Average(*FILTER_1*) by Module Diameter
3	*OUTPUT*	Median(*FILTER_2*)
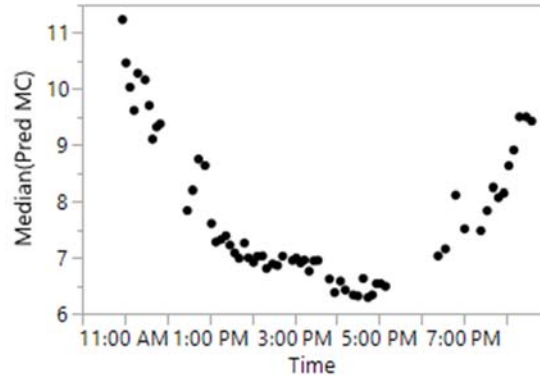
Figure 3.19: Predicted MC response using a median per module on a stripper machine for one day of harvesting showed expected U-shaped trend. Resolution of changes in MC throughout the day from module-to-module also appeared satisfactory.

3.3.2.4   Sensor Face Pressure

Further testing was conducted with the sensor replaced by a panel instrumented with a strain gauge to observe if contact was being made between the sensor and module, or if it was possible that gaps were present and causing discontinuities in the sensor response. This test was conducted on both stripper and picker machines. The force on the plate during the course of forming a round module on both a picker and a stripper are overlaid in Figure 3.20. There were no obvious signs of a gap from the pressure plate data on either pickers or strippers since the force was mostly positive, and with exception of much higher variability in the stripper during rotation. The higher variability in the stripper recordings (even to the point that negative force is recorded) was attributed to the modules being relatively lumpy compared to ones made by a picker.

While no obvious signs of consistent non-contact events were identified during this experiment, the force on the plate appeared to generally increase after the module stopped moving, as can be seen in the periods of low volatility in the signal in the left plot of Figure 3.20. This recording was taken after zeroing the force following the initial influx of material in the module pressed against the sensor. If similar features are present in the dielectric measurement signal as well it could suggest expansion of the module at rest to increase local density.
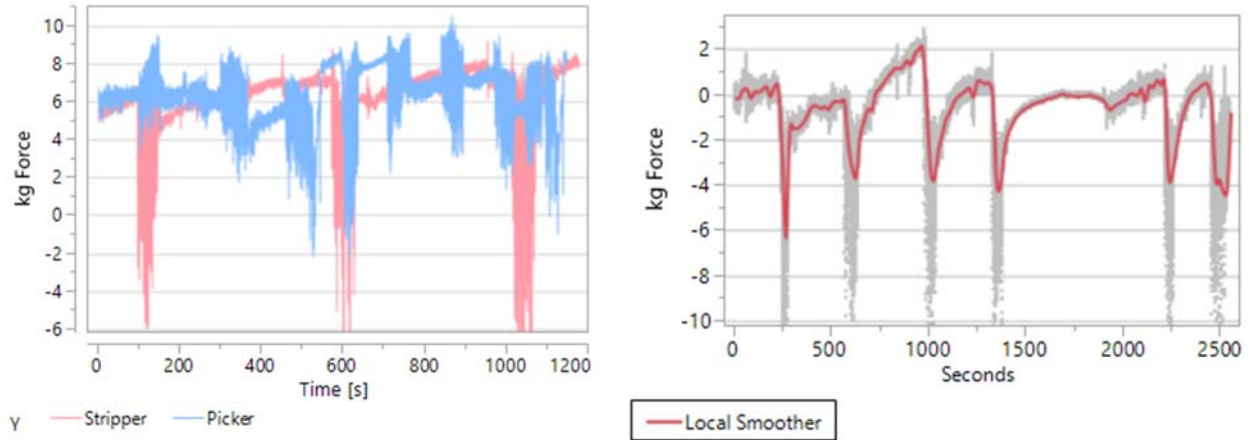
Figure 3.20: (left) Force against strain-gauge plate in place of sensor is compared during the course of making round modules on both a stripper and picker machine. (right) Force on plate while making a module on a stripper is zeroed at the start of a module to facilitate easy comparison to the rest of the module as it is made.

Unfortunately, to measure the force at the exact location of the sensor face the moisture sensor cannot be simultaneously in the machine while the force at the mount location is recorded by the strain gauge, so we are left to compare this to the typical scenario found in other logs. While several instances could be found of the dielectric values increasing while the module is not spinning any new material in during normal harvesting conditions on strippers, the typical response is random and unpredictable, similar to Figure 3.15, in which the values may increase, decrease, or remain constant after the module stops spinning. While these types of changes do imply a sensitivity to small local changes at the sensor to module interface (since the actual material is not changing appreciably), no conclusive or consistent effect is gleaned from the change in force on the plate. When the force during two modules was overlaid and plotted against module diameter (Figure 3.21), a distinct trend emerged which, while intriguing, did not resemble the predicted MC trend in Figure 3.16. Therefore it seems likely that as long as there is contact with the sensor, the force does not have much influence on or direct correlation with changes in predicted MC.
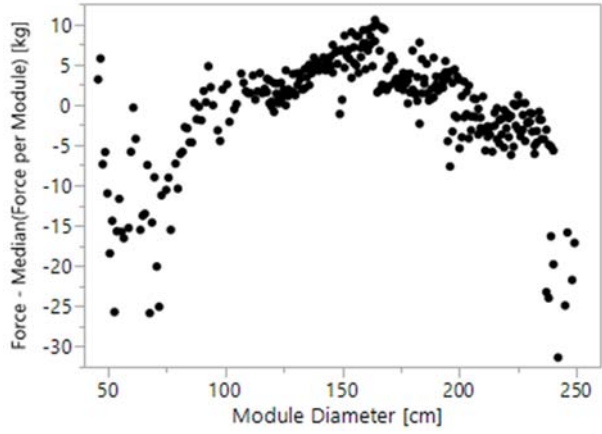
Figure 3.21: Force on plates for two different modules on a picker (each centered at zero by subtracting the median force for each module) overlaid and plotted against module diameter. Trend is distinct but does not bear a resemblance to the averaged predicted MC trend in Figure 3.16, and as such does not suggest any notable influence on dielectric measurements from contact pressure.

3.3.2.5 ███████████████████████

██

██

██

██

██

██

██

██

██

██

██

██

██

██

███████████████████████████████████
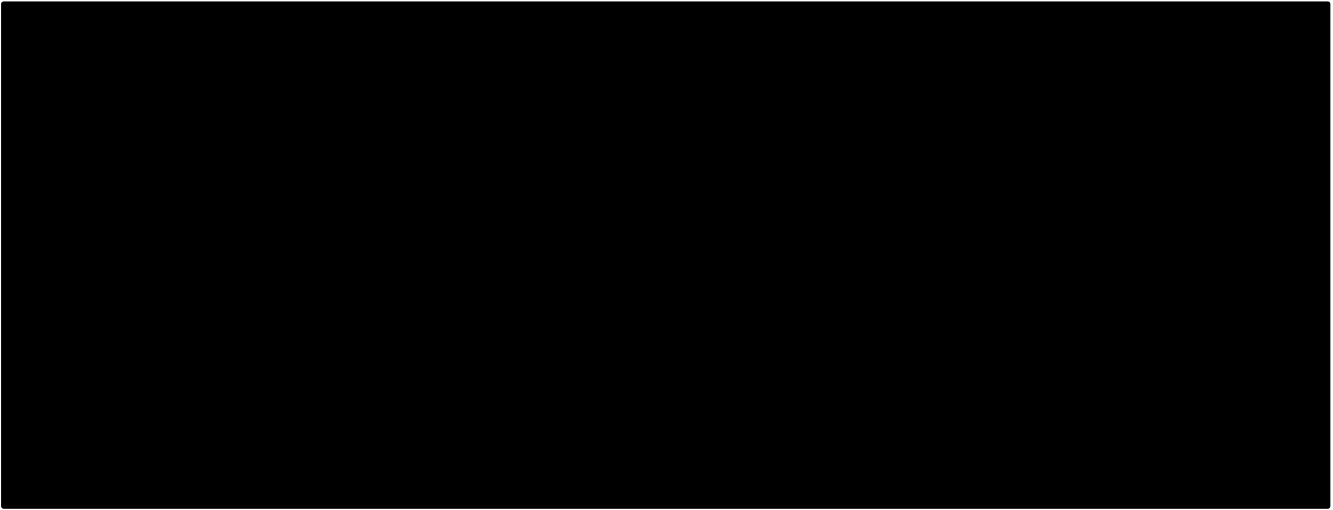
Figure 3.22:

3.3.3   PRE-VALIDATION (TRAINING) OF ON-MACHINE RESPONSE

Using the final output then from the filtering scheme detailed in Table 3.5 to obtain a single value representing the central tendency of predicted moistures per module then, a performance analysis is done on the training data by assessing the predicted (using baseline formulation) against actual MC% determined by sampling the module and oven-drying the samples. As noted earlier, it is not unexpected that some differences may present in the field work between the response generated from lab data and that of field data to cotton of the same dry density and moisture content. Performance was evaluated on the picker data obtained from Arkansas and California in 2014, and stripper data from AU in 2015, by observing the bias and variability of predictions against actual MC% as shown in Figure 3.23. The resulting bias showed picker predictions were biased low by 0.74 MC% and strippers by 2.55% MC. According to the density coefficient found from multivariate regression and shown in Table 3.4, a density on the order of 32 kg/m^3 (2 lbs/ft^3) would be necessary to induce a difference of this magnitude in pickers (and much larger for strippers), were density the cause. If the bias is consistent the problem is easily remedied with a constant offset added to the intercept of the prediction formula. Also, the two regions (AK, CA) can be seen to have clustered trends that may be due to other factors such as regional differences or machine differences, which is difficult to say for certain without controlling for one of these factors.
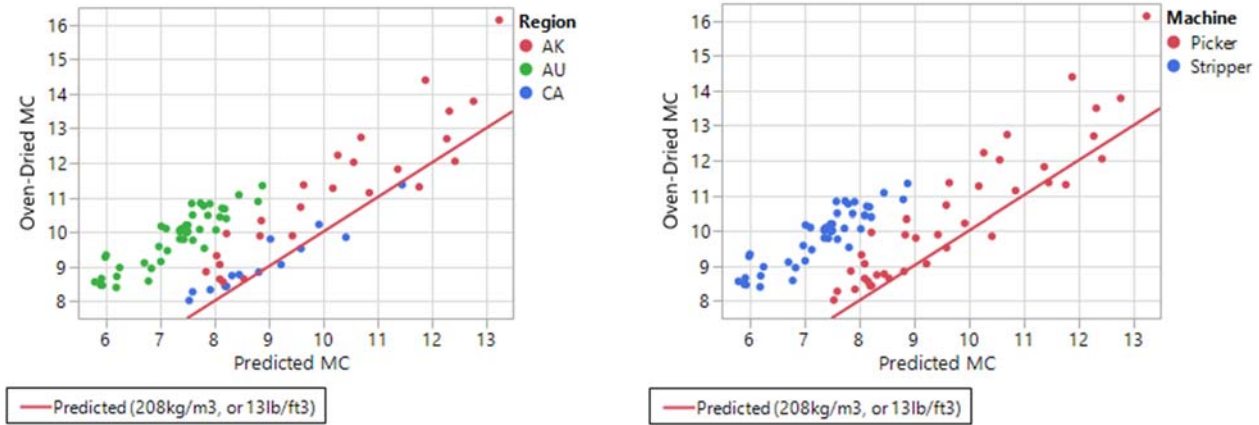
Figure 3.23: (left) The baseline prediction formulation, using machine-based measurements, is plotted against MC% found from oven-drying and colored by region. Overlaid is the perfect prediction line centered at 208 kg/m^3 and indicates a sizable bias in the predictions (right) the same predictions are colored by machine.

Table 3.6: Table of intercept or bias adjustments (from baseline formulation) with associated standard error of the mean when data is adjusted according to two factors, machine and region. In no case is the bias considered statistically the same for any two levels within either factor, but the difference is far larger between machine types than between the two locations from which picker data was obtained.

Factor	Level	Intercept (Bias)	Std Error
Region	Arkansas	1.05	0.165
	Southern California	0.2	0.095
	NSW, AU**	2.55	0.128
Machine	Stripper	2.55 (Same as NSW, AU)	0.128 (Same as NSW, AU)
	Picker	0.74	0.053

** Dry densities obtained from three modules were between 181 to 193.8 kg/m^3 [11.3 to 12.1 lbs/ft^3]

Machine type is an attractive factor to adjust the bias by since it is easy to identify and doesn't change once the sensor is installed. When the baseline prediction formulation is adjusted for by machine type, the resulting residuals across the MC range are fit using Kernel regression (kernel smoother) to find the local MAE (or mean absolute error), with the target of less than 1% MC (which has been stated in the objectives) highlighted by a horizontal line for each machine. This objective is met with a margin of greater than 0.2%MC in both picker and stripper machines through the key range of 6-12%MC.
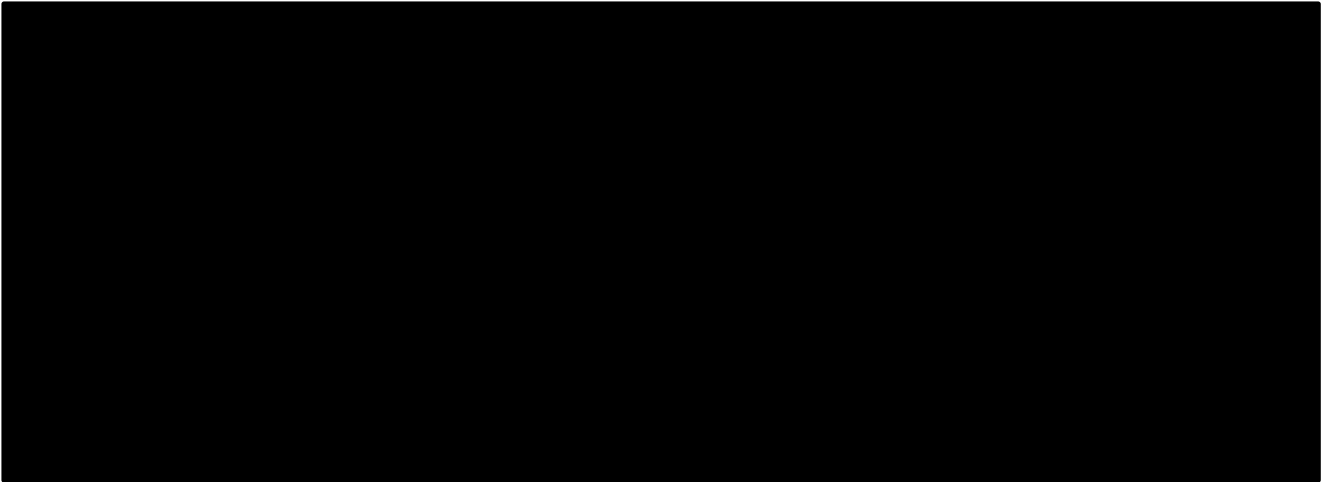
Figure 3.24: ▮▮

3.3.3.1   Field VS Lab Predicted Moisture

As noted in the materials and methods section, the samples collected in 2014 from the round modules in AK and CA (Table 3.2) were sent back to the ISU lab to obtain moisture content by drying in ovens. Prior to drying to obtain MC%, the samples were measured across the same lab test setup used to generate the prediction equation for MC%. Since the lab test stand holds all other factors constant besides moisture and density (which are measured and accounted for), this enables a comparison between the samples from the two regions to determine if material property bias could explain the difference in response on the machine. Variety has been shown to be a factor in previous work [30]. When studied under controlled conditions, the results were very surprising, showing that the mean by region (after accounting for MC and density) amounted to a 1.3% MC offset high in predicted MC for samples from AK compared to samples from CA – which is of opposite sign of the difference seen in the field (p-value < 0.0001). In any case, these results effectively eliminate material properties as a plausible source of the difference for the machine-measured values in this case and suggest multiple sources of bias could be present that are not well understood.
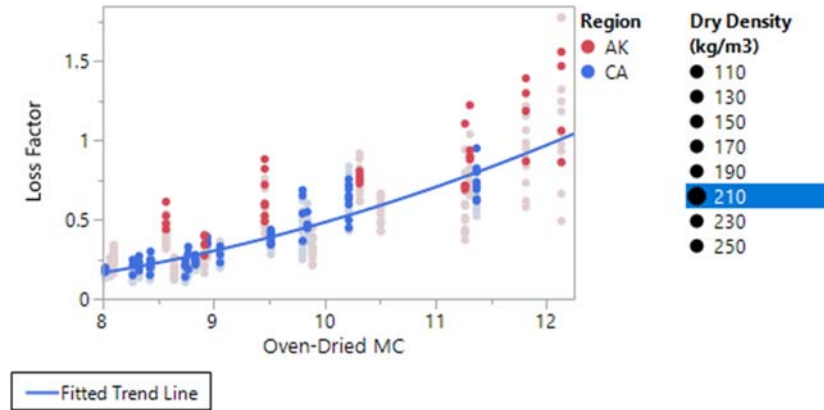
Figure 3.25: For the same MC and density (210 kg/m³ highlighted here) the AK data had a higher dielectric response than the CA data (opposite sign of the difference seen in the field). The dielectric difference amounted to a predicted MC difference of 1.3% MC.

3.3.3.2   *Conclusions from Training Data*

The effect of density on the machine is not fully understood and characterized (including possible interactions with machine type, variety, harvesting conditions, etc) suffice to say it is different than the lab response as shown in Figure 3.22. Additionally, a lab assessment of the samples from CA and AK indicated a difference in the response due to material properties opposite of that seen from the field measured data, further implying multiple factors could be interacting. Adjusting bias by machine appears to be the best (and arguably only) option for validation. It does have advantages though due to simplicity of assumptions and ease of identification when compared to density, variety, field conditions, or operational differences – where the effects of such factors are known. Furthermore, when applied to the training data the results are satisfactory and even have some margin to absorb further variation in validation data while still meeting performance goals.

3.3.4   *FIELD VALIDATION*

As with the training data, the accuracy of the model is assessed by comparing the median predicted MC% per module to estimated MC% of the round modules found through collecting and drying samples from those respective modules. The prediction formulation for validation has been adjusted by machine with the values shown in Table 3.6. Unlike the training dataset though, module wet densities were obtained for all validation data described in Table 3.2 with corresponding moisture samples. Module densities and MC% were collected during other field work for which sensor measurements were not available, for a total of 1052 modules where dry density could be calculated. When observing the distribution of dry densities, it is clear there is a Normal mixture distribution with three modes (tri-modal), which is fit using EM algorithm. The tri-modal distribution implies two seemingly discrete modes or conditions for each machine. Picker and stripper ranges overlap under certain conditions that result in generally higher densities in strippers but lower densities in pickers. The

means from lowest to highest are 172, 195, 211 kg/m^3 [10.8, 12.2, and 13.3 lbs/ft^3], respectively.
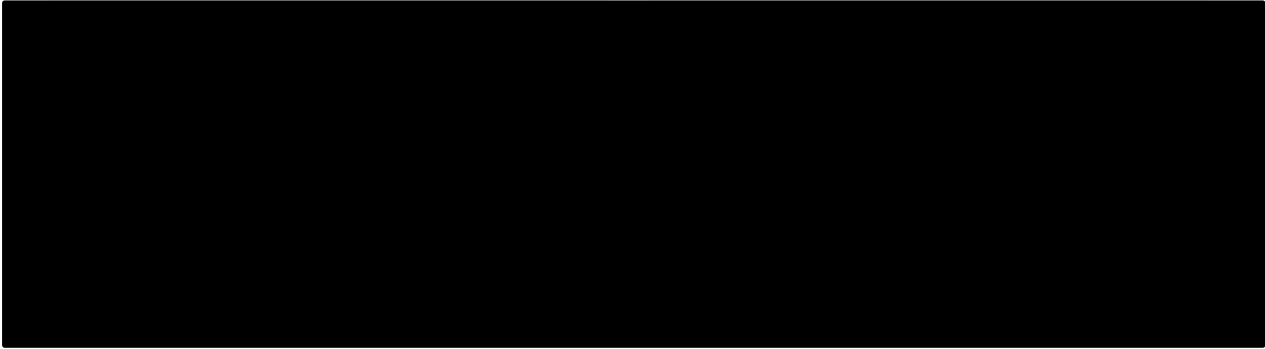
Figure 3.26:

The three density levels, hard-classified by maximum liklihood clustering according to the distribution in Figure 3.26, are colored and shown in a plot of the baseline prediction formulation against the oven-dried MC in Figure 3.27 (left plot). Three trend lines with the same slope as the original are drawn with fitted intercepts and confirm the visual separation between the groups does indeed follow the normal mixture. However, classifying by machine captures most of the difference that density does and with arguably less "noise" (more reliable separation), as shown in the right plot of Figure 3.27. This could be due to error in the density measurements, or possibly other factors causing variation that are yet uncharacterized (such as the difference between CA and AK data displayed in Figure 3.23).
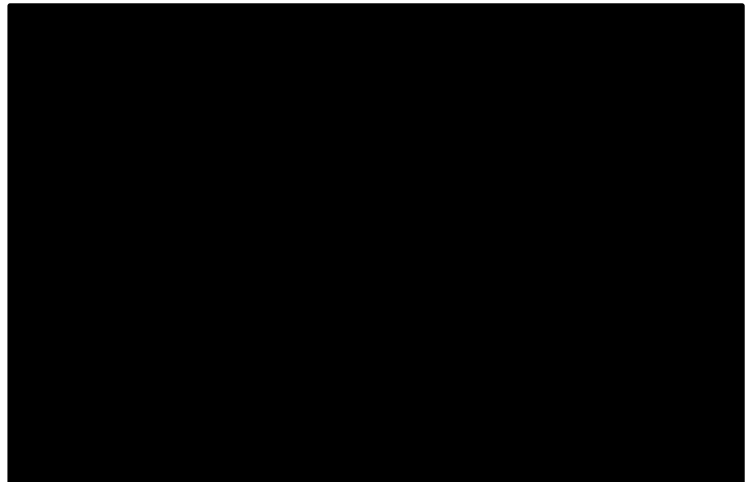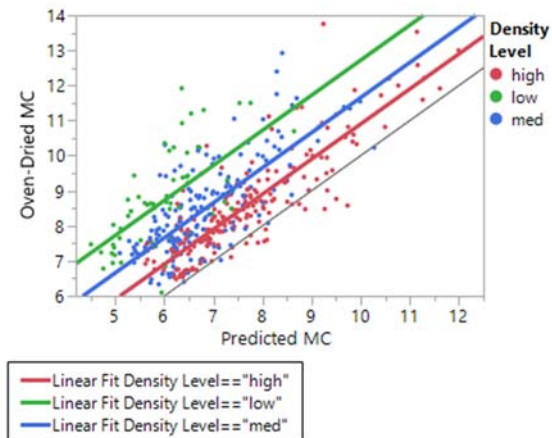
Figure 3.27: (left) All validation data is categorized into three discrete density levels based on maximum likelihood clustering according to normal mixtures in Figure 3.26Error! Reference source not found..

Using the bias adjustments of the MC prediction by machine fit in the training data, the validation data is plotted against and overlaid with the adjusted prediction line in Figure 3.28. One controversial aspect of this type of validation is the number of data points validated in any given condition is very hard to control since it is neither known beforehand nor are all the

influencing factors identified and characterized to facilitate such consideration. For instance, if the oven-dried MC values from pickers are fit using the trained prediction curve and density as fixed effects and region (loosely defined as clusters of data separated by large distances on a map) as a random effect, the region factor accounts for nearly 1/3 of the total variation (this could be machine/operations related, or material properties). As such, an argument could be made to weight the data evenly among spatial clusters (among many other ways to weight the data), but this gives more weight to each sample in conditions with fewer data points, which is also debatable. Therefore, it is recognized that conditional bias is likely present in the data, but still here all data points are still treated as IID in the performance assessment since setting each point as IID is determined by the authors to be as good as any given what is known at this point.
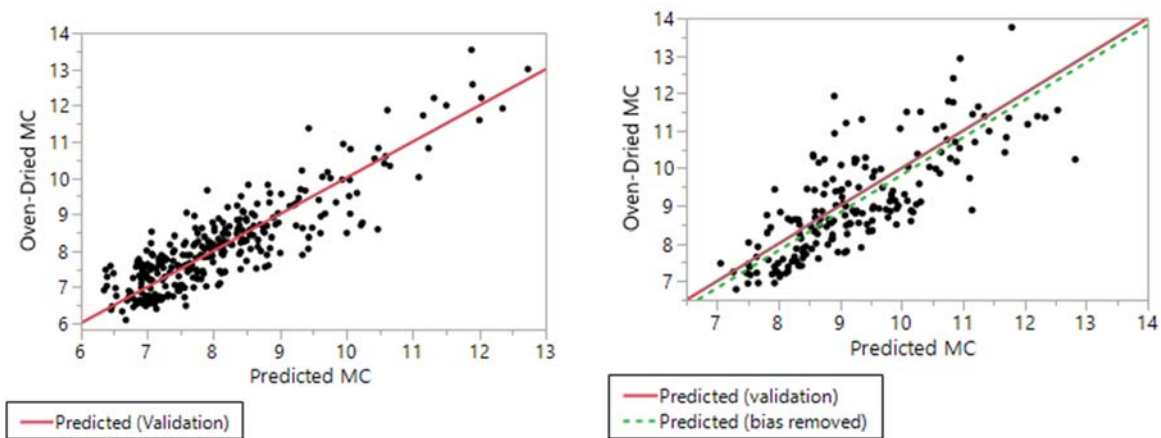
Figure 3.28: (left) Picker field data overlaid with prediction line fit to training data (validation line). The results show a bias of 0 and RMSE of 0.61 MC%. (right) the same for stripper machines using prediction line fit to training data (validation line). These results show a bias of -0.18 and RMSE of 0.89 MC% (when bias is included).

The MAE for validation data is summarized in Figure 3.29 as it was for the training data. ████████████████████ ██ If the small bias present is adjusted for the unbiased fit to MAE would cross at 12%MC. This tends to be the point which operators will no longer harvest, and so it is important for the sensor to be accurate at these moisture levels. For comparison, the performance/accuracy of the picker data is similar to that reported for moisture sensors used for clean lint cotton in commercial gins *after* slope and bias correction and under much stricter conditions of material, temperature, and density, with half of the MC% range seen in this data set [33] [34]. Although the stripper data marginally fails the stated objective, the usefulness of the sensor to achieve enhanced agronomic and machine decision support is apparent in the correlation to ground truth moisture. Furthermore, the sensor seemed to track the daily moisture trends on strippers as well as it did on pickers (Figure 3.32), which weighs heavily in the soft-objective criteria.
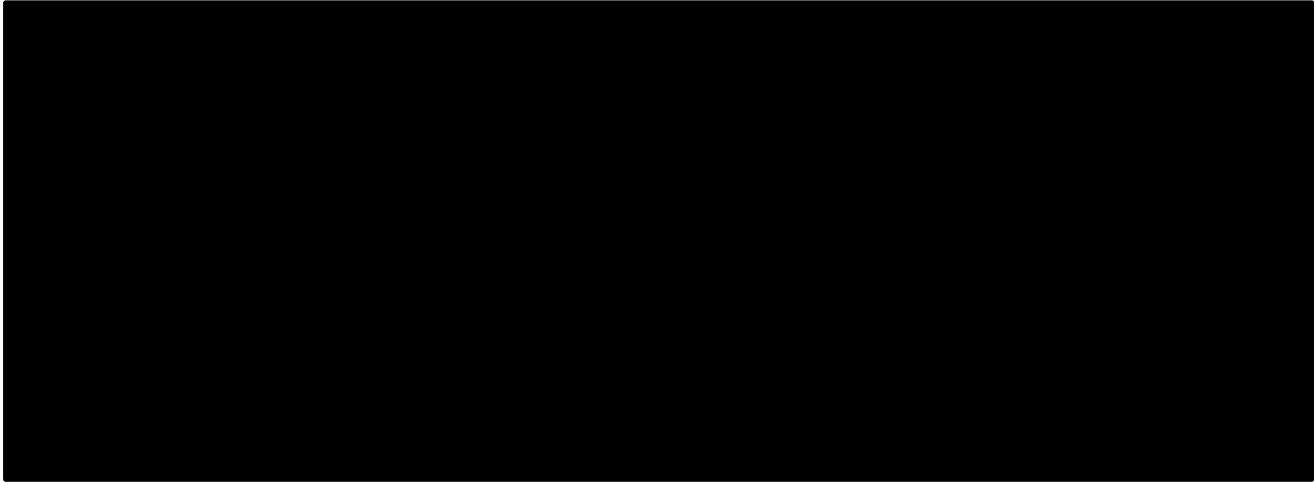
Figure 3.29: ▮▮▮▮▮▮▮▮▮▮▮▮▮▮▮▮▮▮▮▮▮▮▮▮▮▮▮▮▮▮▮

When the picker and stripper data is aggregated and a multivariate model fit with dry density and moisture, the effect of density found was as a change of 0.63 in predicted MC% per 16 kg/m^3 [1 lb/ft^3] change in dry density. Note that fitting with physical density (unadjusted for MC%) produced similar results as dry density, and a real-time implementation of density correction would have to use that since an on-board system exists that could provide it. For the modules included in validation, there was not a significant improvement by using a density correction factor instead of applying a bias by machine since it appeared that the majority of difference due to density is captured when accounting for machine type anyways from Figure 3.27.

3.3.5   REAL-TIME SIGNAL AND FILTERING

3.3.5.1   Real-Time Display of Moisture

During field data collection it was apparent that operators are readily able to gauge when to start harvesting. The primary goal in moisture sensing during harvesting operations pertains to the feedback provided to aid in determining when harvesting conditions are no longer ideal, or possibly identify modules that are wet to a point they might need to be prioritized in processing. The point-to-point real-time signal as seen in Figure 3.15 is not much use to an operator without some kind of filtering though. Averaging the measurements for each incremental module length and then using the median value of those for a single prediction appeared promising though, as seen in Figure 3.19. The characteristic "U" or "V" shaped trend of MC% in the harvested cotton that happens throughout the day [28] [29], with sharp increase in moisture content between 4-6PM each day when the dew point is breached, was found to be typical behavior. The soft-target objective of tracking daily trends still needed to be evaluated though in light of the actual rate of change in moisture at pivotal times of the day, as well as the corresponding variation in both actual and predicted trends compared. From three years of data, two days in

which the most rapid changes in these trends were experienced are shown in Figure 3.30.
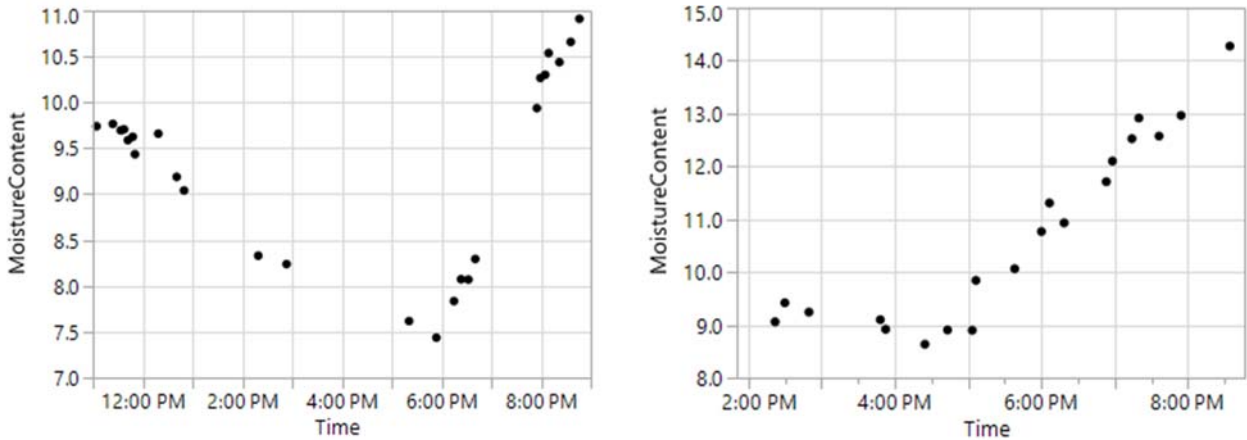
Figure 3.30: Rate of change of moisture (left) 1.27 MC% per hour on 11/21/2015. (right) 1.35 MC% per hour on 12/8/2015

Observing moisture changes throughout the day is obviously most convenient if it can be done on a module-to-module basis since it is a natural unit for this application. From Figure 3.30, even if MC changed 1.5% per hour in very extreme cases, since modules are generally made in under 20 minutes as seen in Figure 3.14, in extreme and unlikely circumstances there is a worst-case resolution of 0.5% changes using the average harvest rate. Most changes in MC% from module-to-module were of similar smoothness as Figure 3.30, and if the predicted MC% trends from module-to-module are nearly as stable, then there is little benefit to providing an output of the MC% within a module since the resolution will be adequate for the primary use cases. Plotting the per-module predicted MC% over the course of a long day of harvesting from AK 2014, the time series output in Figure 3.31 can be seen to be very smooth yet still fully captures the characteristic U-shaped MC% trends found with the oven-dried MC% values (and expected from other references [28] [29]) throughout the day, thus supporting the operator's decision of when to quit harvesting each day. Likewise, the resolution on a per-module basis is adequate for management decisions regarding wetter modules. In this case the bias noted in Figure 3.28 was unaccounted for in the predictions. Further plots of picker and stripper data from 2016 shown in Figure 3.32 account for a bias by machine (using the adjusted values in Table 3.6) in the predictions and depict the usefulness as the predictions accurately follow the trends found in oven-dried samples from the same modules.
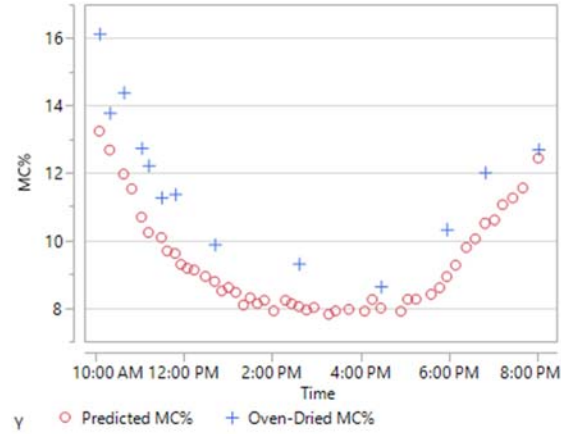
Figure 3.31: Predictions and oven-dried MC% are overlaid during a full day of harvesting. Characteristic U-shaped trend throughout the day is clearly seen. Moisture predictions are unadjusted for bias in this case.

In some cases such as the end of the day in the right plot of Figure 3.32, the predicted MC trend on a per-module basis was clearly more smooth than the trend found from samples from the same modules, thus it could be argued that "unlucky" sampling from the module and/or some error in the lab analysis processing is present and the predicted values are more accurate.
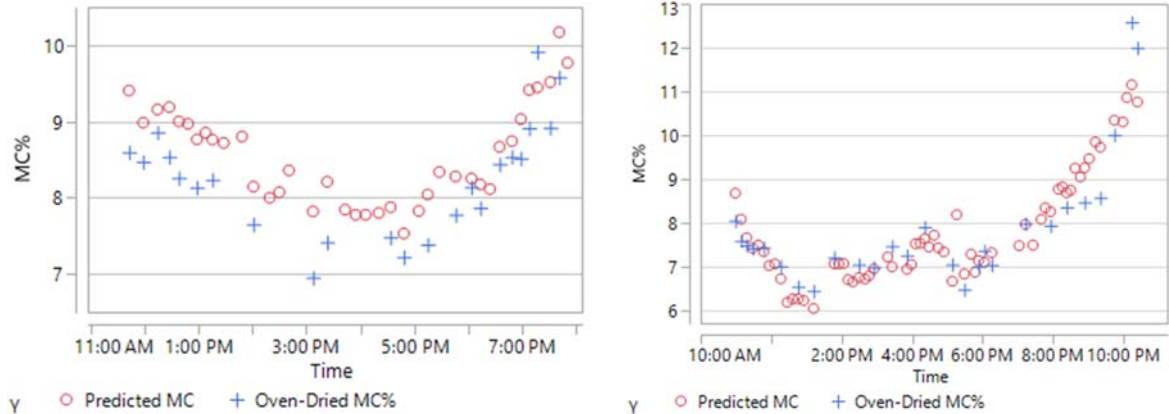
Figure 3.32: MC% prediction overlaid on values found from oven-dried samples throughout a day of harvesting for stripper machine (left) and picker machine (right) from validation set of data. Prediction biases as shown in Table 3.6 is accounted for in both cases.

3.4   CONCLUSIONS

The prediction model developed in this work using a capacitive-based dielectric measurement device, mounted in a location to measure all layers of round-modules on cotton harvesters, proves to be an effective system for moisture prediction of cotton modules. When viewed on a per-module basis, after accounting for bias by machine (picker, stripper), the performance results of the sensor presented in this work are comparable to prediction systems used in gin process control which operates under more stable conditions, consistent material composition, and half the MC% range as a field application.

With the goal of maintaining less than 1%MC mean absolute error for moisture levels less than 12%, the validation results indicated this was achieved with a safety margin for pickers. The aggregated data for strippers nearly passed, and since the predictions tracked moisture changes throughout the day accurately and responsively, ultimately it was considered to meet the performance objectives. Sensitivity to density changes has been explored extensively here and well defined, but the risk of such changes in terms of conditional or operational bias remains a topic for further investigation. Ongoing efforts would include investigating the cause of the bimodal density distribution within each machine type with the hope of identifying a factor that would allow adjustment of the predictions to accommodate such conditions. Exploring ways to decrease the variation in strippers to match the aggregated performance found with pickers would also be of great interest.

3.5   REFERENCES

[1]   S. O. Nelson and S. Trabelsi, "A Century of Grain and Seed Moisture Sensing through Electrical Properties," in *ASABE*, Louisville, Kentucky, 2011.

[2]   *Dielectric Properties of Grain and Seed,* St. Joseph, Mich.: ASABE, 2012.

[3]   C. B. Behringer, "Performance Comparison of Moisture Sensor Technologies for Forage Crops," Madison, Wi, 2004.

[4]   W. Guo, J. Yang, X. Zhu, S. Wang and K. Guo, "Frequency, Moisture, Temperature, and Density-Dependent Dielectric Properties of Wheat Straw," *Transactions of the ASABE,* vol. 56(3), pp. 1069-1075, 2013.

[5]   C. E. Kirkwood, N. S. Kendrick and H. M. Brown, "Measurement of dielectric constant and dissipation factor of raw cottons," *Textile Research Journal,* p. 24:841, 1954.

[6]   A. Kraszewski and S. O. Nelson, "Composite Model of the Complex Permittivity of Cerial Grains," *J. agric. Engng. Res,* pp. 43,211-219, 1989.

[7]   D. K. Cheng, Field and Wave Electromagnetics, Pearson Education, 1989.

[8]   "Impedance Measurement Handbook, 4th Edition," Keysight Technologies, 2014.

[9]   "Basics of Measuring the Dielectric Properties of Materials," Keysight Technologies, 2015.

[10]   "E4990A Impedance Analyzer: Data Sheet," Keysight Technologies.

[11]   S. O. Nelson, "Dielectric properties of grain and seed in the 1 to 50-mc range," *Transactions of the ASAE,* pp. vol. 8, no.1, pp. 38-48, 1965.

[12]   D. Funk and Z. Gillay, "Unified Grain Moisture Algorithm," USDA, 2012.

[13]   D. B. Funk, "New Official Moisture Technology Implementation Briefing," in *NAEGA-GIPSA Regional Meeting*, Destrehan, LA, 2012.

[14]   "GAC 2500-UGMA Grain Analysis Computer," 2 2016. [Online]. Available: http://www.dickey-john.com/product/gac2500/.

[15]   S. O. Nelson, "Dielectric Property Measurements and Techniques," in *AIChE*, Austin, TX, 2004.

[16]   S. O. Nelson, Dielectric Properties of Agricultural Materials and Their Applications, elsevier, 2015.

[17]   W. L. Balls, "Dielectric properties of raw cotton," *Nature,* p. 158: 9–11., 1946.

[18]   L. Han Ming, L. Ma, C. Q. Ma and J. F. Hong , "Estimation of the moisture regain of cotton fiber using the dielectric spectrum," *Textile Research Journal,* p. Vol. 84(19) 2056–2064, 2014.

[19]   C. E. &. D. Team, "Turnout Percentages -- Factors Involved," CSD Extension, 2010.

[20]   B. Goodman and C. D. Monds, "A Farm Demonstrations Method for Estimating Cotton Yield in the Field for Use by Extension Agents and Specialists," *Journal of Extension,* vol. 41, no. 6, 2003.

[21]   S. C. P. Ltd., "Moisture Management a Must," Southern Cotton Pty Ltd., Whitton, NSW, 2013.

[22]   J. Quinn, R. Eveleigh, B. Ford, J. Millyard, A. North and J. Marshall, "Cotton Picking Moisture," Cotton Seed Distributors, Wee Waa, NSW, 2014.

[23]   "Cotton Pcker Management and Harvesting Efficiency," Clemson University Extension, 1996.

[24]   R. Fiore, "Circuit Designers' Notebook, Document #001-927, Rev. E," American Technical Ceramics, 2005.

[25]   "Tests for thermoplastic materials used in the electrical and electronic industries," DuPont.

[26]   "Moisture Restoration of Cotton," USDA-ARS, 2004.

[27]   R. K. Byler, M. G. Pelletier, K. D. Baker, S. E. Hughs, M. D. Buser, G. A. Holt and J. A. Carroll, "Cotton Bale Moisture Meter Comparison at Different Locations," *Applied Engineering in Agriculture,* vol. 25, no. 3, pp. 315-320, 2009.

[28]   M. H. Willcutt, E. M. Barnes, M. J. Buschermohle, J. D. Wanjura, G. W. Huitink and S. W. Searcy, "The Spindle-Type Cotton Harvester," Texas A&M Agrilife Research and Extension Center, Lubbuck, TX, 2010.

[29]   "Cotton Picker Management and Harvesting Efficiency," Clemson University Extension, 1996.

[30]   J. P. Just and M. J. Darr, "COMPOSITE MODEL OF THE COMPLEX PERMITTIVITY OF RAW COTTON," *ASABE,* 2016.

[31]   *Standard Test Method for Moisture in Cotton by Oven-Drying,* West Conshohocken, PA: ASTM International, 2012.

[32]   J. G. Montalvo Jr. and T. M. Hoven, "Review of Standard Test Methods for Moisture in Lint Cotton.," *The Journal of Cotton Science,* pp. 12:33-47, 2008.

[33]   R. K. Byler, "Comparison of Selected Bale Moisture Measurements in a Commercial Gin," in *2012 Beltwide Cotton Conferences*, Orlando, Florida, 2012.

[34]   R. K. Byler, "The Accuracy of Cotton Bale Moisture Sensors Used in a South Texas Commercial Gin with Lint Moisture Restoration," in *2014 Beltwide Cotton Conferences*, New Orleans, LA, 2014.

[35]   D. Cash and H. F. Bowman, "Alfalfa Hay Quality Testing," Montana State University Extension, Bozeman, MT, 1993.

[36]   W. K. Coblentz, "Spontaneous Heating," in *Idaho Alfalfa and Forage Conference Proceedings*, Burley, Idaho, 2013.

[37]   W. Coblentz and M. Bertram, "Effectiveness of Buffered Propionic-Acid Preservatives for Large Hay Packages," Midwestforage.org, 2011.

[38]   K. E. Webster, M. J. Darr, J. C. Askey and A. D. Sprangers, "Production Scale Signle-pass Corn Stover Large Square Baling Systems," in *2013 ASABE Annual International Meeting*, Kansas City, MO, 2013.

[39]   J. P. Just and M. J. Darr, "COMPOSITE MODEL OF THE COMPLEX PERMITTIVITY OF RAW COTTON," *ASABE,* 2017.

[40]   J. Just and M. Darr, "Real-Time Moisture Prediction on Round-Bale Cotton Harvesters," *ASABE,* 2017.

[41]   D. Funk, "Engineering Considerations for Dielectric On-Line Grain Moisture Measurement," in *ASABE*, Kansas City, MO, 2013.

[42]   J. O. Rawlings, S. G. Pantula and D. A. Dickey, Applied Regression Analysis: A Research Tool, Second Edition, Springer, 1998.

[43]   "Impedance Measurement Handbook, 5th Edition," Keysight Technologies, 2015.

[44]   G. E. Shewmaker and R. Thaemert, "Measuring Moisture In Hay," in *Proceedings, National Alfalfa Symposium*, San Diego, CA, 2004.

[45]   M. Rankin, "Understanding Corn Test Weight," UW Extension Team Grains, 2009.

[46]   J. T. Documentation, "Standard Least Squares Report and Options -- Row Diagnostics," JMP From SAS, [Online]. Available: http://www.jmp.com/support/help/Row_Diagnostics.shtml#184200. [Accessed 17 Jan 2017].

[47]   S. O. Nelson and S. Trabelsi, "Use of Grain and Seed Dielectric Properties for Moisture Measurement," in *Southeastcon. 2011 Proceedings of IEEE*, Nashville, TN, 2011.

[48]   D. M. Mitchell, J. Johnson and C. Wilde, "IMPACTS OF DECREASING COTTONSEED TO LINT RATIO ON COTTONSEED MARKETS," in *Beltwide Cotton Conference*, New Orleans, 2007.

[49]   D. Blackham, F. David and D. Engelder, "Dielectric Materials Measurements," in *RF & Microwave Measurements Symposium and Exhibition*, 1990.

[50]   D. Funk, B. Gillay, S. Burton and Z. Gillay, "Engineering Considerations for Dielectric Online Grain Moisture Measurement," in *2013 ASABE International Meeting*, 2013.

[51]   R. K. Byler, "Resistivity of Cotton Lint for Moisture Sensing," *Transactions of the ASABE,* vol. 41, no. 3, pp. 877-882, 1998.

[52]   M. Digman and K. Shinners, "Technology Background and Best Practices: Yield Mapping in Hay and Forage," in *Proceedings, Idaho Hay and Forage Conference*, Burley, ID, 2013.

[53]   R. Benning, S. Birrell and D. Geiger, "Development of a Multi-Frequency Dielectric Sensing System for Real-TIme Forage Moisture Measurement," in *2004 ASAE/CSAE Annual International Meeting*, Ottawa, Ontario, Canada, 2004.

[54]   J. Banta, "Bale Weight: How Important Is It?," AgriLife Communications.

CHAPTER 4: REAL-TIME PREDICTION OF ALFALFA MOISTURE CONTENT ON LARGE SQUARE BALERS

John Just, Matt Darr

ABSTRACT

In this work, a capacitive-based dielectric sensor design was used to predict the moisture content of large square alfalfa hay bales. A lab characterization of the dielectric response using the probe design was performed which focuses on moisture content from 10-60% range and density of 16 – 192 kg/m³ [1-12 lbs/ft³], while controlling for confounding variables experienced when mounted on a machine. A Keysight E4990A impedance analyzer was used to measure impedance of raw cotton from a custom planar capacitive probe. This same probe design was also tested as a packaged unit with a specially designed impedance measurement circuit ████████████████████████████, which was intended for the on-machine moisture sensing application. The E4990A measurements clearly showed the sensitivity of the dielectric properties to these two main influencing variables leading to the conclusion that moisture has a stronger influence than dry material for the same weight and density of material. ██ ████████████████████████████████████ Sources of variation arising from the application are discussed and quantified using data (e.g. sampling variability of moisture content within a bale). Mounting of the sensor on a machine and field testing is described in light of potential confounding factors such as density (which is not available in real-time) and saturation issues with the packaged sensor. Over 10,500 bales were measured between July 2015 and December 2016 during the field research, with 1075 of them core-sampled for moisture content and used for development of the prediction model and further performance assessment. This includes both hay (<30%MC) and silage (>30%MC). Factors such as temperature and machine function states are recorded during operation, and density is obtained during sampling and used to assess sensitivity of the prediction model to these factors. Additionally, data is collected on a microwave-based sensor (competing technology which is limited to hay) and included to serve as a baseline performance comparison. Both the microwave sensor and the capacitive-based sensor were found to have similar accuracy for hay with approximately 2% standard deviation of error. Due to the saturation of the packaged sensor, feature engineering was employed and an artificial neural network (ANN) fitted that overcame sensor limitations in silage. Finally, an on-line (real-time) filtering algorithm using a Kalman filter is presented and compared to other traditional methods such as windowed (FIR) and IIR filtering. Oscillations observed in the prediction signal are investigated via spatial techniques (semi-variogram), and a final qualitative performance assessment of the signal shows plots of the prediction signal overlaid with oven-dried MC found from sampling to observe how well the prediction signal follows the actual trend for various days of baling.

4.1 INTRODUCTION

Knowledge of the moisture levels of hay and forage bales drives harvesting, management, and storage decisions. In large bale alfalfa hay, baling in the 17-20% MC range is optimal in the sense that it minimizes leaf loss that occurs when baling lower moistures, while mitigating microbial activity that occurs at higher moisture contents. Quality is significantly affected by these factors since leaves comprise 70% of the nutritional value [35], and mold growth will not only reduce quality but can cause heating and in turn combustion of the bales [36]. In the 20-30% range, applying preservative to maintain quality is necessary [37]. However, since the most significant controllable factor influencing quality is maturity of the crop [35], operations may need more flexibility regarding when they can bale than weather may permit. In this case preservatives can be applied to very wet material that would normally spoil if harvested. It is added as the windrow is processed by the baler, but this additional input adds cost. Timely feedback regarding the moisture content of the material is necessary to apply only when needed to prevent spoilage. Real-time moisture sensing facilitates automatic control of such a system that can optimize the application.

In this work a capacitive-based sensor is used to measure dielectric properties of large square alfalfa hay bales less than 30%MC, as well as extending into silage bales up to 50%MC. The response of the probe design is initially investigated in a laboratory setting for moisture levels from 10% - 60%+ MC, and a packaged/mobile version of the design with embedded electronics (intended for machine mounting) is compared to the measurements obtained using the same probe design. A Keysight impedance analyzer serves as a validation of the mobile sensor measurements. During operation, the mobile sensor is located within the bale chamber, thus allowing for real-time measurement and prediction. These measurements are used to predict moisture content, which provides information for harvesting decisions, preservative application, identification of wet bales, and adjustment of moisture for yield monitoring.

With the goal of prediction, several statistical models are presented herein for prediction of moisture content in alfalfa as it is baled and dielectric measurements taken in the bale chamber. The data is divided into train/test or train/validation/test portions (depending on modeling technique) to fit the model and assess performance. In pursuit of a real-time feedback signal for control of preservative application, a few signal processing methods are also compared such as simple FIR/IIR digital filters to remove noise, as well as more advanced techniques using Kalman filtering as an optimal recursive estimator with minimal delay. Data from a commercially available microwave-based moisture sensor (Gazeeka by Vomax) is also

assessed to provide a baseline performance comparison. Although the data was taken from a capacitive-type planar probe sensor with focus on large square alfalfa bales, the methods presented herein can be readily extended to other forage applications and sensor designs.

4.1.1   FORAGE FORMS AND TYPES OF MATERIAL

In the context of this work, for discussion it is useful to understand the breakdown of the different forms and types of forage material. Forage is considered an all-encompassing term in this paper and refers to the harvested leaves and stems of plant material intended to feed grazing livestock. It is further subdivided into hay and silage; which is primarily defined by the moisture content and storage method. The name silage is derived from the process of ensiling, which involves storing forage with moisture contents of roughly 30% or higher in an oxygen-limited environment to encourage anaerobic fermentation. Hay on the other hand is forage that is purposely dried or otherwise dry enough to store in an open-air environment. Note though that there is risk of spoilage and/or fires due to microbial activity and heating in bales for moisture contents above 20% and preservatives must be added to mitigate this risk.

Forage is harvested in either bulk form (loose) or baled (cylindrical bales or square bales). *This work focuses on moisture sensing in large square balers*. Large square bales are found in sizes from 0.91x0.91x2.4 m [3x3x8 ft] to 1.2x1.2x2.4 m [4x4x8 ft], and 90% of 10,500 bales made during the course of this research were found to weigh between 363 – 907 kg [800 – 2000 lbs]. This is in contrast to small square bales which are closer to 0.3x0.3x0.91-1.2 m [1.5x1.5x3-4 ft] and weigh in the range of 32-36 kg [70 to 80 lbs].

Types of forages can substantially be classified as either grass, grain, or legume. Examples of grasses are fescues, timothy, and Bermuda. Example grains can be wheat, oat, and barley. And legumes include alfalfa, and clover.

4.1.2   CURRENT TECHNOLOGY/METHODS

A summary of technologies used for monitoring moisture content in forages are classified and described below.

4.1.2.1   Conductance

As the most common commercial moisture meter due to low-cost, several combinations of meters and probes are available from various manufacturers that allow for measurement of moisture both in-chamber and post harvesting. This style depends on electrodes that make contact with the bale in some way (either by pressing a probe against the surface of the bale or by inserting a probe into the bale). While the dry material is hardly conductive, the moisture in the bale has enough ionic content that an applied voltage between the electrode and cathode on the probe allows for a measurement of the conductance between them, using the moisture bale material as the conducting medium. As moisture content increases, the resistance of

the conducting path between the electrode falls, and thus a higher conductance is measured. This path can be highly variable though since it depends on the network of material within the bale. Factors such as compaction (density), temperature, material structure, and constituents can all affect the conductivity of the network between electrodes.

4.1.2.2   *Microwave*

Higher priced options for moisture measurement include sensors that operate within the microwave region of the electromagnetic spectrum. With microwave-based sensors, three quantities are typically of interest: reflectance, transmittance, and absorption. In simple homogenous material cases, reflectance (or the reflection coefficient) is a property of the interface between the sensing unit and material, calculated as the ratio of complex amplitude of the reflected wave over the incident wave (or original wave). Transmittance and absorption then are properties of the bulk material, and describe the parts of the wave that are absorbed into the material and transmitted through to the other side, respectively. Gazeeka (by Vomax) functions by a transmit and receive unit and allows for measuring through the bale just before the bale drops off the end of the machine, but other options are also available that operate without a receiver (TEWS model MW-1000) and act as a probe with more localized sensing. The dielectric properties of the material determine the transmittance and absorption quantities, and since the dielectric constant of water (at a value of 80) is generally about a magnitude larger than most other materials, measurement of moisture is enabled. This technology is significantly costlier than conductance or capacitance-based products, but has been noted to be very accurate up to the preset limit of 28% MC [38]. However, since it is mounted outside of the bale chamber there is a two-bale delay from the time of harvest which is not as useful for real-time control of preservative or correction of moisture for yield monitoring. Designs which rely on transmission are also not as easily mounted on a machine for any given application as sensors which rely on capacitance or reflectance alone (e.g., a silage chopper chute). It is primarily marketed for finding especially wet bales and marking them.

4.1.2.3   *Capacitive*

By using the very low to high frequency spectrum (per the ITU designations), the MUT is treated as the dielectric of a capacitor. In doing so the dielectric properties appear in the circuit as a complex impedance and can be measured as if it were part of the circuit. Like the microwave approach, since water heavily influences dielectric properties the detection and quantification of MC% is enabled. Commercial product options targeting the baled crops market are far more limited than conductance-type sensors. Like conductivity sensors, capacitive-based sensing is cheap and can easily be mounted to get in-chamber measurements. Drawbacks are similar to conductance-based sensors and included inaccuracy and sensitive to density [3].

4.1.2.4   Infrared

By projecting light in the IR spectrum onto a material and measuring the reflectance as a percent of the transmitted intensity, it has been found that material properties such as moisture content, among others, can be predicted from the response. The John Deere HarvestLab is one such example and is marketed primarily for estimation of nutritional quality of the forage (determination of constituent quantities), although it outputs predicted moisture content as well. The HarvestlLab though is intended for the spout of a forage chopper, and some modification would be necessary for hay applications. Some downsides include very high cost (three times that of the Gazeeka at the time of writing), penetration depth (only measures surface material), and any application be very careful about contamination from other light sources with IR content.

4.1.3   OPPORTUNITIES IN HAY MOISTURE SENSING

The impetus for further research in the area of moisture sensing for baled crops arises from several gaps in this market. The lower cost technology currently available, which uses conductance, has not been found to be very accurate [3]. Some laboratory results evaluating the response of complex permittivity in a frequency under 1 MHz to moisture and other factors showed promise [4], and so extending the concept to mobile equipment is a logical next step. Microwave sensing has shown decent performance in two studies [3] [38], but the higher price tag is a deterrent and it is generally limited to less than 30%MC bales. Also, the mounting location is on the end of the machine, which is approximately two bales behind the infeed and thus a large time delay between harvesting and feedback exists. Bale-chamber mounting on the other hand can provide feedback close to when material is harvested, thus making it more useable for yield monitoring and preservative application control. Variations in moisture can occur quickly over the length of a field from conditions such as elevation changes, end rows, and exposure (shade/sun, wind), and therefore achieving real-time feedback requires measuring material as close to the infeed point as possible. This work targets moisture sensing using a probe that can be mounted in-chamber and obtain measurements of complex permittivity in the low MHz range.

4.2   MATERIALS AND METHODS
4.2.1   LAB EXPERIMENTATION WITH ALFALFA

A small lab study was performed to assess the response of a planar capacitive-based sensor design to moisture and density of alfalfa forage under controlled conditions, (i.e. without other confounding factors such as temperature fluctuations, machine dynamics, and dew vs stem moisture that a sensor mounted in a machine during typical operations will experience). This also allowed for a one-to-one sample to measurement, which mitigates the variability introduced in the field when sampling material from a bale that was not directly measured by the sensor. The setup used to contain the material, compact

to pre-determined densities, and obtain dielectric measurements was successfully used in cotton for the same purpose and is previously described [39].

The full test involved three replications with six moisture levels and three densities per replication. The five replications were of five different alfalfa samples that began as extremely wet (60% MC) and were incrementally air-dried to in target step sizes of 10% MC to achieve six moisture levels (60,50,40,30,20,10) per sample across the typical industry range for alfalfa hay and silage. Dielectric measurements were taken of the samples at each moisture level. Within each moisture level per replication, three discrete densities were induced by compressing the material to pre-determined heights. For 95% of the data, these heights translated to densities between 1.5 - 34 lb/cu-ft wet (1.15 – 10.6 lbs/cu-ft dry). The frequency measurements were swept over 1kHz to 30MHz for a total of 201 measurements on a log-interval, ███████

████████████████████████████████████

███

Table 4.1: Treatment factors and levels for lab characterization of alfalfa dielectric response

Factor	*Levels*
Density	Low, med, and high compressed heights per sample per moisture level. Dry density is proportional to the inverse of the compressed height. Dry densities from 1-176 kg/m^3 [1-11 lb/ft^3] were obtained.
Moisture Content	10,20,30,40,50,60 [%]
Frequency	1kHz – 30MHz range sweep at uniform intervals on a log10 scale. ████████████

4.2.2   FIELD MACHINERY

The data included in this work was taken from three different large square balers, two of them forming bales with end dimensions of 0.91x1.2 meters [3x4 feet] and a small amount of data from a 0.91 meter [3-foot] square baler. Over 10,500 bales were made during this research. With these types of balers, 50% of the bales were made at rates between 2 and 3.8 cm per second, with a median of 2.9 cm/sec. Nominal lengths for bales were typically either 244 cm or 229 cm depending on the farmer's preference. The middle 50% of bale weights fell in the 544 kg [1200 lb] to 658 kg [1450 lb] range, with 95% between 408 kg [900 lbs] and 907 kg [2000 lbs]. An example large square baling machine is shown in Figure 4.1.

Figure 4.1: Typical large square baler baling corn stover.

4.2.3 ███████████████████████████████

██

██

██

██
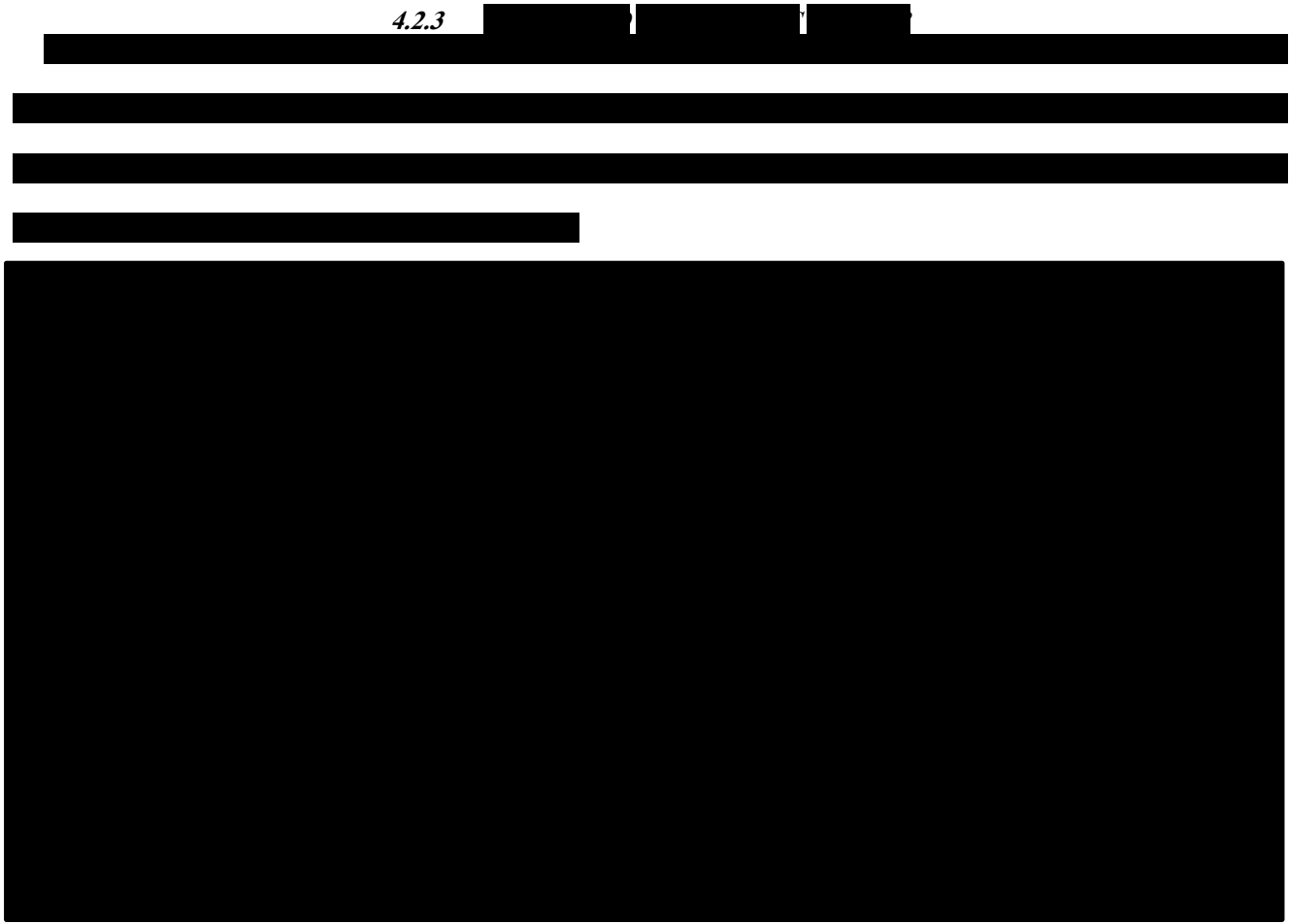
Figure 4.2: ███
██

4.2.4   DETERMINATION OF BALE DENSITY

Bale weights and lengths were necessary to calculate density. The length was measured manually. Bale weights were obtained by inserting a row of steel prongs/forks attached to load cells into the bale, and then lifting the bale off the ground and recording the sum weight of the load cells. The weigh-system was built as a three-point attachment and a tractor was used as the carrier (Figure 4.3).   The resulting data obtained is in terms of a wet-weight (wet basis) and thus the bales are adjusted to a dry material weight using the moisture content found by a core sample taken and oven-dried for the same bale.

Figure 4.3: A three-point scale attachment used to obtain bale weights. Forks attached to load cells were used to lift the bale off the ground and obtian a weight.

4.2.5   DETERMINATION OF MOISTURE CONTENT

In order to estimate moisture content of bales, cores of four inches in diameter and 24" deep were taken from the ends of bales. Moisture content was determined by drying samples in a forced-air oven per ASABE S358.3.

4.2.6   SUMMARY OF FIELD DATA

Confidence in the performance of any predictive algorithm is directly proportional to the range of conditions it has been trained and tested in. The data is summarized in Figure 4.4 and Table 4.2 with respect to factors that implicate the range of conditions tested, such that it can serve as a baseline to extend the conditions and drive further research and development. This research intended for data collection during "typical" conditions as much as possible, which maximized the amount of

data that could be collected by minimizing interruption to farming operations that facilitated this work. Gathering data across different days increases the likelihood that possibly confounding environmental conditions were included in the dataset. Of the 10,500 bales for which dielectric measurements were recorded, only roughly 10% were sampled for moisture content analysis. Although not every bale was sampled to determine MC and density, they still play an important part in the development of a reliable real-time prediction algorithm and assessment of the real-time signal quality.

The majority of data collected for this work was taken from Arizona where conditions and internal plant (or "stem") moisture are typically on the dryer side (<15%MC), and baling is more often done when dew has formed to increase moisture content, minimize leaf loss, and help compaction. This is reflected in the right plot of Figure 4.4, which shows the vast majority of data was collected during morning (stopping before noon) baling when dew is highest. Conversely, in areas where internal (or "stem") moisture is higher and is a hindrance to storage baling will typically occur as the material is drying down and no dew is present, and therefore the mid-afternoon times would be more ideal.

Since detection of moisture content is the purpose of this work, the range of coverage for this variable is of primary importance. Classical analysis using multiple linear regression is performed on a subset of the data for which the sensor dielectric measurements agreed with that expected by physics (i.e., monotonic and exponential increase in dielectric values with MC). This amounted to bales which the MC was less than 30% and required other filtering conditions to be met which intended to detect saturation in the hardware at higher MC. Most of the data (1014 samples) fell into this category. The remaining 169 samples, those between 30-50% or otherwise showed evidence of an uncharacteristic response, are included in an analysis using more advanced regression techniques. It is of important note that most of the bales with MC% greater than 30 were obtained under special circumstances, i.e. they were "one-off" bales and not baled in consistent harvesting conditions. For the classic analysis, the data is divided arbitrarily into a 60-40 ratio of train-test sets. For advanced regression, the data is divided into 40-40-20 train-validate-tests sets, with the validation set being used to optimize tunable parameters, and the test set being the independent evaluation.
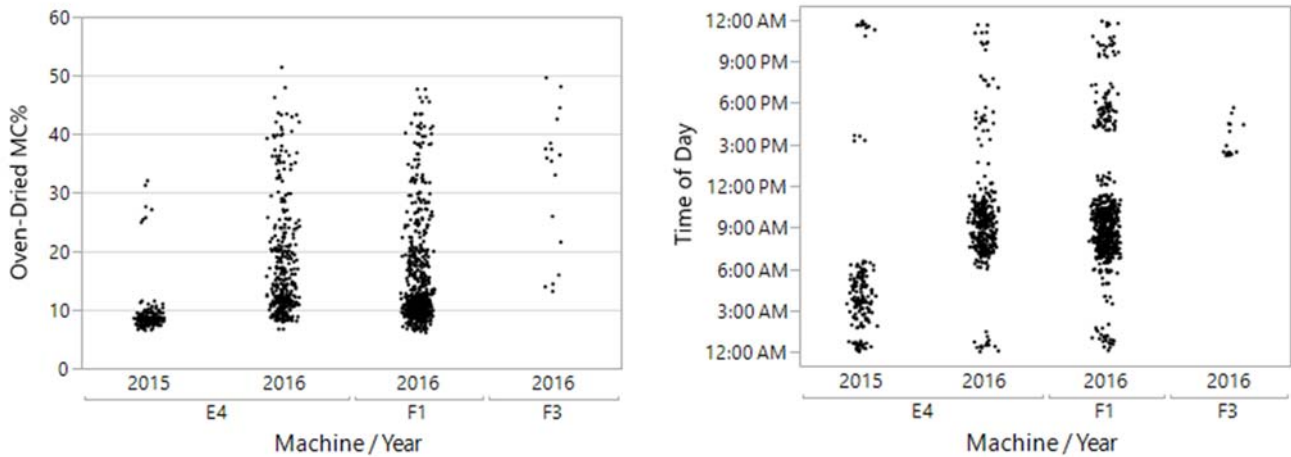
Figure 4.4: Point densities of samples included in this work/analysis summarized by (left) machine/year vs MC% and (right) machine/year vs time of day which the samples were collected. The time of day can be an important factor since it is related to the type of moisture that is dominant (dew VS stem moisture). Note: Points are jittered in the figures to aid in visualizing point densities.

Table 4.2: Data quantities included in analysis, grouped by machine/year/ location. The number of different days over which samples were collected is also included to show coverage of conditions beyond a single day (or short time period).

Machine	Year	Location	# of Samples	# Days Harvesting
E4	2015	AZ	160	8
	2016	AZ	356	51
F1	2016	AZ	650	65
F3	2016	WI	17	3

4.3   RESULTS
4.3.1   *LAB CHARACTERIZATION OF RESPONSE*

4.3.1.1   Measurements with E4990A

The equivalent circuit for permittivity measurements is typically modeled as a parallel resistor and capacitor. While this lab setup has been shown to accurately measure the dielectric constant for PTFE and Acetal [39], the dielectric properties of alfalfa and water are significantly higher than common industry plastics. The response of the dielectric constant and loss factors of alfalfa forage to moisture content and density is shown in Figure 4.5. A value of 80 for the dielectric constant of water can be found in any introductory text on electromagnetics [7]. However, the values found for very wet and dense alfalfa in this work were well beyond the known dielectric constant of water, while it was presumed they would be less than that of water. This is similar to results reported in other work on wheat straw [4]. Research by Funk et al [41] contends that the values, which are higher-than-expected by dipolar relaxation, are a consequence of conductivity effects (electrode polarization, Maxwell-Wagner relaxation) [41], and is thus expected but otherwise not ideal. Regardless, for any given

density level strong trends with MC% can be seen (after applying a log-transform on permittivity), and thus since prediction

is of primary concern the exact physical mechanism of the response only need-be consistent.
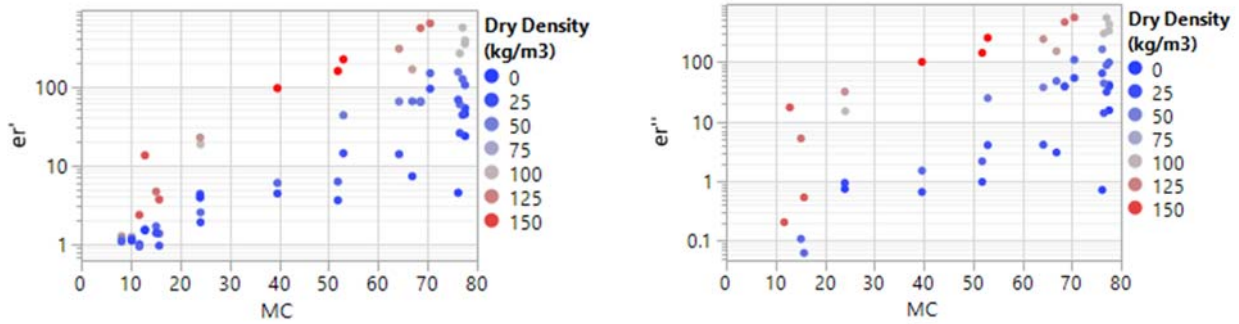
Figure 4.5: **The logarithm of the dielectric constant (left) and loss factor (right) at 2.1 MHz can be seen to increase linearly with moisture content. The points are also colored by dry density and as such it can be seen that for a given moisture content, increasing the density has a large effect on the measured permittivity values.**

Other work on the dielectric properties of wheat straw found values for the dielectric constant to increase approximately

exponentially with the multiplicative change factor for moisture content (i.e., a doubling of the moisture content from 10 to

20% MC results in an approximate change factor of exp(2) in the dielectric value) [4]. Therefore, these results appear to

agree with that found in other published work, and since a strong and stable response was found to both moisture and density

that would facilitate prediction of either quantity, the probe design was deemed adequate for the intended purpose.

4.3.1.2 ███████ ███████████████████████████

Figure 4.6: ██

4.3.1.3 *Dry Material VS Moisture Response*

Continuing with the lab measurements from the E4990A as a baseline investigation of the physical response for the chosen probe design, a natural question that arises from these results is whether moisture or density changes have a stronger effect on the dielectric measurements. Since the intended application is for measuring moisture content, it is desirable for the solution to be uninfluenced (or minimally influenced) by density. Previous research noted density as having a "stronger" effect than moisture for capacitive-based measurements (with little qualification of what "stronger" meant), which would be concerning for this application [3]. In order to answer this, certain stipulations must be stated regarding the context. Since the range of moisture content (wet basis by weight) is generally anywhere from 5 to 70% in alfalfa, a good metric is examining the dielectric response when maintaining the same [wet] density of material, while replacing the equivalent amount of forage by weight with water. This is trivial to do using multivariate regression, and it is shown for both the dielectric constant and loss factor in Figure 4.7 and Figure 4.8, respectively. Note that dry densities in the field were generally found to range from 10-20 lbs/cu-ft, and although the level of densities induced in the lab is low, the range is about the same and is sufficient to draw conclusions on the effects. Ultimately, moisture commands a higher dielectric response than hay for the equivalent weight, which is shown in two separate ways. The left plots indicate for a given wet density, as the dry density decreases (hay replaced by equivalent weight of water) the dielectric values increase. The right plots are the leverage plots [42] of moisture in a multivariate regression of MC and wet density, and the positive slope indicate that a change in MC for the same wet density increases the dielectric values, after accounting for wet density. For the dielectric constant, the rate of increase [slope] is 1 unit of sqrt(diel. Cons.) per 13% weight of forage replaced with water. The rate of increase [slope] for the loss factor is 1 unit of sqrt(diel. loss) per 14.5% weight of forage replaced with

water. Similar multi-variate regression models with dry density instead of moisture content have a negative slope (as would be expected by aforementioned relationships). Thus, by this experiment it is concluded that moisture, and not density, is the dominant component in the response. However, the potentially confounding effect of density should not be overlooked. Nevertheless, the lab work provided the intuition needed to understand the individual effects of moisture and density.
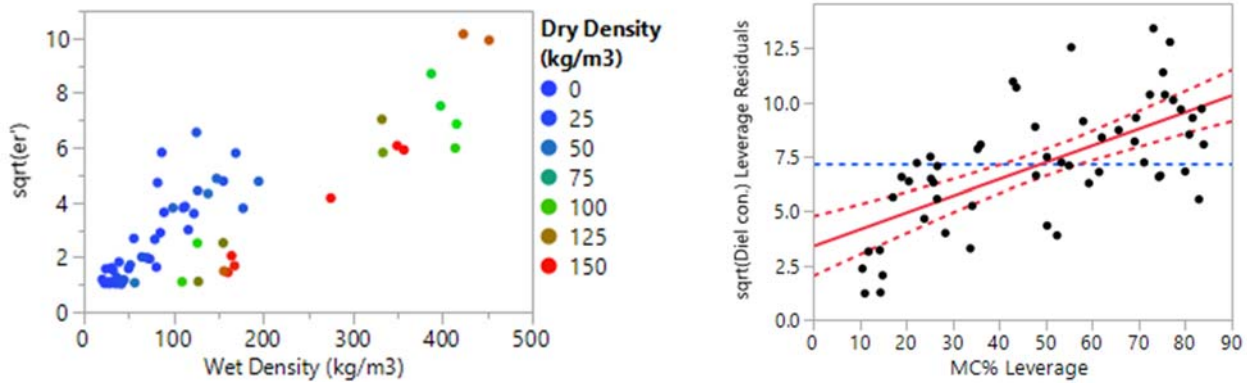
Figure 4.7: (left) a plot of the dielectric constant against wet density, with the dielectric constant transformed by a sqrt function to linearize the relationship. The points are colored by dry density to show that for the same wet density, replacing moisture with material *DECREASES* the dielectric constant. (Right) Likewise, this same relationship is shown from the vantage of the results of a multivariate fit using a leverage plot. Again it can be clearly seen that replacing a given weight of forage material with water while controlling wet density will result in *HIGHER* dielectric values. The rate of increase [slope] is 1 unit of sqrt(diel. Cons.) per 13% weight of forage replaced with water.
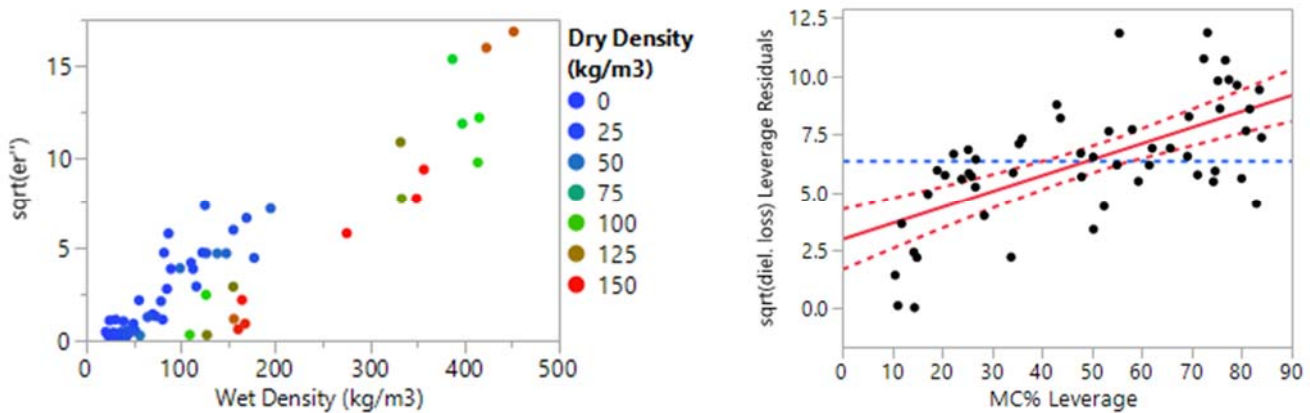
Figure 4.8: The effect on the dielectric loss factor of replacing forage material with an equivalent weight of moisture is very similar to the dielectric constant. The positive slope of the leverage plot for moisture content (right) indicates forage dielectric properties are not as strong as those of moisture. Here rate of increase [slope] is 1 unit of sqrt(diel. loss) per 14.5% weight of forage replaced with water.

4.3.1.4   *Impedance Range of Alfalfa*

While permittivity is of interest for the formulation of a moisture prediction model, knowledge of the impedance range is useful when designing sensors for such applications, since permittivity is estimated by impedance measurements. The

impedance is estimated under the presumption of a parallel RC circuit, which is the classic and typical equivalent circuit assumed for permittivity measurements [39] [43]. The figures below show the lab-measured parallel impedances ▮▮▮ ▮▮▮, from whence statistical models are fit using moisture content and density.
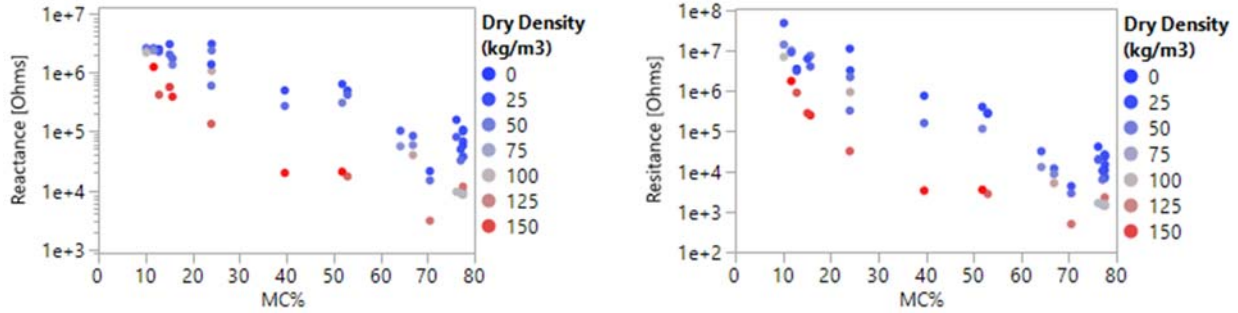
Figure 4.9: (left) Parallel reactance and (right) parallel resistance in Ohms as measured by E4990A during testing in lab. The higher limit of the impedances as seen in the field over the same moisture range is expected to be the lower limit in these plots since range of densities found in field were in the 10-20 lbs/cu-ft range.

A multivariate regression model of the impedance using moisture content and dry density as predictors found the relations shown in Table 4.3. Note that the dry density is in units of lbs/ft^3. These can be combined in typical fashion of parallel circuit elements to obtain total impedance, which should be considered a liberal estimate of impedance for design purposes (i.e., a margin of safety should be included in the design). A similar method to determine the necessary impedance range of the circuit can and should be performed for different fixture designs and/or frequencies used.

Table 4.3: A statistical model helps to numerically understand the sensitivity of measured impedance to moisture content and dry density. Here the reactance and resistance are shown separately, but total impedance may be found by simply adding the impedances in parallel.

Impedance Quantity	Equation
Parallel Reactance (Xp)	$e^{14.8} * e^{-0.071*MC} * e^{-0.3*DryDensity}$
Parallel Resistance (Rp)	$e^{18.8} * e^{-0.114*MC} * e^{-0.462*DryDensity}$

These equations are combined in parallel using $|Z| = \dfrac{1}{\sqrt{\left(\frac{1}{R}\right)^2 + \left(\frac{1}{X}\right)^2}}$ to obtain the magnitude of impedance and a plot of the impedance response to MC and dry density is shown below for reference.
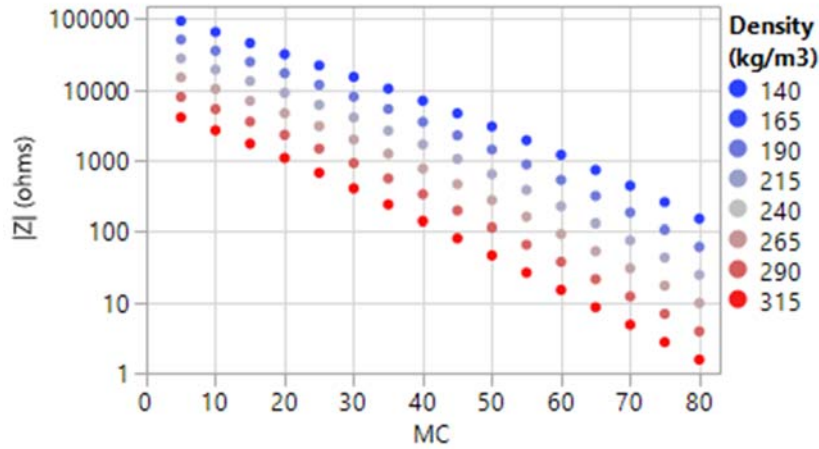
Figure 4.10: Equivalent impedance magnitude plotted against moisture content and colored by dry density.

4.3.2   SOURCES OF VARIATION

Sensor development is concerned with factors that cause bias and variability when attempting to measure the quantity of interest (MC% in this case). Confounding factors are what determine the potential limit of any given sensing technology, and also are key considerations in development and performance test plans. While development in the lab offers convenience, speed, and ease of matching each sample dielectric measurement with an oven-dried MC%, it is difficult to fully replicate the real-time harvesting on a machine for which the sensor is intended. Development and validation of a capacitive sensor targeting moisture of a biological material, which is intended for an in-field application such as real-time moisture prediction on balers, has many challenges due to the various factors that affect both dielectric properties and consistency of matching any given on-machine measurement to a lab-determined moisture of the same material. Data collected in the field during harvesting can introduce additional confound factors and sources of variability that are not easily accounted for or seen in a lab environment [40] [41]. The transport process of samples to the lab and associated time delay risks microbial activity or other compositional changes. Sampling variability can have a sizable impact depending on variation encountered during a single bale, and bias can be a plausible factor if moisture gradients in the windrow are carried into the bale such that the sensor location typically measures a different part of the windrow than the sampled area. Other factors such as the material interface with the sensor, moisture type (dew VS stem), bale density, temperature, and chamber material dynamics are all candidates of influencing the measurements that may be difficult to emulate correctly in the lab. As such, a model built from measurements in a static lab environment will likely be suboptimal. Therefore, major sources of variation and plausible mitigation options are discussed.

4.3.2.1   Dew VS Stem Moisture

The types of moisture, dew and stem, are disparate enough to warrant consideration. While dew forms as physical droplets of water visible on the forage and is easily evaporated by the elements (wind/sun), stem moisture is already "absorbed" (or more internal) and is not as quickly and easily removed by evaporation as dew [44]. Dew droplets are also more discrete and separate while stem moisture is more evenly distributed in the plant. Research from the grain industry has indicated that dielectric measurements can change as a non-uniform distribution of moisture in a material permeates and equalizes across the material [41]. Unless conditions are perfect, harvesting forage involves cutting and leaving the material in windrows and either waiting for additional moisture (which comes from condensation/dew) or for the material to dry by the elements (wind/sun). In the former case the moisture present when baling is dominated by dew, while the in later case the dominant moisture type is stem moisture. Given what has been seen in grain, since the dew moisture is distributed differently than stem by the very nature of how it forms, it is projected the different moisture sources could potentially produce different dielectric responses for the same MC% as measured by an oven-dried method.

4.3.2.2   Sampling Variability (Variation of MC within a Bale)

Variation of moisture content within any given bale leads to variability in sampling from the bale in an attempt to quantify the moisture level. It is very difficult to obtain and match a core sample to real-time measurements since the sensor is mounted in the floor of the bale chamber and core samples are taken from the middle of the bale. Furthermore, it would be very time consuming and difficult to core sample the bottom of a bale, and contact with the ground would risk contamination with other water or material that wasn't part of the measurement. Thus the sampling variability is examined and quantified in order to understand the additional variation introduced. To do so, 57 bales over a wide range of moisture contents were sampled at least four times as shown in Figure 4.11. The results indicate the standard deviation of moisture content within a bale generally increases with mean moisture content. If the fitted linear trend is used to draw conclusions, then the standard deviation increases by 0.13 % points per 1% mean increase in moisture content. In this case, the coefficient of variation at 30% mean mc is around 9%. This is especially important information since validation of the sensor cannot show better performance than sampling variability. This accuracy was deemed adequate for this research, but if a tighter accuracy specification is desired then a more complex and costly strategy would need to be considered, or a different sensor mounting location that is more conducive to matching measurements to samples would need to be devised.

Figure 4.11: (left) The bales were sampled two times on the leading and trailing ends for a total of four samples per bale to quantify variability of MC% within a bale. (right) A total of 57 bales were included in the variability investigation. A clearly increasing trend appears of the stdev of MC% with the mean MC% of each bale.

4.3.2.3   *Aggregating Measurements for Ground Truth Matching*

While each bale has an oven-dried MC% with it, there are many dielectric measurements for each bale. In order to do regression, it is desirable to have one dielectric measurement for each bale that is representative of the material that was sampled. A simple mean of the dielectric measurements for the entire bale is one way, but this would overlook the variability of the infeed rate of material and assign more weight to time which feeding was slower. Instead, the median value for each flake is taken, and from this subset the median value is taken as the estimated dielectric value for the bale. It is recognized that not matching up the sample with a dielectric measurement of that exact material may introduce some variability (as discussed in the sampling variability section), but it is also presumed the error will be normally distributed which poses no issue when using typical statistical fitting techniques.

4.3.2.4   ███████ ███████████████████████

███

███

███

███

███

███

███

███

██

Table 4.4: ███

██

Figure 4.12: ██
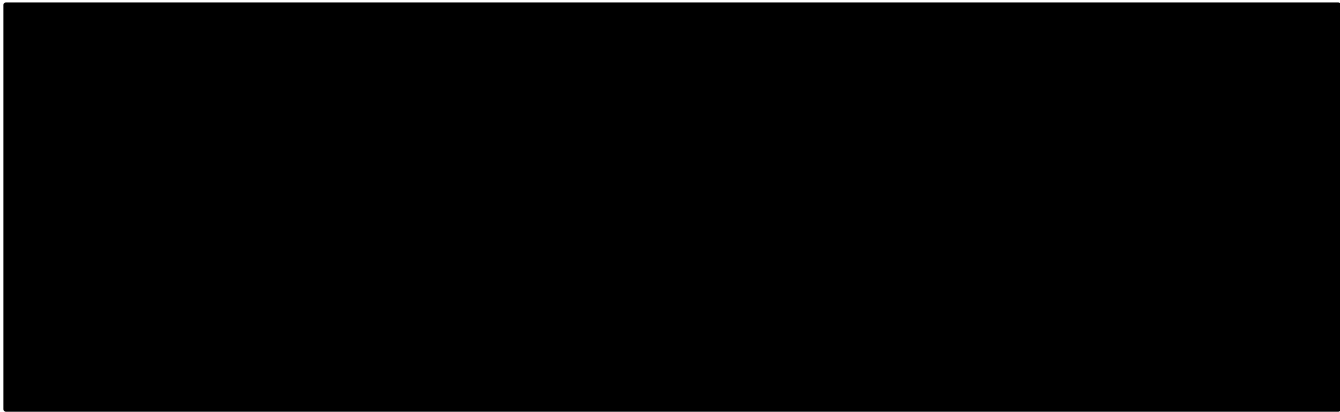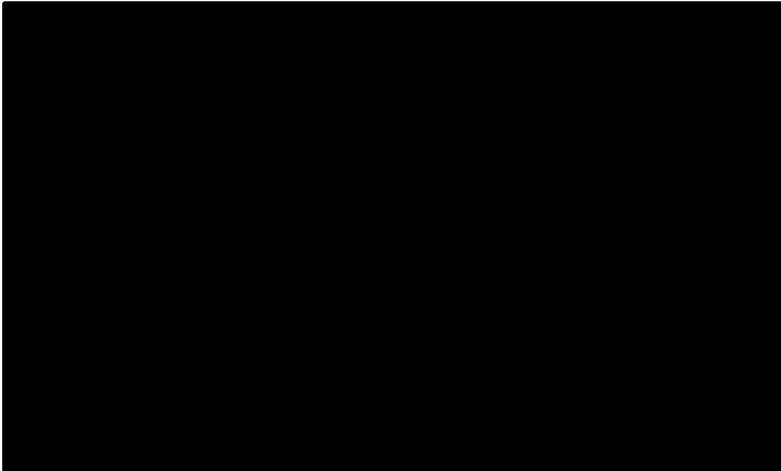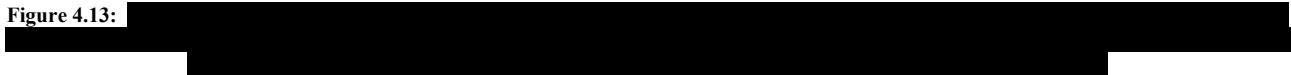██

Figure 4.13:

Figure 4.14:

4.3.2.5 Bale Speed

Since the moisture variability in alfalfa can be very high, and since the sensor has shown limitations in higher moisture content, it is desirable that the sampling rate be relatively high compared to the linear speed of the material to allow for additional filtering of the signal. In the case of this sensor the sampling rate is 1-Hz. Lengths of the large square balers were available via a star-wheel that turned as bales advanced and facilitated measuring linear distance. While not as accurate as a manual measurement, it provides a good estimate by examining the movement of nearly 500k flakes, with the median flake size of 5.4 cm found (shown in Figure 4.15). A median of 3.7 cm/sec movement speed, and typical bale length of 243

cm, the sensor measurement frequency translates to 66 measurements per bale. This quantity provides ample opportunity to assess hardware limitations and engineer features from each bale.
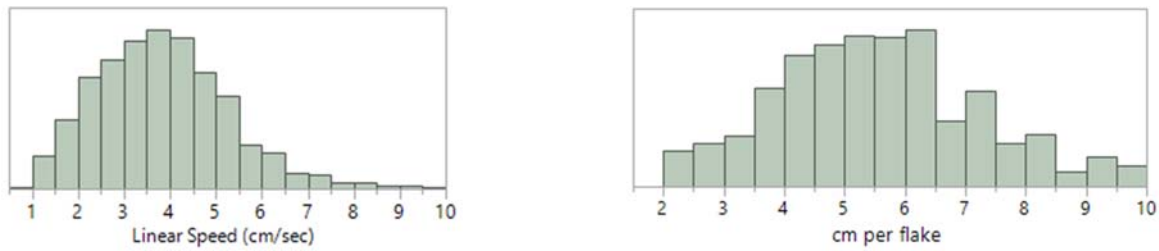
Figure 4.15: Distributions per bale of (left) linear speed of material and (right) length of flakes.

4.3.2.6   Windrow

Windrowers cut the forage material and leave them in straight piles lengthwise along the field called windrows. During that time, the outer part of the windrow, which is exposed to the elements such as wind and sun, can dry more than the inner parts and induce a gradient of moisture from outer to inner parts. Conversely, if baling when the dew is coming on, the exterior would be wetter than the interior of the windrow. Since such types of gradients conceivably exist, the moisture sensor could experience higher variability in MC that may be difficult to separate from variability due to other confounding sources, thus presenting more difficulty in the noise filtering problem. It is also possible that biasing could occur if one part of the windrow is consistently found more at the bottom of the bale where the sensor is located. In this research this particular source of variation and/or bias is noted but not extensively investigated due to limiting scope to the factors projected to have the largest impact, of which sampling variability and density were deemed of much greater potential for introducing bias and/or variability.

Figure 4.16: Grass cut and left to dry for day or two before baled. Windrow can have disparate MC between outside and inner parts due to exposure to elements.

4.3.2.7   *Density & Temperature*

Like cotton, the density of forage is mostly referring to the bulk density, which is not so much an intrinsic property since the material has a low bulk modulus, and this fact is manipulated to compact bales tightly and save room for logistical purposes. Density has also been reported as having a strong effect on dielectric properties [3] [41] [39] [4]. This was investigated specifically for alfalfa and results presented in the lab testing section earlier as well. Although moisture was shown to have a stronger effect, density was still very significant.   The lab test stand operation is such that when material is compressed it is forced directly against the sensor (i.e., force is perpendicular to the sensor face plane), while the plunger action on the machine is parallel with the face plane of the sensor. Seemingly small details such as this may have a sizable impact since even a small gap (~0.1") has shown to significantly reduce the response for this particular sensor design/plate configuration [39]. The effect of density on the dielectric properties is investigated for the in-field response in a similar manner as in the lab; using multivariate analysis. Before doing so, the importance of accounting for moisture content when exploring the effect of density is discussed in light of the correlation between MC% and density (both wet and dry) shown in Figure 4.17 for bales with MC% less than 30% collected during this research.
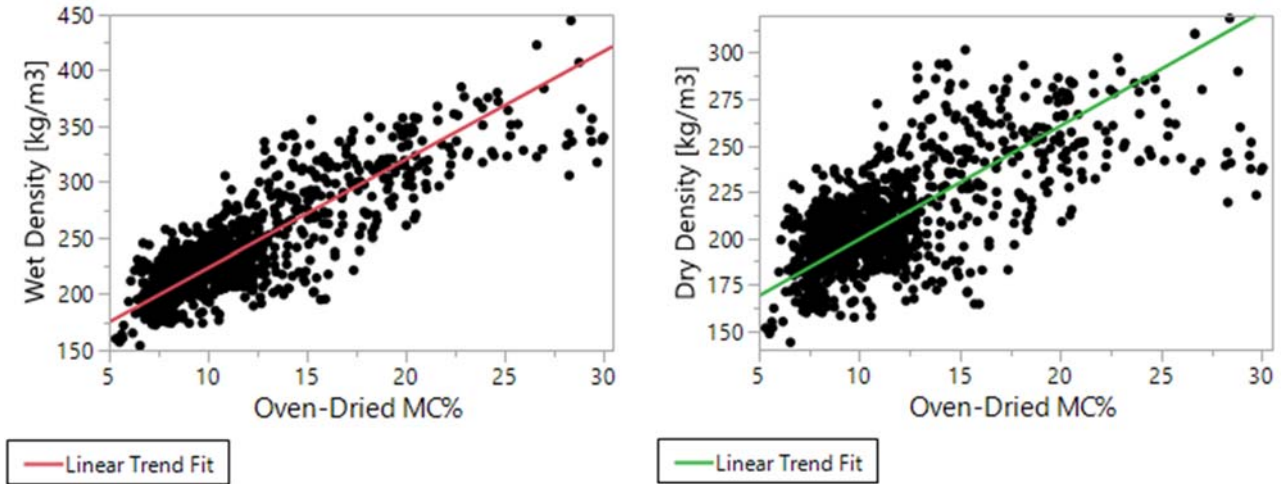
Figure 4.17: (Left) Wet density has a strong correlation with moisture content (R^2=0.73). (Right) Dry density for the same data showed correlation with MC (R^2=0.47) as well. Fitted trend lines are overlaid on both plots.

While a trend of wet density with MC% would seem reasonable, the trend with dry density is most curious. In grains it has been well noted that adding moisture to kernels causes them to expand, and thus even after adjusting the weight for moisture content the density is decreased due to a larger physical size of the kernels [45]. This particular relationship in alfalfa is clearly positive though (not negative like grains), and after some thought one can imagine an analogous situation of trying to squeeze a wet cloth or paper towel, and how the cohesive properties of water facilitate higher compressed densities of the material. I.e., higher wet and dry density is achievable with higher moisture. Therefore, it is necessary to account for MC% in any model that explores a relationship between density and dielectric properties to obtain meaningful results and qualify any conclusions regarding a relationship between permittivity and density in alfalfa.

Temperature is used as part of the prediction model by the Unified Grain Moisture Algorithm (UGMA) for grains developed by GIPSA [12]. It was also found to have significance in research on dielectric properties of wheat straw [4]. Temperature was recorded at the face of the sensor while harvesting during this research in order to facilitate an investigation in this work as well. This particular temperature sensing design was found to accurately detect relative changes (in deg C) over a wide range of temperature in grains when comparing to a Dicky-John GAC2500, albeit with a bias of 5 deg-C high due to internally generated heat. In this case where the sensor is mounted in a rail on the bed of the bale chamber, higher-than-ambient values are expected due to heat from the machine, friction from hay moving across the sensor, and a bias from internal heating.

Using MC%, dry density [kg/m^3], and temperature [deg-C] as predictors then, the log-transformed ▮▮▮▮ dielectric constant (denoted as f3) is fit in a multivariate model since this particular transform maximized the R^2 in both the transformed

and untransformed response spaces. Since there is no need for interpretability in the original units, the log-transformed units are used. Effect leverage plots (Figure 4.18) show the effect of each predictor on the residuals of the response after accounting for other predictors and removing correlation with other predictors. They are an excellent way to observe significance of, and sensitivity to changes in, each predictor after accounting for the others [42] [46]. As is evident by the nonzero slopes in the leverage plots, MC%, density, and temperature were all statistically significant (P-value < 0.0001), and are ordered from left to right in terms of decreasing effect on f3.
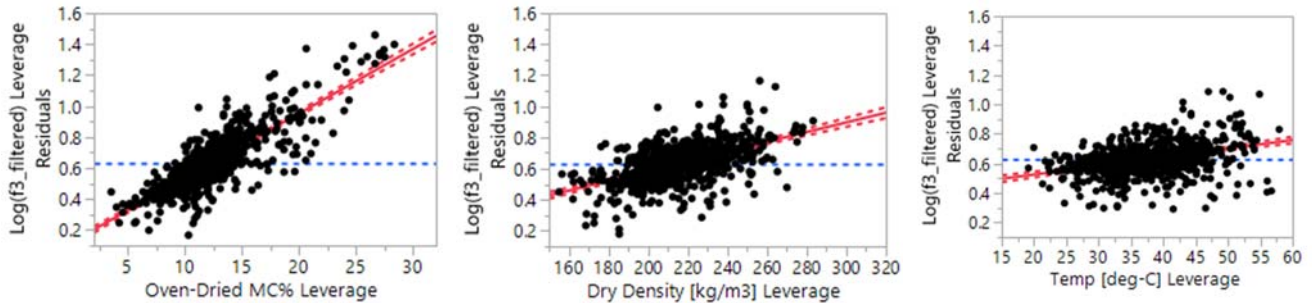
Figure 4.18: The log-transformed f3-filtered leverage residuals after fitting a multivariate model with dry density, MC%, and temperature as recorded at the sensor probe surface. P-values found were < 0.0001 and the leverage plots confirm the visual significance of each variable (i.e., that the P-value was not strongly influenced by a small number of outliers). The leverage plots also facilitate easy discernment of the sensitivity of the dielectric constant to each individual factor, which in this case is ordered from left to right in terms of sensitivity.

It is of interest to quantify the "risk" associated with density changes inducing notable spurious changes in moisture prediction, since density is not measured in real-time and included in the prediction model. Shown in Figure 4.19 is a distribution from 110 days of baling, and in 90% of cases the range of dry density experienced within in a day changes no more than 48 kg/m³ [3 lbs-cu/ft]. Additionally, over 50% of all bales collected are in very narrow range of 201 +/- 19 kg/m³ [12.6 +/- 1.3 lbs/cu-ft]. Examination of the sensitivity indicates a change of 16 kg/m³ [1 lbs-cu-ft] in dry density could result in a change of approximately 0.09 for the f3 value at 12%MC (where the curve is very sensitive to moisture), which is not a significant change in light of the right plot in Figure 4.13. This sensitivity could be absorbed in the performance without much problem.
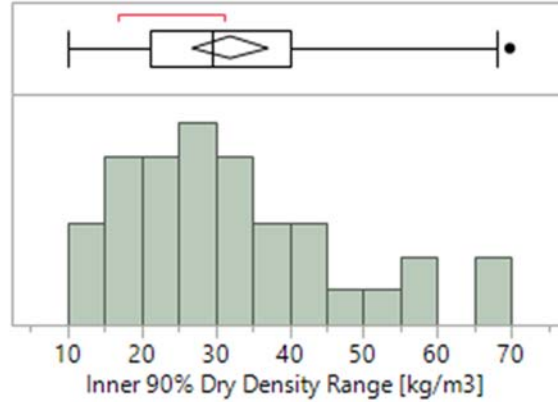
Figure 4.19: From 110 days of harvesting, the inner 90% range for each day is usually (in 90% of cases) is less than 48 kg/m³ [3 lbs/cu-ft].

With large square balers the panels on either of the side walls are on pivots at the front part of the baler, and at the rear force can be controlled to the panels to increase or decrease resistance to the plunger force on the bale at the front of the chamber. Since this system's function is primarily intended for control of bale density, it was investigated for any effect on dielectric measurements. This was done simply by adding the median tension pressure per bale (as recorded from the vehicle communications bus, or CANbus), to the multivariate regression with MC%, density, and probe temperature. For the most part, the significance and sensitivity of the 20MHz dielectric constant (f3) to each of the other effects remained similar to that shown in Figure 4.18. Adding tension panel pressure (measured in psi on the hydraulic cylinder) showed significance statistically (P-value < 0.0001) and a clear trend in the leverage plot in Figure 4.20 after accounting for the other predictors. Since it is available in real-time, this factor can be tested for usefulness in a prediction model for MC%.
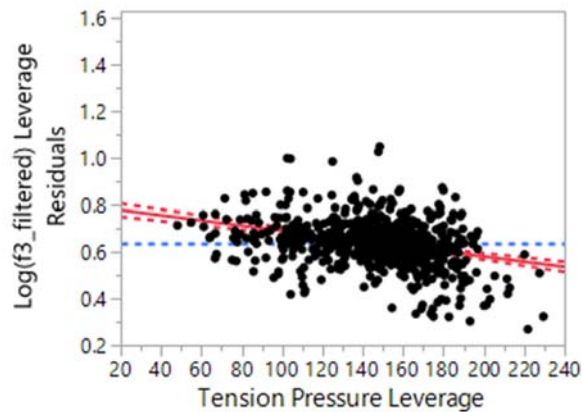

Figure 4.20: Tension panel pressure showed significance as an influencing factor after accounting for other factors.

4.3.3   COMMERCIAL MICROWAVE SENSOR
A commercially available microwave-based sensor was mounted on two different machines over the course of four

months (March-July of 2016) and 90 data points were collected from 7%mc to 65%MC. A setting of "General" was used since it proved effective on previous research [38] although a "Legume Hay" options is also available. The unit is pre-programmed with a hard limit of 31.5%mc and will not predict above that amount.

The performance of the microwave unit was very competitive when evaluated on a per-bale basis, with a 2.48%MC RMSE found with leave one out cross-validation from a 2nd order fitted-line shown in Figure 4.21 (the bias is obviously zero due to fitting). A linear reference line highlights the need for using a higher-order polynomial or basis functions. Note though that the data points colored red were ignored since the signal had clearly saturated by that point and a maximum prediction is not likely to be above 40%MC. The microwave unit outputs readings at regular intervals, but since it is mounted at the rear of the machine, these measurements are not very useful for real-time feedback. Therefore, the primary use of this device is finding wet spots in bales (it can be set to trigger a spray-paint can when moisture reads above a certain user-specified threshold) and monitoring general harvesting conditions.
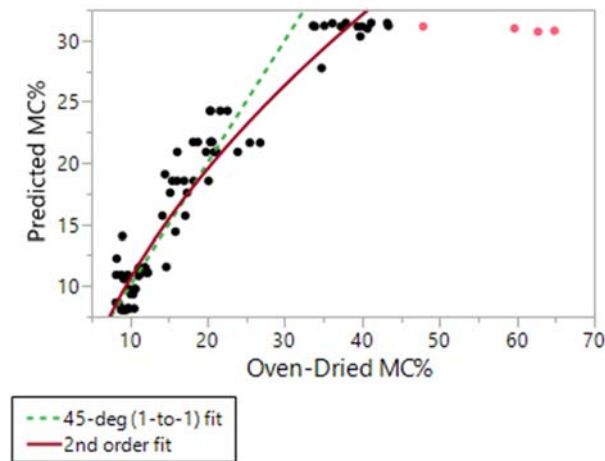
Figure 4.21: Standard deviation of residual MC from 2nd order fitted line is 2.3%. Stdev of residual of 45-deg line is 3.4%. The residual spread is similar to what was found with the capacitive-based sensor.
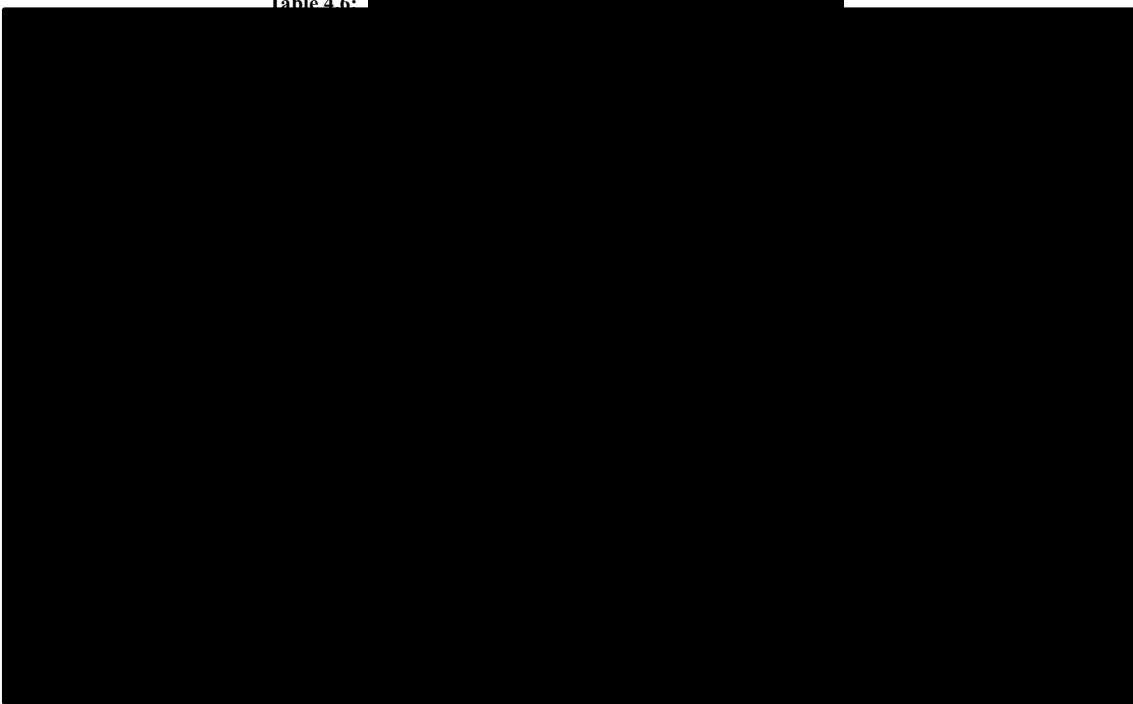
4.3.4   PREDICTIVE MODELING AND PERFORMANCE ANALYSIS

4.3.4.1   Classical Multivariate Analysis and Performance

The classical model utilizes the predictors found earlier to be significant in a multivariate model to predict MC%. Specifically the ▮▮▮▮ permittivity (f3), tension panel pressure in lbs/in^2 (psi) on hydraulic cylinder, and probe temperature in Celsius (density was excluded since it is technically not known at run-time). The data consists of the 1014 data points that are split into 60/40 train/test sets (561/453 in terms of samples for each). All three predictors were found significant in both P-value (< 0.0001) and leverage plots. The training and test sets had virtually identical RMSE at 1.86/1.87 MC%,

respectively. Certainly by these numbers the capacitive units would seem competitive with the commercial microwave sensor, but it is not quite a one-to-one comparison since the capacitive sensor was evaluated on an order of magnitude more bales, and some data from the capacitive sensor had to be ignored/eliminated due to non-characteristic response. The microwave unit had no such issues with data that was available.

Figure 4.22: (Left) Training data with R²=86, RMSE=1.86, and mean absolute error MAE=1.36 (Right) Test data for independent performance assessment with R²=84, RMSE=1.87, and MAE=1.4 has nearly identical performance as the training set.

Table 4.5: Prediction equation using classic multivariate model.

Prediction: MC% = A +B*(log(abs(f3)))+C*(Probe Temp)+D*(Tension Pressure)		
Factor	Coefficient Designation	Coefficients
Intercept	A	11
Log(Abs(F3))	B	13.2
Probe Temp	C	-0.11
Tension Pressure	D	-0.02

4.3.4.2 ███████ ████████ ████

Table 4.6: ████████████████

██
██
██

██

Table 4.7: ████████████████

██
██
██
██

5 10 15 20 25 30 35 40 45 50
Oven-Dried MC%

10 15 20 25 30 35 40 45 50
Oven-Dried MC%

10 15 20 25 30 35 40 45 50
Oven-Dried MC%

Figure 4.23:

Figure 4.24:

Table 4.8:

4.3.5   *REAL-TIME SIGNAL AND FILTERING*

The real-time signal represents a pivotal part of the sensor application. For this investigation the formulation from the classic [multivariate] analysis is used and each data point in the signal is one flake of the bale. If multiple measurements were made during a given flake the median was taken. All sensors have some kind of noise, which is essentially defined as part of the measurement that is not of value to the application, regardless of if it is accurate or not. In this case the real-time signal presents some interesting and challenging features beyond the classic Gaussian measurement noise around a slowly varying mean (representing the true moisture) that is to be explored and filtered to support the use cases mentioned earlier. A realization of the signal is shown in Figure 4.25 as measured during a day of harvesting alfalfa, and illustrates the type of structures that can be present in the signal. A kernel smoother is overlaid to highlight the slower trend, and also make the oscillations more visible. The various colors highlight different bales – note that the period of the oscillations last anywhere between two and four bales and appears to usually have a rigid edge between oscillations that coincides with different bales. These oscillations look suspiciously like the result of machine controls, although the primary suspect to affect density is

tension pressure and this has already been included in the model. Spatial correlation and density are explored for any plausible explanation for the source.
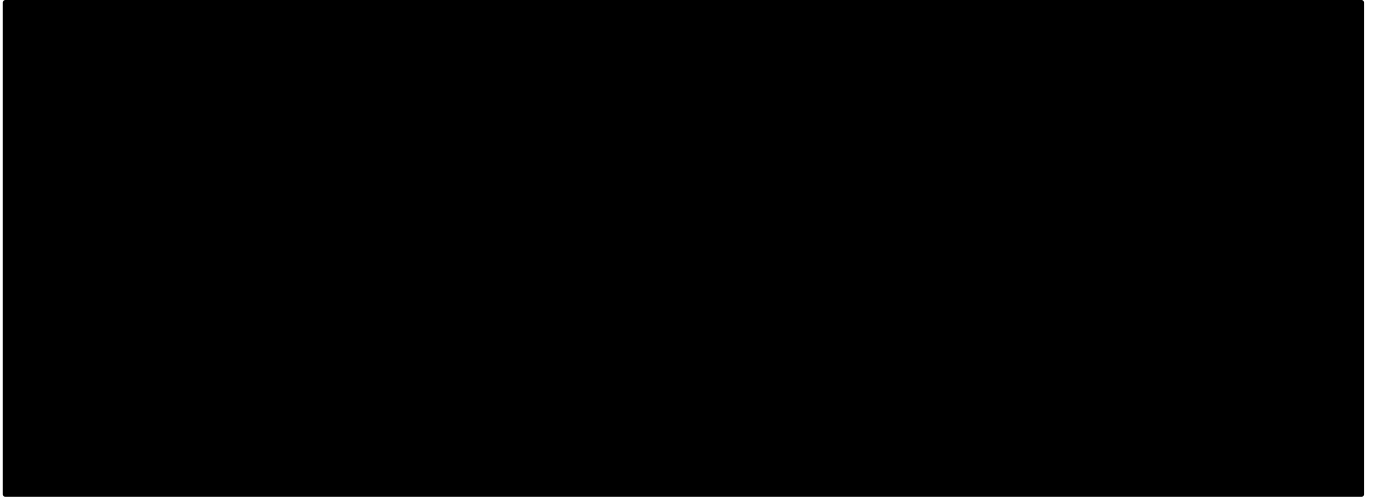

Figure 4.25:

4.3.5.1   Filter Training

While local smoothers (e.g., Lowess) are easy to implement off-line, they are not causal and not an option for online use. Causal filters such as FIR filters (a common example being a windowed average) can be an option but the delay is always a concern and minimum filter order to achieve low pass filtering can still be very large and increase computational burden. IIR filters are a good alternate to FIR filters for online use, but can still suffer from long phase delays. Another option which is employed for this task is building a signal model and subsequent prediction using a Kalman Filter (KF). As long as the signal model extends reasonably well to most cases, the foreknowledge of the process contained in the model facilitates a much shorter delay. Another advantage is that the state-space form of the model allows certain features to be extracted independently (and for "free" since all states are updated during the KF recursion algorithm), and thus support different use cases with one calculation. To obtain the same from non-parametric methods (such as IIR filter) a filter bank would be necessary, thus increasing computational burden.

While the more classic method of filtering is not used for the online algorithm, they still present a useful method to train the signal model. More specifically, the model is trained using non-causal (zero-phase) filters. Kernel smoothing could also serve as a training basis but IIR filtering allows a more analytical means to design the filters used for training. Visual inspection of the signal indicates a random walk will work well for the slowly changing mean and a discrete representation of a sinusoid as an AR2 process with no damping is a good candidate for the oscillatory part of the process. For this the

formulation is shown below with three parameters of the model to be fit: the frequency of the AR2 model and the process

driving noises for both the random walk and AR2.

Equation 3: Signal model shown in state space form that supports typical Kalman Filter implementation.

$$\begin{bmatrix} random\ walk \\ AR2 \\ \end{bmatrix} = \begin{bmatrix} x_k \\ n_k \\ n_{k-1} \end{bmatrix} = \begin{bmatrix} 1 & 0 & 0 \\ 0 & cos\omega & -1 \\ 0 & 1 & 0 \end{bmatrix} \begin{bmatrix} x_k \\ n_{k-1} \\ n_{k-2} \end{bmatrix} + \begin{bmatrix} \sigma_{rw} \\ \sigma_{ar2} \\ 0 \end{bmatrix}$$

$$z_k = \begin{bmatrix} 1 & 1 & 0 \end{bmatrix} \begin{bmatrix} x_k \\ n_k \\ n_{k-1} \end{bmatrix} + \sigma_z^2$$

To support training these three parameters, a slower moving local trend line and a faster moving filter to capture

oscillations but reject higher frequency part of signal are needed. Welch's method is used to estimate the power spectral

density (PSD) of the training signal and is shown below. Low-pass Butterworth filters are designed per the cutoff frequencies

determined from the PSD. KF parameters are optimized via minimum MSE criteria.
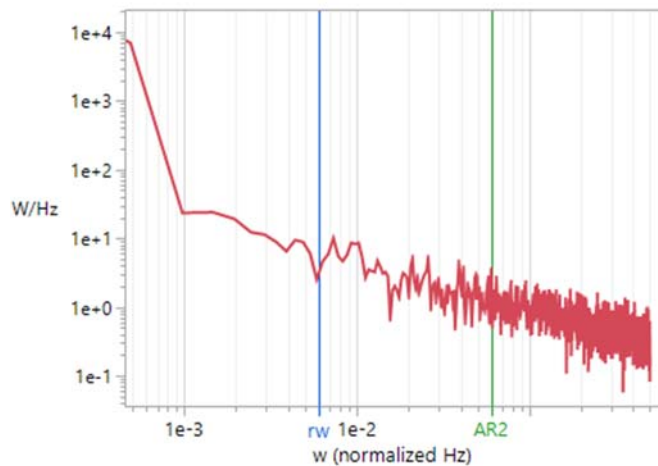
Figure 4.26: Power spectral density of signal recorded during harvesting a field. Lines are drawn to show the cut-off frequencies at which the filters are built.
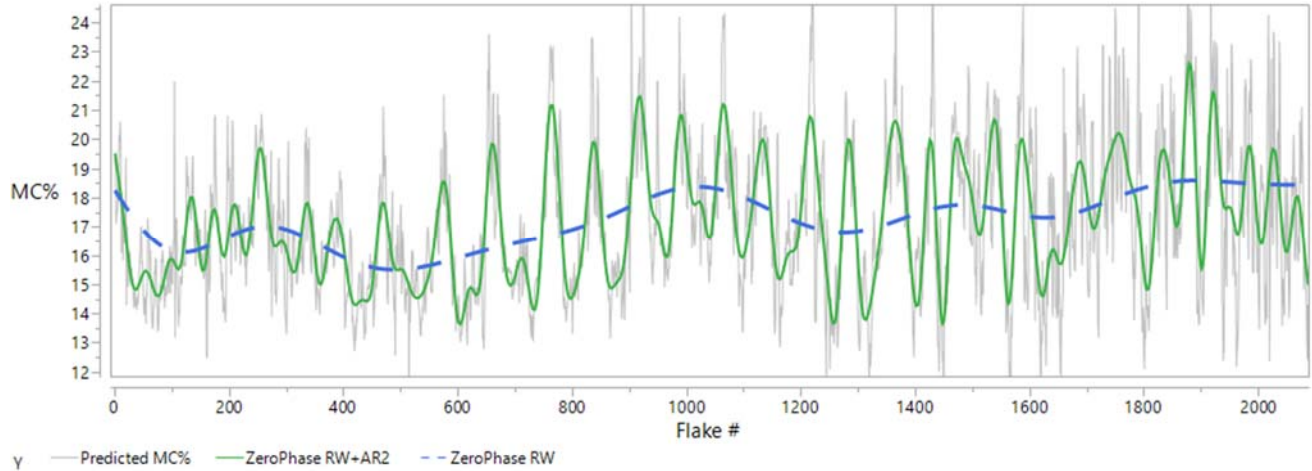
Figure 4.27: The results of applying the filters are overlaid on the original signal for a subset of the training data.

The signal is broken into the random walk and ar2 when comparing results of the trained KF algorithm to the zero-phase and causal IIR filters below. The resulting solution when fitting the three model parameters are as follows: $\omega = \frac{2\pi}{100}, \sigma_{rw} = 1E^{-4.5}, \sigma_{ar2} = 1E^{-5.5}$. The measurement noise, σ_z^2, also requires some value and it is sufficient to enter a small nominal value for stability of the calculations (0.2 worked sufficiently well here). If the oscillation frequency in the signal slows down by much, there is a chance of spectral overlap between the random walk and ar2 states that would present as the slower moving trend picking up some part of the oscillations. In such case the only option is to decrease the driving noise on the random walk.

In the top plot of Figure 4.28 The slower moving trend did not differ significantly between the KF and causal filters, with both closely following the zero-phase filter output as can be seen in the top plot of the following figure. Further comparison between the residuals of the KF and causal filter is shown in the bottom plot in terms of difference, or error, from the zero-phase filter output. The KF is slightly less biased in general, and at times where the local trend changes more quickly it is apparent the KF has less delay (and bias) than the causal IIR filter.
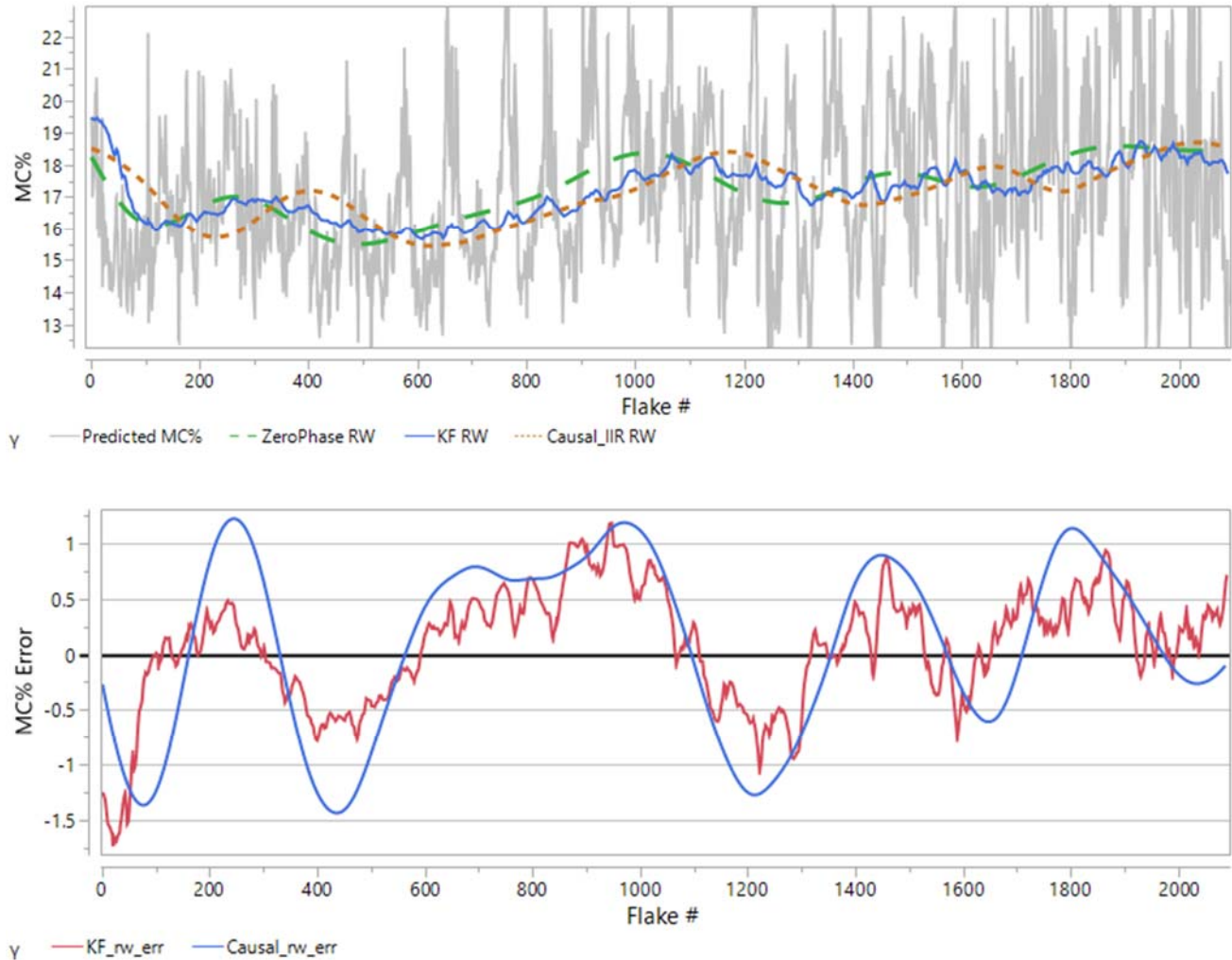
Figure 4.28: (top) Overlaying the zero-phase, KF, and causal random walk (or causal IIR filter) outputs shows much similarity between them and very reasonable tracking of the slow trend during harvesting an entire field. (bottom) The difference between the zero-phase filter output and the KF and causal version of the filter as overlaid as a comparison and examination of biasedness.

The oscillations are examined in the top plot of Figure 4.29 on a smaller time scale to make them more visible. The zero-phase filtered value has been subtracted from the original signal to obtain the "Oscillations" part of the original signal that is plotted with the rest of the data. A similar procedure was used to get the "zero-phase ar2" and "causal_ar2" parts. The KF filter naturally extracts this part of the signal as a state and thus no additional work is required to obtain it. The delay seen is on the order of six flakes for the KF output and 25 flakes for the causal filter. Additionally, the error between the zero-phase and KF and causal IIR filters is shown in the bottom plot of Figure 4.29, indicating the KF output tracks the signal much more closely than the IIR filter.
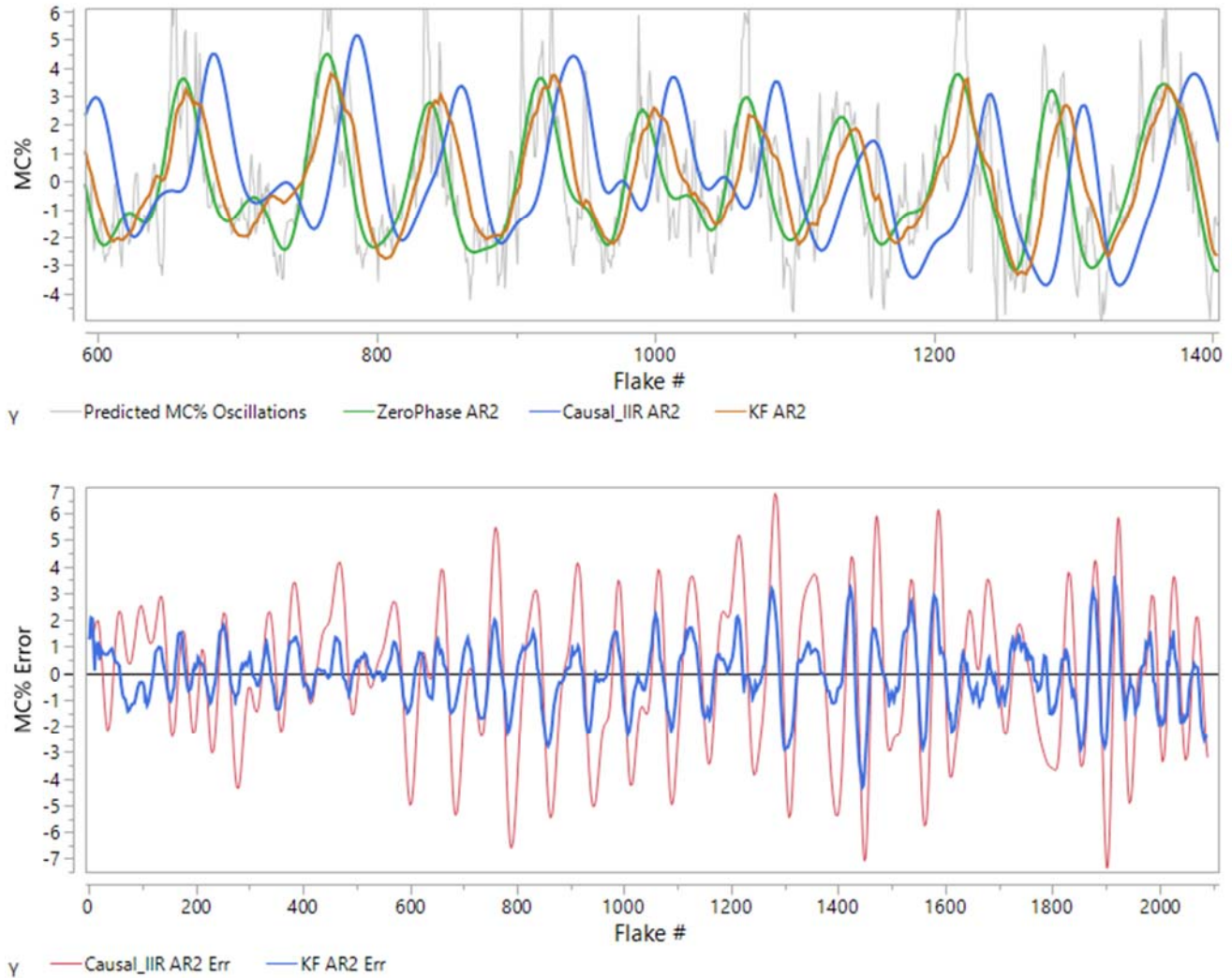
Figure 4.29: (top) Performance of tracking is shown by overlaying on the original signal residual "Oscillations" with the zero-phase, KF, and causal AR2 outputs. The long filter delay of the causal IIR is stark **(bottom)** The difference (or "error") between the online filters (KF, causal IIR) and the ideal (zero-phase IIR) over the same time period is shown and emphasizes the advantage of the KF over IIR filtering.

After training the parameters of the KF, the model was tested on the signal from a different day of harvesting. The output from the KF is overlaid on the raw signal in Figure 4.30 and appears to track the mean and oscillations very well while rejecting higher-frequency noise.

Figure 4.30: The trained KF was tested on harvest data from a different day than training data, and overlaid on the original signal. The resulting trends appear to track the signal very accurately while eliminating the higher frequency movement.

Circling back to the intended use cases, from the KF output the slower moving trend could support both general harvesting decisions and feedback control. Assuming the oscillations are not due to real moisture changes, the residual part of the original signal (after subtracting slower moving trend and oscillations) could be used to identify wet "slugs" in the bale relative to other parts. It is important to recognize that with the current model the residual part of the signal is not a white noise sequence, and thus a further AR1 term could be used to model that sequence for smoothing purposes if desired.

4.3.5.2 ███████ ███████████

118

Figure 4.31: ███

Figure 4.32: ███

Figure 4.33: ██
██

██

██

██

4.3.5.3   Real-Time Performance

As a final qualitative check on performance of the real-time prediction, data is taken from longer periods of baling in which a multitude of bales were also core-sampled, and the prediction signals overlaid with the oven-dried moisture content. To validate usefulness and validity of the signal, it is important to see the prediction trends follow the trend in moisture found from the core samples through the baling period. The plot in Figure 4.34 contains both raw & KF filtered prediction signals in addition to oven-dried MC for select bales. The "KF RW+AR2" contains the oscillations that were shown to be unlikely due to MC earlier, and are included in Figure 4.34 but would best be ignored/removed from the online signal. The slow moving trend is slightly biased between flakes 2000-2500, but otherwise tracks the oven-dried MC% trend closely. Further harvesting events from the dataset in Figure 4.35 similarly showed good tracking between the smoothed (by KF) prediction signal and trend in MC% found with oven-dried samples from the same bales.
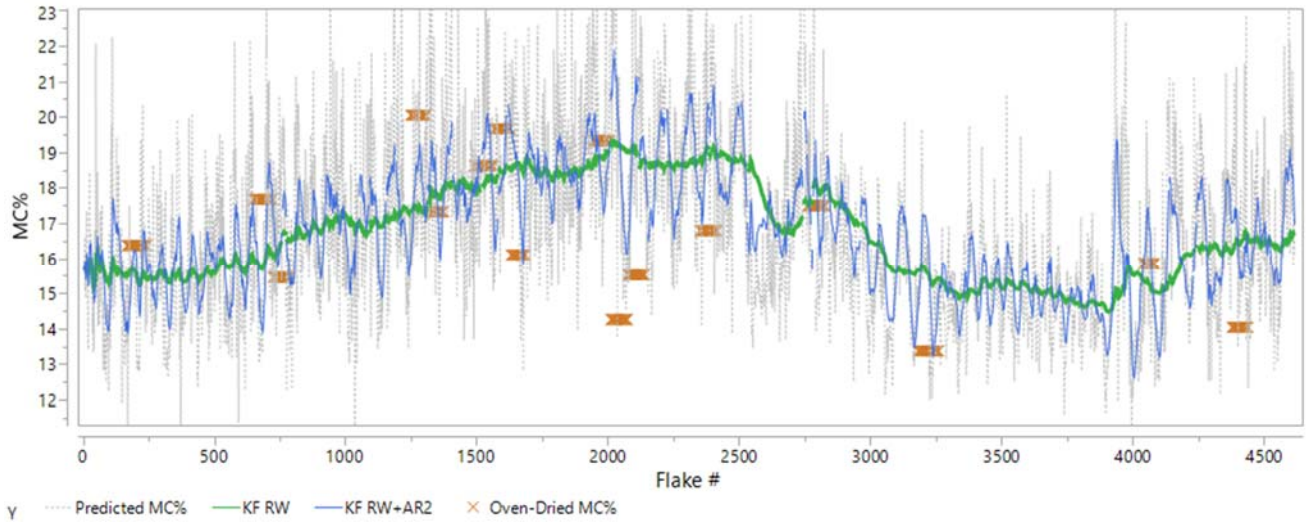
Figure 4.34: A typical signal is overlaid with KF output and oven-dried moisture content found from core sampling select bales. Since oscillations were shown to be unlikely due to moisture changes, the focus is on how the slower moving trend follows the trend found from the oven-dried core samples.
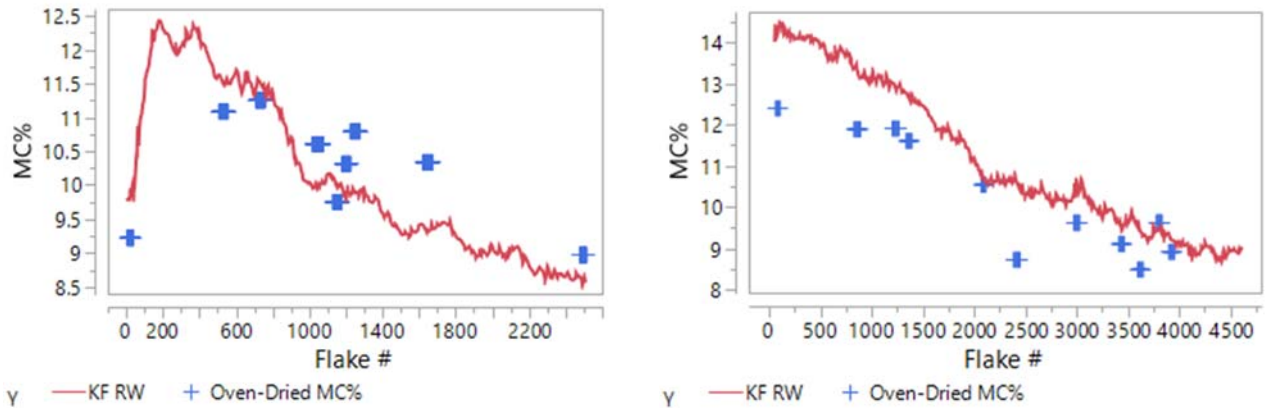

Figure 4.35: Two additional examples of the KF RW component output of predicted MC% tracking the trend found with oven-dried samples from the same bales.

On a final note, the KF filter functions well under the presumption that harvesting is relatively continuous. If this is not the case then large biasing may result as shown in Figure 4.36. It is possible to overcome this by resetting (or reinitializing) the KF filter after a maximum idle time (or non-harvesting state).
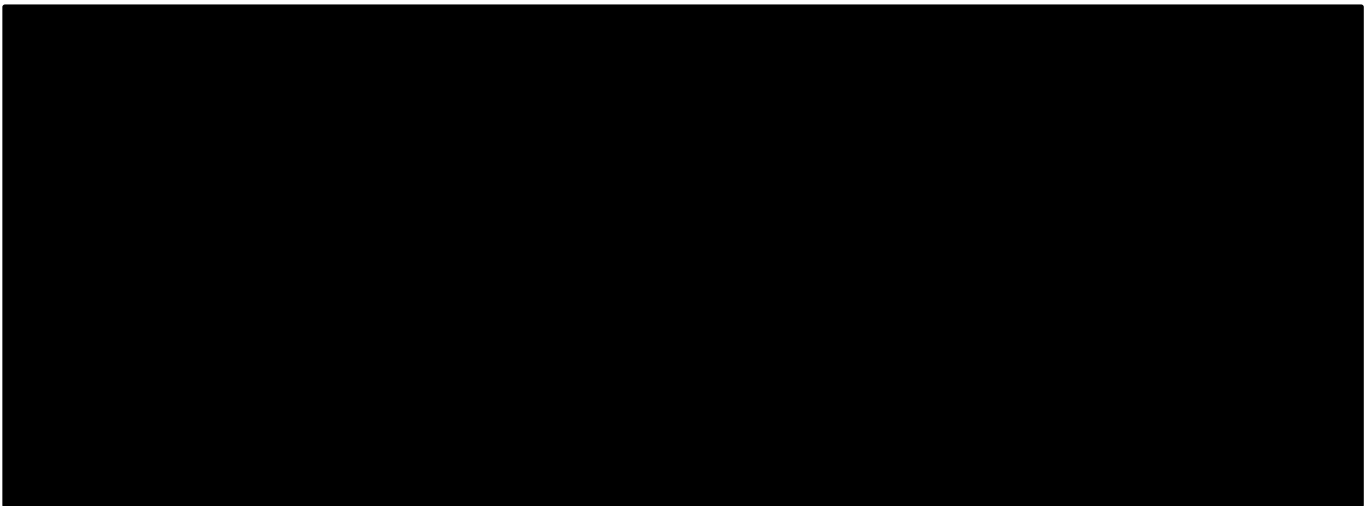
Figure 4.36:

4.4   CONCLUSIONS

The main use cases of a moisture sensor in the alfalfa hay business are correction of mass by MC for yield monitoring, general harvesting decisions, preservative application, and identification of wet spots. With regards these, the evidence detailed herein has shown the capacitive-based sensor has potential as a cost-effective solution with accuracy on par with other more expensive technology (microwave sensor), and can support all primary use cases. With advanced filtering methods the sensing moisture range will be larger than with microwave technology as well. The sensitivity to confounding factors described (e.g. density) is determined to be acceptable. The Kalman filter algorithm for described for online prediction provides a useful basis for implementation, with a nominal amount of additional logic likely necessary to handle initial values to the filter and transitions between fields/conditions or where any other discontinuous harvesting occurs. In light of the positive performance observed thus far, opportunities exist primarily in gathering more data for moisture contents greater than 30% to better train the ANN, and inclusion of wet density information in the predictive model [such as when combined with a yield monitor] may lead to a more accurate prediction of moisture content. More creative feature engineering may also lead to further improvements.

4.5   REFERENCES

[1]   S. O. Nelson and S. Trabelsi, "A Century of Grain and Seed Moisture Sensing through Electrical Properties," in *ASABE*, Louisville, Kentucky, 2011.

[2]   *Dielectric Properties of Grain and Seed,* St. Joseph, Mich.: ASABE, 2012.

[3]   C. B. Behringer, "Performance Comparison of Moisture Sensor Technologies for Forage Crops," Madison, Wi,

2004.

[4]   W. Guo, J. Yang, X. Zhu, S. Wang and K. Guo, "Frequency, Moisture, Temperature, and Density-Dependent Dielectric Properties of Wheat Straw," *Transactions of the ASABE,* vol. 56(3), pp. 1069-1075, 2013.

[5]   C. E. Kirkwood, N. S. Kendrick and H. M. Brown, "Measurement of dielectric constant and dissipation factor of raw cottons," *Textile Research Journal,* p. 24:841, 1954.

[6]   A. Kraszewski and S. O. Nelson, "Composite Model of the Complex Permittivity of Cerial Grains," *J. agric. Engng. Res,* pp. 43,211-219, 1989.

[7]   D. K. Cheng, Field and Wave Electromagnetics, Pearson Education, 1989.

[8]   "Impedance Measurement Handbook, 4th Edition," Keysight Technologies, 2014.

[9]   "Basics of Measuring the Dielectric Properties of Materials," Keysight Technologies, 2015.

[10]   "E4990A Impedance Analyzer: Data Sheet," Keysight Technologies.

[11]   S. O. Nelson, "Dielectric properties of grain and seed in the 1 to 50-mc range," *Transactions of the ASAE,* pp. vol. 8, no.1, pp. 38-48, 1965.

[12]   D. Funk and Z. Gillay, "Unified Grain Moisture Algorithm," USDA, 2012.

[13]   D. B. Funk, "New Official Moisture Technology Implementation Briefing," in *NAEGA-GIPSA Regional Meeting*, Destrehan, LA, 2012.

[14]   "GAC 2500-UGMA Grain Analysis Computer," 2 2016. [Online]. Available: http://www.dickey-john.com/product/gac2500/.

[15]   S. O. Nelson, "Dielectric Property Measurements and Techniques," in *AIChE*, Austin, TX, 2004.

[16]   S. O. Nelson, Dielectric Properties of Agricultural Materials and Their Applications, elsevier, 2015.

[17]   W. L. Balls, "Dielectric properties of raw cotton," *Nature,* p. 158: 9–11., 1946.

[18]   L. Han Ming, L. Ma, C. Q. Ma and J. F. Hong , "Estimation of the moisture regain of cotton fiber using the dielectric spectrum," *Textile Research Journal,* p. Vol. 84(19) 2056–2064, 2014.

[19]   C. E. &. D. Team, "Turnout Percentages -- Factors Involved," CSD Extension, 2010.

[20]   B. Goodman and C. D. Monds, "A Farm Demonstrations Method for Estimating Cotton Yield in the Field for Use by Extension Agents and Specialists," *Journal of Extension,* vol. 41, no. 6, 2003.

[21]   S. C. P. Ltd., "Moisture Management a Must," Southern Cotton Pty Ltd., Whitton, NSW, 2013.

[22]   J. Quinn, R. Eveleigh, B. Ford, J. Millyard, A. North and J. Marshall, "Cotton Picking Moisture," Cotton Seed Distributors, Wee Waa, NSW, 2014.

[23]   "Cotton Pcker Management and Harvesting Efficiency," Clemson University Extension, 1996.

[24]   R. Fiore, "Circuit Designers' Notebook, Document #001-927, Rev. E," American Technical Ceramics, 2005.

[25]   "Tests for thermoplastic materials used in the electrical and electronic industries," DuPont.

[26]   "Moisture Restoration of Cotton," USDA-ARS, 2004.

[27]   R. K. Byler, M. G. Pelletier, K. D. Baker, S. E. Hughs, M. D. Buser, G. A. Holt and J. A. Carroll, "Cotton Bale Moisture Meter Comparison at Different Locations," *Applied Engineering in Agriculture,* vol. 25, no. 3, pp. 315-320, 2009.

[28]   M. H. Willcutt, E. M. Barnes, M. J. Buschermohle, J. D. Wanjura, G. W. Huitink and S. W. Searcy, "The Spindle-Type Cotton Harvester," Texas A&M Agrilife Research and Extension Center, Lubbuck, TX, 2010.

[29]   "Cotton Picker Management and Harvesting Efficiency," Clemson University Extension, 1996.

[30]   J. P. Just and M. J. Darr, "COMPOSITE MODEL OF THE COMPLEX PERMITTIVITY OF RAW COTTON," *ASABE,* 2016.

[31]   *Standard Test Method for Moisture in Cotton by Oven-Drying,* West Conshohocken, PA: ASTM International, 2012.

[32]   J. G. Montalvo Jr. and T. M. Hoven, "Review of Standard Test Methods for Moisture in Lint Cotton.," *The Journal of Cotton Science,* pp. 12:33-47, 2008.

[33]   R. K. Byler, "Comparison of Selected Bale Moisture Measurements in a Commercial Gin," in *2012 Beltwide Cotton Conferences*, Orlando, Florida, 2012.

[34]   R. K. Byler, "The Accuracy of Cotton Bale Moisture Sensors Used in a South Texas Commercial Gin with Lint Moisture Restoration," in *2014 Beltwide Cotton Conferences*, New Orleans, LA, 2014.

[35]   D. Cash and H. F. Bowman, "Alfalfa Hay Quality Testing," Montana State University Extension, Bozeman, MT, 1993.

[36]   W. K. Coblentz, "Spontaneous Heating," in *Idaho Alfalfa and Forage Conference Proceedings*, Burley, Idaho,

2013.

[37] W. Coblentz and M. Bertram, "Effectiveness of Buffered Propionic-Acid Preservatives for Large Hay Packages," Midwestforage.org, 2011.

[38] K. E. Webster, M. J. Darr, J. C. Askey and A. D. Sprangers, "Production Scale Signle-pass Corn Stover Large Square Baling Systems," in *2013 ASABE Annual International Meeting*, Kansas City, MO, 2013.

[39] J. P. Just and M. J. Darr, "COMPOSITE MODEL OF THE COMPLEX PERMITTIVITY OF RAW COTTON," *ASABE,* 2017.

[40] J. Just and M. Darr, "Real-Time Moisture Prediction on Round-Bale Cotton Harvesters," *ASABE,* 2017.

[41] D. Funk, "Engineering Considerations for Dielectric On-Line Grain Moisture Measurement," in *ASABE*, Kansas City, MO, 2013.

[42] J. O. Rawlings, S. G. Pantula and D. A. Dickey, Applied Regression Analysis: A Research Tool, Second Edition, Springer, 1998.

[43] "Impedance Measurement Handbook, 5th Edition," Keysight Technologies, 2015.

[44] G. E. Shewmaker and R. Thaemert, "Measuring Moisture In Hay," in *Proceedings, National Alfalfa Symposium*, San Diego, CA, 2004.

[45] M. Rankin, "Understanding Corn Test Weight," UW Extension Team Grains, 2009.

[46] J. T. Documentation, "Standard Least Squares Report and Options -- Row Diagnostics," JMP From SAS, [Online]. Available: http://www.jmp.com/support/help/Row_Diagnostics.shtml#184200. [Accessed 17 Jan 2017].

[47] S. O. Nelson and S. Trabelsi, "Use of Grain and Seed Dielectric Properties for Moisture Measurement," in *Southeastcon. 2011 Proceedings of IEEE*, Nashville, TN, 2011.

[48] D. M. Mitchell, J. Johnson and C. Wilde, "IMPACTS OF DECREASING COTTONSEED TO LINT RATIO ON COTTONSEED MARKETS," in *Beltwide Cotton Conference*, New Orleans, 2007.

[49] D. Blackham, F. David and D. Engelder, "Dielectric Materials Measurements," in *RF & Microwave Measurements Symposium and Exhibition*, 1990.

[50] D. Funk, B. Gillay, S. Burton and Z. Gillay, "Engineering Considerations for Dielectric Online Grain Moisture Measurement," in *2013 ASABE International Meeting*, 2013.

[51]   R. K. Byler, "Resistivity of Cotton Lint for Moisture Sensing," *Transactions of the ASABE,* vol. 41, no. 3, pp. 877-882, 1998.

[52]   M. Digman and K. Shinners, "Technology Background and Best Practices: Yield Mapping in Hay and Forage," in *Proceedings, Idaho Hay and Forage Conference*, Burley, ID, 2013.

[53]   R. Benning, S. Birrell and D. Geiger, "Development of a Multi-Frequency Dielectric Sensing System for Real-TIme Forage Moisture Measurement," in *2004 ASAE/CSAE Annual International Meeting*, Ottawa, Ontario, Canada, 2004.

[54]   J. Banta, "Bale Weight: How Important Is It?," AgriLife Communications.

CHAPTER 5:   GENERAL SUMMARY

While the area of rapid determination of moisture content via capacitive means is a 65 year-old topic, new technology, ideas, and analytical methods shown in the three papers presented in this dissertation have enabled advancement in this area. From leveraging FEA software to utilizing machine learning methods, a simple planar probe design coupled with relatively inexpensive impedance measurement hardware becomes a novel invention for moisture sensing during harvesting operations of cotton and alfalfa.

Opportunity for further research exists for both improving on the probe design as well as extending the sensor into other applications. Some type of constrained evolutionary optimization of the design of the probe geometry may yield a probe design that more efficiently links flux through the material between source and sink electrodes, and/or with further penetration into the material. Other planar designs such as concentric patterns of the electrodes should be examined, although may be harder to manufacture. Due to the planar design, this sensor can be used in virtually any type of crop and so there is much opportunity to apply this sensor in other bale crops as well as grains in the same ways presented in the second and third papers. Fusion of signals from other sources that produce information correlated to specific properties like density, but not highly correlated with permittivity, could also be used to increase accuracy of the predictions.